Evaluating the Trade-offs Between Microalgal Biomass Production Rate and Nutrient Reduction in Dairy Waste Whey Permeate-amended Culture

By

Tatyana Bouffard-Martel

Submitted in partial fulfilment of the requirements
for the degree of Master of Science

At

Dalhousie University
Halifax, Nova Scotia
April 2024

Table of contents

List of tables

List of figures

Abstract

Leveraging microalgae for food production and aquaculture feeds utilizing waste offers an economically efficient and circular solution to food challenges while promoting nutritional sustainability. This research investigates the potential of whey permeate (WP), a by-product of cheese making, as a nutrient-rich substrate for algal cultivation. The first part (Chapter 2) delves into the preparation of WP powder and its integration into culture media, revealing that autoclaving WP with NaOH, resulting in browning reactions, supported algal growth, especially with 1 M NaOH. Media adjustments at pH 7 optimized biomass, and aging enhanced growth of the green alga *Tetraselmis suecica*, possibly due to calcium-phosphate resolubilization. The solvent used with WP influenced phosphorus availability, while a light exposure experiment explored WP degradation. The cryptophyte *Chroomonas mesostigmatica* had higher growth in WP media with a headspace, emphasizing the importance of gas exchange. A second part (Chapter 3) extends to larger-scale exploration by characterizing biomass from four algal species in closed systems using WP as a phosphorus substitute and organic carbon source. Signs of mixotrophic growth were observed in *T. suecica* and the diatom *Chaetoceros muelleri*, suggesting lactose assimilation from WP. The pinguiophyte *Pinguiococcus pyrenoidosus* showed comparable eicosapentaenoic acid (EPA) productivity rates in WP media during exponential phase, highlighting a promising strain for omega-3 production. *C. muelleri* had significant fatty acid accumulation in stationary phase with WP media, hinting at its suitability for biofuel production. *T. suecica* and *C. mesostigmatica* emerged as potential candidates for protein production, and *C. muelleri* and *C. mesostigmatica* seemed suitable for WP remediation, given their luxury uptake of phosphorus. This work lays the foundation for large-scale production of algae-based valuable compounds using dairy waste WP as a growth substrate.

Résumé

Tirer parti des microalgues pour la production alimentaire et les aliments aquacoles, en particulier en utilisant des déchets, offre une solution économiquement efficace et circulaire aux défis alimentaires tout en favorisant la durabilité nutritionnelle. Cette recherche explore le potentiel du lactosérum (whey permeate: WP), un sous-produit de la fabrication du fromage, en tant que substrat riche en nutriments pour la culture d'algues. La première partie (chapitre 2) se plonge dans la préparation de la poudre de WP et son intégration dans les milieux de culture, révélant que l'autoclavage du WP avec NaOH, entraînant des réactions de brunissement, favorisait la croissance des algues, surtout avec 1 M NaOH. Des ajustements du pH des milieux à 7 ont optimisés la biomasse, et le vieillissement du milieu de WP a amélioré la croissance de *T. suecica*, probablement en raison de la re solubilisation du phosphate de calcium. Le solvant utilisé avec le WP a influencé la disponibilité du phosphore, et une expérience d'exposition du media à la lumière a exploré la dégradation du WP. *C. mesostigmatica* dans un milieu de WP avec un espace libre a démontré une croissance supérieure, soulignant l'importance de l'échange gazeux. Une deuxième partie (chapitre 3) s'étend à l'exploration à plus grande échelle en caractérisant la biomasse de quatre espèces d'algues dans des systèmes clos en utilisant le WP comme substitut du phosphore et source de carbone organique. Des signes de croissance mixotrophe, en particulier chez *C. muelleri* et *T. suecica*, ont été observés, suggérant une assimilation du lactose provenant du WP. *P. pyrenoidosus* a montré des taux de productivité d'eicosapentaenoic acid (EPA) comparables dans les milieux de WP pendant la phase exponentielle, mettant en évidence une souche prometteuse pour la production d'oméga-3. *C. muelleri* a présenté une accumulation significative d'acides gras en phase stationnaire avec des milieux de WP, laissant entendre sa pertinence pour la production de biocarburants. *T. suecica* et *C. mesostigmatica* ont émergés comme des candidats potentiels pour la production de protéines, et *C. muelleri* et *C. mesostigmatica* ont semblé adapter à la remédiation du WP, compte tenu de leur absorption luxueuse de phosphore. Ce travail établi des bases de la production à grande échelle de composés de valeur à base d'algues en utilisant le lactosérum comme substrat de croissance.

List of Symbols and Abbreviations used

Symbols	Definition	Units
μ	Fluorescence-based specific growth rate (Equation 3.6)	d^{-1}
μ_{max}	Fluorescence-based maximum specific growth rate observed during exponential phase based on Blackman or Gompertz models.	d^{-1}
a	Absorbance from the spectrophotometer	Dimensionless
Chla	Chlorophyll-*a* concentration	$\mu g\ L^{-1}$
d	Optical pathlength	m
d*F*/dt	Instantaneous rate of change of fluorescence	Arb.
dX/dt	Instantaneous rate of change of biomass (X)	mg biomass (X) $L^{-1}\ d^{-1}$
F	Dark-acclimated Chla fluorescence in vivo, measured with Turner fluorometer	Arb.
F_0	Minimum dark-acclimated Chla fluorescence in vivo, from FIRe induction curve	Rhodamine Eq.$^{-1}$
F_{init}	Initial ln-transformed value of *F* in batch culture	Arb.
F_m	Maximum dark-acclimated Chla fluorescence in vivo, from FIRe induction curve	Rhodamine Eq.$^{-1}$
F_{max}	Final ln-transformed value of *F* in batch culture	Arb.
F_t	Time-dependent value of ln-transformed *F*	Arb.
F_v	Variable fluorescence, calculated as (F_m - F_0)	Rhodamine Eq.$^{-1}$
F_v/F_m	Ratio of variable to maximum dark-acclimated Chla fluorescence in vivo, calculated as (F_m - F_0)/F_m	Dimensionless
OD	Optical density	Dimensionless
t	Time (day)	d
t_{gen}	Generation (i.e., doubling) time	d
t_{sat}	Time to saturation in growth curve (from λ to STA phase)	d
λ	Duration of lag phase	d
σ	Sigma: Absorption cross section representing the area of the antenna's pigments	$Å^2$

Abbreviations	Meaning
ANOSIM	Analysis of similarity
ANOVA	Analysis of variance
C-box	CO_2-generating system
CCM	Carbon-concentrating mechanism
CTRL	Control media
CTRL ± DIC	Both treatments CTRL and CTRL+DIC
CTRL+DIC	Control media with 2 mM of sodium bicarbonate added
DIC	Dissolved inorganic carbon
DIN	Dissolved inorganic nitrogen
DIP	Dissolved inorganic phosphorus
EPA	Eicosapentaenoic acid
EXP	Exponential phase of growth curve
FA	Fatty acid
FIRe	Fluorescence Induction and Relaxation system (Satlantic)
MDS	Multidimensional scaling
mo	Month(s)-old
NCMA	National Center for Marine Algae and Microbiota
PSII	Photosystem II
PUFA	Polyunsaturated fatty acid
SD	Standard deviation
SDGs	United Nations Sustainable Development Goals
SIMPER	Similarity percentage
STA	Stationary phase of growth curve
WP	Whey permeate
WP+DIC	WP-amended media with 2 mM of sodium bicarbonate added
WP ± DIC	Both treatments WP and WP+DIC

Acknowledgements

I extend my highest gratitude to my supervisor, Dr. Hugh MacIntyre, for his unwavering belief in my abilities, his continuous challenges that pushed me beyond my perceived limits, and for being an exceptional mentor and human being. His guidance and support were instrumental throughout this journey, and I appreciate the nurturing environment he created for his students in Halifax.

I am sincerely thankful to the members of my supervisory committee, Dr. Stefanie Colombo, Dr. Patrick McGinn, Dr. Carolyn Buchwald, and Dr. Christopher Algar for their valuable insights and contributions to my work.

Special appreciation goes to the dedicated members of the MicroAlgal Process and Evaluation Laboratory (MAPEL), especially our lab manager, Cat London, whose commitment has enriched the research environment. I am grateful to the co-op students—Kylie Santella, Griffin Finkbeiner, Mikaela Ermanocovics, Emma Taniguchi, Ryan Molin, Ainhoa Boyle, Danielle Baribeau, Kasey Manolikakis, and Rori Mulholland—who played a crucial role in data collection for this thesis.

I would also like to thank our lab technicians, Julia Cantelo, Mackenzie Burke, and Rose Latimer, for their technical expertise and support. Special thanks to an excellent research assistant, Chris Latimer, who greatly contributed to Chapter 2. I am appreciative of the support and friendships built with my fellow graduate students, Jessica Oberlander, Marie Egert, and Laura Figueira Garcia.

To my friends — Serena Feeney, Graeme Guy, Jérémie Al-Simaani Goulet, Ève Gagnon, Isabelle Ouellette, Thomas McClellan, Marine Ceillier, and George Poitra-Tremblay — and my family — Sylvain Martel, Nadia Bouffard, Francis Martel-Bouffard, and Luba Laurin — I extend heartfelt thanks for being pillars of support throughout this degree.

Last, my sincere appreciation to everyone who, in various ways, contributed to my research. This work was made possible through the generous funding provided by the Weston Foundation, Nature's Way, and the Ocean Frontier Institute and through the acquisition of dairy waste substrate provided by Agropur. Your support has been crucial to the success of this research.

Chapter 1: Introduction

1.1. Context: Addressing sustainability

Some may have come across the concept of Earth's Overshoot Day, which is when human demand for resources exceeds our planet's ability to renew them within the same year (Global Footprint Network 2023). In 2023, Canada reached this point on March 13, highlighting the country as one of the least sustainable consumers in the world. This pressing concern urges us to examine our consumption patterns and ecological footprint.

Global Food Problem

A significant factor contributing to the Overshoot calculation is food production, with half of the Earth's biocapacity being used to feed human populations (Global Footprint Network 2023). The global food problem is a challenge that necessitates responsible consumption and production, as underscored by the United Nations Sustainable Development Goals (SDGs) 2030, particularly Goal 12 (The Global Goals 2023). This goal identifies several critical targets, including the need for "*Achieving sustainable management and efficient use of natural resources*", to "*Halve per capita global food waste at the retail and consumer levels and reduce food losses along production and supply chains, including post-harvest losses*", and to "*Support developing countries to strengthen their scientific and technological capacity to move towards more sustainable patterns of consumption and production*". Central to these targets and the concerns they aim to address is the need to explore sustainable food production and consumption approaches, focusing on enhancing food quality and minimizing waste and losses in the supply chain.

Aquaculture feeds

Aquatic food production is forecasted to increase by 15 % by 2030, which is seen as beneficial to feeding the growing world population (FAO 2022). It is recognized that because of the state of world capture fisheries, this growth will need to be supported by growth in aquaculture production. The aquaculture industry plays a major role in the global food system, as half of the seafood consumption in the world comes from it (Fry et al. 2016). Effective and sustainable use of resources like energy and feeds within aquaculture systems is a pressing need (Boyd et al. 2020). The nutritional quality of cultivated seafood is contingent upon the animal's diet. Lipids, particularly omega-3 fatty acids (FAs), are crucial for many aquaculture animals at various growth stages (Roy and Pal 2015). Additionally, supplying amino acids and proteins is vital for increasing biomass in aquaculture ponds (Boyd et al. 2020).

The aquaculture industry has heavily relied on wild catches of small fish to provide essential feeds, constituting a significant portion of the global wild catch (Boyd et al. 2020). The declining stocks of these smaller fish in the oceans pose a notable challenge to the sustainability of aquaculture. Consequently, the aquaculture industry is pivoting towards incorporating land crops as a feed ingredient, raising ecological concerns related to land usage, freshwater utilization, and fertilizer and pesticide application (Fry et al. 2016). Moreover, this shift towards land crops as feeds has resulted in aquaculture products with suboptimal nutritional profiles, including reduced omega-3 content, potentially affecting human nutrition and health (Fry et al. 2016). Alternative sources of proteins and lipids for aquaculture feeds are needed to solve this issue and improve the nutritional quality of farmed animals (Wurts 2000; Roy and Pal 2015).

1.2. One solution: Microalgae as feeds

To confront these challenges, one avenue of great promise lies in microalgal culturing. Algal biomass offers versatile compounds extending to both human and aquaculture animal consumption. Microalgae have gained increasing attention, and efforts of mass-culturing have intensified worldwide, driven by the recognition of their rich nutritional profiles.

Microalgae have a rich history of cultivation and remain a valuable source of various compounds, including proteins, carotenoids, xanthophylls, omega-3 FAs, bio-colorants, and more (Cardozo et al. 2007; Abreu et al. 2012). Commercial markets for algal biomass include pharmaceuticals, health supplements, cosmetics, aquaculture feeds, and biofuels (Becker 2007; Cardozo et al. 2007). Cultivating microalgae for biofuel production using triacylglycerides has a lengthy history, yet it has proven to be less economically viable compared to the production of nutritious compounds intended for consumption. The consumption of algae has also been linked to a range of health benefits. These benefits extend from improved cardiovascular health, thanks to omega-3 FAs, to enhanced antioxidant protection due to carotenoids (Cardozo et al. 2007). Incorporating algae into diets can play a pivotal role in supporting overall well-being and mitigating the risks associated with inadequate nutrition. Moreover, using microalgae as a primary ingredient in aquaculture feeds offers a sustainable approach to meet the increasing demand for fish production. This method can reduce the use of land crops while providing highly nutritious food to the cultivated organisms. Extensive research has examined the utilization of

microalgae in aquaculture feeds, demonstrating success, particularly in the supply of essential amino acids (Brown 1991; Roy and Pal 2015).

The cultivation and utilization of microalgal biomass holds great promise in addressing the complex challenges of global food insecurity, sustainable aquaculture, and improved human nutrition. However, large-scale algae cultivation can present important economic challenges due to the significant costs and investments required. The costs of supplying nutrients and light to sustain these cultures are high. One solution to this challenge is intercepting industrial effluents and using their wastes as a low-cost nutrient supply for the cultures.

1.3. Bioremediation of food-grade wastes

Waste management

Utilizing waste as a nutrient source for algal cultures not only offers a promising means to reduce the costs of mass culturing but also serves a critical role in waste management. The food industry generates substantial volumes of by-products that often go to waste due to limited commercial uses. While growing efforts are made to reduce food-grade waste, it remains inevitable. Conventional remediation treatments are employed to address the environmental challenges associated with these by-products, including the risk of eutrophication, hypoxic areas (Diaz and Rosenberg 2008; Rabalais et al. 2009; Glibert et al. 2018), and Harmful Algal Blooms, as the need for effective and eco-friendly waste management is a pressing concern.

Aligned with the United Nations SDG 12, there is a recognition of the necessity to "*achieve the environmentally sound management of chemicals and all wastes throughout their life cycle, in accordance with agreed international frameworks, and significantly reduce their release to air, water and soil in order to minimize their adverse impacts on human health and the environment*" (The Global Goals 2023). The process of cleaning waste effluents from nutrients and harmful components often involves expensive processes. Chemical treatments, for instance, may employ hazardous substances to oxidize organic matter, generating substantial volumes of secondary sludge and thereby introducing additional forms of pollution (España-Gamboa et al. 2011; Jiang et al. 2012; Ahmed et al. 2018).

Using microalgal cultures to bioremediate waste holds considerable promise for both waste management and the algal biomass production sectors. Microalgae, with their high photosynthetic

efficiency and rapid growth rates, demonstrate significant potential for effective remediation (Olguín 2003). This strategy has the potential to contribute to sustainable waste management while fostering the production of high-quality food at lower costs. The transformation of non-desired waste into valuable algal biomass serves as an excellent illustration of resource efficiency and circular economy principles, making it a win-win approach.

The dairy industry – Whey permeate

The dairy industry in Canada produces more than 500 million kilograms of cheese per year, accounting for 38 % of the total milk that is transformed (Statista Canada 2023). The by-product of cheesemaking is whey, a creamy white liquid containing high concentrations of lactose and protein, that constitutes 90 % of the initial milk volume (Confectionery Production 2016; Trivino et al. 2016; Coopérative Agropur 2021). Whey can be processed again for further use, notably by ultrafiltration, to obtain concentrated whey protein, a valuable product for the dairy, food, and pharmaceutical industries (Trivino et al. 2016). The permeate of that ultrafiltration, whey permeate (WP), is predominantly composed of lactose, often reaching concentrations of up to 70 % or more. It contains varying protein levels, some phosphorus (P), and organic nitrogen (N), with a DIN:DIP (dissolved inorganic nitrogen and phosphorus) ratio of 1:4.3. The dairy waste also contains vitamins and elements such as potassium, calcium, and sodium (Zall 1992; Danalewich 1998; Durham 2009; Confectionery Production 2016).

Whey permeate's high lactose content makes it suitable for different applications, including fermentation for methane/alcohol production and baked goods, mixes, and sauces (Zall 1992; Coopérative Agropur 2021). Its uses are, however, limited. Drying it for lactose powder is costly, and cheese production greatly exceeds the few uses for WP. Consequently, a significant portion is discarded as fertilizer on land or as waste (Marwaha and Kennedy 1988; Zall 1992; Tsakali et al. 2010). Exploring creative and sustainable methods for using WP is crucial to minimize waste and optimize resource utilization in the dairy sector. Whey permeate presents a global challenge for the industry, demanding effective disposal solutions (Marwaha and Kennedy 1988). Given its nutrient-rich composition, WP is a prospective substrate for algal growth.

1.4. Microalgae and organic matter

Mixotrophy in cultures

To cultivate microalgae using media amended with organic carbon (C) substrate such as that offered by WP, it is essential to understand the potential metabolic modes. Photosynthesis requires inorganic C, like CO_2 or bicarbonate, as substrates. However, when labile organic compounds are present, some microalgae species can transition from photoautotrophic to mixotrophic growth, combining both photosynthesis and heterotrophy (Ceron Garcia et al. 2006), and in rarer cases, they may adopt heterotrophic growth alone. An alga's capacity to remediate organic-rich waste – and so generate valuable biomass – relies on its ability to absorb and utilize the organic substrates, thus facilitating either mixotrophic or heterotrophic growth. Mixotrophic metabolism in cultures is well-documented. Mixotrophy can significantly boost the productivity of biomass in cultures and, for certain species, can increase the cellular content of valuable compounds, like FAs, when compared to photoautotrophic cultures (Ceron Garcia et al., 2006; Heredia-Arroyo et al. 2010; Ummalyma and Sukumaran 2014; Bashir et al. 2019; Baldisserotto et al. 2021).

Mixotrophy in the oceans

While mixotrophic metabolism is well-documented and extensively researched in cultures, it remains a vital ecological trait among marine microalgal groups. Surprisingly, this globally distributed trait has yet to receive the level of attention it deserves in ocean ecosystem research. Most ocean and climate change models still adhere to a simplistic binary classification, distinguishing organisms as either phytoplankton or zooplankton. However, there is an expectation that mixotrophy in the oceans could have far-reaching effects on higher trophic levels (McManus et al. 2023). In natural ecosystems, we observe various possible metabolic modes, including photoautotrophy, mixotrophic phagotrophy, mixotrophic osmotrophy, and heterotrophy. They refer, in turn, to growth solely by photosynthesis C acquisition, growth by combined photosynthetic and heterotrophic C acquisition through consumption of particles (phagotrophy) or dissolved organic substrate (osmotrophy), and growth solely by consumption of organic C. It is imperative to incorporate these diverse metabolic modes into biogeochemical models to understand the environmental drivers of food webs and, potentially, to enhance our ability to predict phenomena like Harmful Algal Blooms. Understanding the diverse metabolic modes observed in natural ecosystems, including the potential for mixotrophic growth, becomes particularly relevant in the context of this research project, which aims to cultivate microalgae using organic substrate, potentially promoting mixotrophic growth strategies.

1.5. Research objectives

The main objective of this research is to assess biomass composition and productivity rates in marine microalgal cultures cultivated using whey permeate, with the goal of developing a sustainable method for efficient remediation by recycling WP nutrients through algal cultivation. Striking a balance between these two objectives is essential, as the cost of remediation can only be justified by increasing biomass production rates and, thus, the commercial profitability of algal biomass.

To reach these objectives, specific targets have been defined:

- Identify an optimal formulation for WP solution that ensures the availability of essential growth nutrients (C and P) for the algae – Chapter 2;
- Compare mixotrophic growth of four species of microalgae (*Pinguiococcus pyrenoidosus*, *Chaetoceros muelleri*, *Tetraselmis suecica*, and *Chroomonas mesostigmatica*) in WP-amended media with photoautotrophic cultures in regular media ± dissolved inorganic C, in stationary- and late exponential-phase of growth – Chapter 3;
- Analyze photosynthetic parameters to gain insights on potential shifts in metabolic processing in WP media. – Chapter 3;
- Analyze nutrient uptake by comparing initial dissolved inorganic nutrients in the medium with final particulate nutrients in the cultures (C, N, P) to gain insights on remediation efficiency – Chapter 3;
- Analyze biomass composition and calculate biomass productivity rates of total fatty acids, EPA, and particulate N as a proxy for proteins to help identify strains of microalgae and conditions in which biomass production is maximized – Chapter 3.

I hypothesized that species with ready access to organic C (lactose) and P in WP will have higher yield rates of proteins and valuable FAs. The most rapid rates of biomass productivity are expected in cultures harvested during exponential phase of growth (i.e. in nutrient-repleted conditions). Additionally, it is hypothesized that cultures amended with WP will display more complete remediation and higher biomass productivity rates to cultures in regular media. Cultures in WP media are likely to down-regulate their photosynthetic apparatus during mixotrophic growth, resulting in reduced light absorption per nutrient assimilated and biomass produced. This is a critical factor in determining the standing stock in a photobioreactor when growing microalgae at scale. The outcomes will likely depend on the species of microalgae cultivated, the concentration and composition of WP, and the environmental conditions of the experiments.

Chapter 2: Optimizing whey permeate powder as a substrate for algal growth: testing preparations, concentrations, and transformations.

Abstract

Whey permeate (WP), a by-product of cheese making often discarded as waste, holds potential as a substrate for algal growth, offering a promising avenue to remediate dairy waste and reduce the production costs of valuable algal biomass. This research aims to identify a suitable method for preparing WP powder and integrating it into culture media. The series of experiments show the dynamics of algal growth in various prepared WP-amended media. Autoclaving WP dissolved in NaOH revealed that browning reactions (Maillard reaction and/or caramelization) significantly support algal growth, particularly when 1 M NaOH is employed. pH-adjustment experiments underscored the pivotal role of pH levels, with cultures at pH 7 exhibiting optimal biomass. Furthermore, storing WP media for seven months enhanced *T. suecica*'s growth, possibly through calcium-phosphate resolubilization. The choice of NaOH as a solvent influenced phosphorus availability during autoclaving. An abiotic experiment with light exposure explored WP degradation and sterilization by autoclaving. Finally, *C. mesostigmatica* growth in WP media with a headspace in closed tubes demonstrated superior growth rate and yield, emphasizing the critical role of gas exchange in closed systems. These observations reveal the effects of nutrient availability, pH, aging, and gas exchange on algal cultivation within WP-based media. These set the stage for larger-scale experiments in Chapter 3 aimed at characterizing algal biomass and nutrient uptake.

2.1. Introduction

2.1.1. Context dairy waste: whey permeate

The dairy industry is a significant sector responsible for valuable dairy products but also generates significant waste. Whey permeate (WP) is a by-product of ultrafiltration of liquid whey, a cheese production residue (Marwaha and Kennedy 1988; Zall 1992). The procedure is used for deproteinization, removing most of the proteins from the whey, although a significant portion remains in the permeate. Liquid WP contains no more than 6 % solids (Durham 2009). When dehydrated, most of the powder is lactose, often reaching concentrations up to 70 % or more of the total dry weight. The protein content in dry WP can vary between cheese manufacturers, typically from 0 to 5 % of the mass, but it can be as high as 15 % (Zall 1992; Durham 2009; Confectionery Production 2021). The P content fluctuates between 0 and 20 % (Zall 1992; Durham 2009), with primary P forms being orthophosphates, polyphosphates, and organically bonded P (Danalewich 1998). Organic N is also present in the dairy waste (Danalewich 1998). Whey permeate may contain significant amounts (> 0.5 %) of elements such as calcium, potassium, and sodium, with others in smaller amounts (< 0.5 %) like iron, magnesium, and zinc (Zall 1992). Additionally, WP contains eighteen amino acids, as well as vitamins such as riboflavin and thiamin (B1) (Zall 1992; Confectionery Production, 2016). The composition of WP varies with factors such as cow diet, cheese manufacturer practices, the permeate extraction method, and the type of porous ultrafiltration membrane used (Zall 1997).

Whey permeate is used commercially as a fermentation feedstock, and refined or hydrolyzed lactose products derived from it are integrated into baked goods, dry mixes, soups, and sauces (Marwaha and Kennedy 1988; Coopérative Agropur 2021). Despite these applications, its use is minor compared to its production in cheese making, leading to a large portion being inevitably discarded as waste (Zall 1992; Tsakali et al. 2010). Whey permeate is a promising substrate for commercial microalgal cultures due to its properties. Abundant in inorganic P, it could support photoautotrophic growth, while its substantial lactose content offers the potential for mixotrophic growth via organic C assimilation. Utilizing WP to enhance microalgal cultivation has proven successful, often yielding increased lipid and protein content along with overall biomass in cells when introduced to the culture medium (Abreu et al. 2012; Espinosa-Gonzalez et al. 2014; Borges et al. 2016; Mondal et al. 2016; Vieira Salla et al. 2016; Girard et al. 2017; Salati et al. 2017; Nham et al. 2023). Most studies have used fresh/liquid WP from the dairy industry, demonstrating its favorable characteristics as a substrate. This study explores the use of dehydrated WP as a nutrient supply, expanding the potential applications of this waste product.

2.1.2. Technical considerations for commercializing algal biomass using WP

Whey permeate can be obtained in two forms: as a liquid after the whey ultrafiltration process or as a dehydrated powder. The dehydration is expensive, and the current applications for WP do not justify the cost (Domínguez-Niño et al. 2017). However, producing valuable algal biomass could provide a compelling reason to consider this investment. In a commercial context, there are two main approaches to utilizing dairy waste for large-scale microalgal culturing. One method involves situating an algal facility next to or near a cheese factory, where the liquid WP could be transported through pipes directly to the facility. Alternatively, the WP could be dehydrated and then transported to the culturing facility. The choice between these approaches depends on transport efficiency and the cost/benefit of dehydration versus biomass production's increased value.

Prior microalgal studies using WP to supplement nutrients predominantly used it in liquid form (Kothari et al. 2013; Girard et al. 2014; Ummalyma and Sukumaran, 2014; Mondal et al. 2016; Girard et al. 2017; Nham et al. 2023). This liquid WP obtained freshly from the dairy factories, was refrigerated before being integrated into the culture media. Typically, liquid WP has an acidic pH ranging from 5.5 to 6.8 (Mondal et al. 2016; Girard et al. 2017; Nham et al. 2023). The feasibility of commercializing biomass products using fresh liquid WP largely depends on the proximity of the cheese factory and the algal facility, which may present logistical challenges. This study explores the potential of using dehydrated WP as an algal growth substrate. Efficient dissolution of the powder is facilitated by using an alkaline solvent such as sodium hydroxide (NaOH), mainly due to substantial components like residual proteins and peptides that have higher solubility at high pH. Exploring further processing of WP powder becomes crucial to optimize its applicability in algal cultivation.

2.1.3. Alteration of WP during solubilisation and sterilization

Sterilization is essential to preparing a WP solution for amending the culture media. Autoclaving was chosen due to its straightforwardness and reliability. However, during this autoclaving step, a cascade of reactions can be initiated when WP interacts with an alkaline environment at high temperatures, resulting in the browning of the solution. The browning could stem from caramelizing the sugar (lactose) due to heat or could also arise from Maillard reaction products (Zall 1992; Lund and Ray 2017). Given the calcium content in WP, the autoclaving process could also induce precipitation of calcium phosphate, potentially decreasing P available for algal growth (Fairbrother 1991).

Using NaOH as a solvent to dissolve WP powder results in elevated media pH, with a pH of approximately 10 in a media amended with 0.5 g L^{-1} WP. pH plays a role in influencing the composition of dissolved inorganic C in the media. At pH 7, there is a higher concentration of carbon dioxide (CO_2) compared to higher pH levels, where CO_2 is converted to bicarbonate (Henderson 1908). Many marine microalgae have evolved carbon-concentrating mechanisms (CCMs) to manage and utilize the available forms of inorganic C in their environment (Badger et al. 1998). Additionally, pH can directly impact algal growth by reducing growth rates and biomass yields or altering cell membrane properties (Taraldsvik and Myklestad 2000). The pH at which growth becomes limited varies depending on the cultivated species (Lundholm et al. 2004; Oberlander et al. 2023).

2.1.4. Algal and bacterial cultures

This study primarily focuses on utilizing the green alga *Tetraselmis suecica* CCMP9306 for the series of tests on WP due to its favourable attributes, such as high growth rate, ease of cultivation, and widespread use as an aquaculture feed. *T. suecica* is versatile and can grow across a broad pH range, which makes it a suitable candidate (Almutairi and Toulibah, 2017). Tests involving *Chroomonas mesostigmatica* CCMP1168 were also conducted in WP media, with cultures confined within closed tubes.

The stock cultures used were bacterized so the bacterial community associated with the alga coexisted in the culture medium. The presence of organic matter in WP can enhance the heterotrophic bacterial population, competing for resources and thereby influencing the algal population dynamics (Nham et al. 2023). On the other hand, growth-promoting bacteria may impact algal growth by increasing their biomass and lipid production (Liu et al. 2020) or by degrading organic matter (Arora et al. 2012).

2.1.5. Objectives of the Chapter

The main objective of this study is to identify a suitable method for preparing WP as a nutrient supply for algal cultures. To achieve this goal, several sub-objectives were established:

- Test the most effective NaOH concentration for dissolving WP powder.
- Investigate the sterilization techniques used while preparing the WP, focusing on the effects of autoclaving on dissolved nutrients and the extent of browning reactions during the process.
- Assess the influence of the initial pH of the media on algal growth in both WP- and lactose-amended media, serving as a comparison to WP.

- Assess the effect of pH on the abundance of bacterial and algal cells in the cultures.
- Evaluate how the age of WP media might influence algal growth.
- Explore light exposure to test its potential for enhancing nutrient availability in WP-amended media.
- Test the effect of adding a headspace to cultures growth in closed systems.

2.2. Material & Methods

A series of experiments were conducted to explore different formulations of WP solutions and their impact on algal growth. Each experiment involved the preparation of stock solutions by dissolving 50 g of WP powder (Agropur, Lot# 321190702-22; collected on August 22nd, 2019) in 1 L of solvent. NaOH was selected as the solvent due to its alkaline nature, allowing efficient WP powder dissolution. The stock solutions underwent sterilization through autoclaving using a vacuum steam sterilizer (Lancer LSS 275) in glassware bottles for 45 minutes at 121 °C and a pressure of about 100 kPa (15 PSI). For most of the experiments, some measurements of the solutions were taken before the bioassay inoculation. These included pH measurements using a pH-probe (Thermo Scientific, Orion 2-star pH benchtop), absorbance from 200 to 750 nm using a spectrophotometer (Agilent Cary 4000), and nutrient analyses done by Dr. Douglas Wallace's laboratory at Dalhousie University.

Unless stated otherwise, the bioassays were carried out in 24-well polystyrene culture plates covered with a porous membrane to facilitate gas exchange. These plates were placed inside a sealed, transparent box containing a CO_2-generating system (C-box) on a light table (Dr. Patrick McGinn, personal communication, 2018). The CO_2 was generated from an internal reservoir containing 100 mL of 1 M sodium bicarbonate solution placed next to the culture plate. To maintain atmospheric CO_2 levels, 400 µL of 10 % hydrochloric acid was added daily following monitoring immediately before sealing the box. The cultures were maintained under continuous illumination with an intensity of 80 µmol photons m^{-2} s^{-1} in a temperature-controlled room at 18 °C. Unless stated otherwise, each experiment received its inoculum from a bacterized parent culture maintained in balanced growth (MacIntyre and Cullen 2005) in control medium (L1; Guillard and Hargraves 1993).

Growth in the well plates was monitored with a multimode microplate reader (BioTek, Synergy 4) with Gen5 1.11 software using fluorescence measurements. Fluorescence was monitored daily until the

culture had been in stationary (STA) phase for a time equivalent to three generations during exponential (EXP) growth, following Equation 2.1 (Wood et al., 2005). The growth rates were determined by fitting the growth curve to a modified Blackman model (Jones et al. 2014), modified to include a non-zero intercept and a lag phase in which either there was no growth or growth was undetectable because the signal was below the lower limit of detection of the instrument (Eq. 2.2a, b). The maximum growth rate, μ_{max}, is obtained as the slope of the change in fluorescence in the growth phase (Eq. 2.3). Upon harvest, unless stated otherwise, cell counts were conducted using a hemocytometer (Bright-Line™; Lot# 3110) and a microscope (Leitz dialux 20 EB) at 125 X magnification.

$$t_{gen} = \frac{\ln(2)}{\mu_{max}} \quad \text{(Eq. 2.1)}$$

where t_{gen} is generation time (d) and μ_{max} (d^{-1}) is the maximum specific growth rate observed during EXP phase.

$$F = F_{init} \text{ for } t \leq \lambda \quad \text{(Eq. 2.2a)}$$

$$F = \frac{(F_{max} - F_{init}) \times (t-\lambda) + t_{sat} - |(t-\lambda) - t_{sat}|}{2 \times t_{sat}} + F_{init} \text{ for } t > \lambda, \quad \text{(Eq. 2.2b)}$$

$$\mu_{max} = \frac{F_{max} - F_{init}}{t_{sat}} \quad \text{(Eq. 2.3)}$$

where F is ln-transformed fluorescence at time t (d), F_{init} is the ln-transformed initial fluorescence, F_{max} is the ln-transformed maximum fluorescence (i.e., in STA phase), λ is the duration of the lag phase (d), t_{sat} is the time (d) of the growth phase from λ to cessation of growth (STA phase).

2.2.1. Effect of solvent (NaOH) concentration in WP solutions on algal growth

The first experiment investigated the effect of solvent concentration on nutrient availability in WP solutions and its impact on algal growth. Six WP-NaOH solutions were prepared at 50 g L^{-1} of WP powder in the alkaline solvent and then autoclaved. The NaOH concentrations used were 100, 180, 300, 560, 1000, and 3000 mM, respectively. The pH of the six WP-NaOH solutions was measured before and after autoclaving, as well as after diluting them into the seawater culture media described below. Light absorption (optical density; OD) of the diluted solutions was measured from 250 to 750 nm, and normalized absorbance was obtained as the ratio of absorption to the mean value over the full spectrum to compare the peak's positions. The absorption coefficients (m^{-1} nm^{-1}) were calculated by converting from $\log_{10}$ to $\log_e$ units and correcting for residual scattering and the optical pathlength (Eq. 2.4). Nutrient analyses were conducted to determine the concentrations of dissolved phosphate, nitrite, nitrate, and ammonium based on colorimetric analysis (Whitledge et al., 1981) using a Skalar autoanalyzer.

$$a[\lambda] = \frac{2.3 \times (OD[\lambda] - OD[750])}{d} \quad \text{(Eq. 2.4)}$$

where a[λ] is the absorption coefficient (m^{-1} nm^{-1}) at wavelength λ nm, OD[λ] and OD[750] are the optical densities at wavelength λ and 750 nm (dimensionless), and *d* is the optical pathlength (m).

For the bioassay, the six WP-NaOH solutions were diluted to a final concentration of 2 % (equivalent to 1 g L^{-1} of WP) in a modified L1 seawater culture media (Guillard & Hargraves, 1993). The modified media lacked phosphate but included 200 µM nitrate and L1 concentrations of silicate, trace metals, and vitamins. The control media had 50 µM phosphate added to match the concentration of the WP amendment. The bioassay was carried out in 24-well plates placed inside C-boxes. Each well was inoculated with *Tetraselmis suecica* CCMP906 at a volume ratio of 5 % of the total 1 mL culture per well. Monitoring was done through fluorescence (see above), and cultures were harvested for cell counts once they reached the equivalent of three generations in STA phase.

2.2.2. Effect of pH-adjusted WP-amended media on algal growth

The effect of the pH of WP media on culture growth was tested. Two WP-NaOH solutions were prepared using 100 mM and 1 M NaOH and autoclaved. The WP-amended and control media were prepared as described in Section 2.2.1, except that the WP was prepared with the two concentrations of NaOH. The pH of the media was adjusted to 7, 8, 9, and 10 using sterile-filtered (Sarstedt filtropur S 0.2) 10 % hydrochloric acid and 1 M NaOH. *T. suecica* culture was inoculated into 24-well plates, each of the wells containing one of the twelve prepared media. The plates were placed inside C-boxes, and the cultures were monitored daily (see Section 2.2.1). On harvest, cultures were sampled, and cell counts were conducted.

2.2.3. Effect of pH-adjusted lactose- and WP-amended media on growth of *T. suecica* and bacteria

A follow-up experiment on pH was conducted to assess the effect of WP- and lactose-amended media on both algal and bacterial growth. The WP solution was prepared by dissolving 50 g L^{-1} WP powder in 1 M NaOH, followed by autoclaving. The lactose solutions were prepared using Alpha-D-lactose monohydrate (ACS Thermo Scientific, Lot: Y091011). One lactose solution contained 50 g L^{-1} lactose in E-pure water and was subsequently autoclaved. A second lactose solution had the same concentration but was autoclaved in a volumetric flask before being solubilized in E-pure. The absorbance of the solutions

was measured from 200 to 700 nm after dilution with E-pure water, and absorption coefficients (m^{-1} nm^{-1}) were calculated following Equation 2.4.

Solutions of lactose and WP, with a concentration of 0.5 g L^{-1}, were added to a modified L1 seawater culture media as described in Section 2.2.1, except that nitrate was added at 176.4 µM. The control and lactose media were supplemented with 72.4 µM phosphate instead of the WP amendment. Before inoculation, all media were adjusted to pH 8, 9, and 10, as described in Section 2.2.2. The bioassay was conducted in 24-well plates placed inside C-boxes. Half of the wells were inoculated with a xenic culture of *T. suecica* and bacteria, while the other half were inoculated with only the associated bacteria. Algae were filtered out effectively using Whatman GF/F filters (effective pore size 0.7 µm). Algae were monitored until STA phase through fluorescence (see above), while bacteria were monitored using absorbance at 600 nm with the same multimode microplate reader (BD Synergy 4 with Gen5 1.11 software).

Cultures were harvested, and biomass yields were assessed from cell counts and chlorophyll-*a* (Chla) concentration. Chla concentrations were determined according to Welshmeyer (1994) using DMSO: 90 % Acetone (3:2) as the extraction solvent (Shoaf and Lium 1976). The fluorometer (Turner Designs 10-005R) was calibrated with purified Chla (Sigma C6144). Cell counts were made with a BD Accuri™ C6 flow cytometer with BD CSampler Plus software after the cells were stained with the DNA stain SYBR Green (Gasol and Del Giorgio 2000). Accurate counts could not be obtained on the WP-amended cultures because the cells formed irregular clumps (see below). Bacterial and algal counts were differentiated based on particle size and scatter (Marie et al. 2005). Cells counted by epifluorescence microscopy were also stained with SYBR Green, collected on AMD polycarbonate filters (pore size 0.22 µm), and viewed with 3.5 µL of immersion oil under the cover slip. Microscope pictures were taken at 200X magnification using a Leica microsystem (CMS Gmbh; DFC365 FX; Serial no. 0767390416) microscope and a mobile phone camera.

2.2.4. Testing algal growth in WP media in successive cultivation

After evaluating different preparations of WP to amend the media in well-plate cultures, a tube experiment was conducted to assess the feasibility of growing cultures on a larger scale for biomass characterization. The WP-amended medium was prepared as described in 2.2.1, except that nitrate was added at 220.5 µM. The culture of *T. suecica* was inoculated in a 40-mL borosilicate closed tube.

Monitoring was carried out daily by measuring dark-acclimated fluorescence in the growth tube with a Turner Designs 10-005R fluorometer and Fluorescence Induction and Relaxation (FIRe) system (Satlantic, FIRe, Serial no: 031). The batch culture was monitored until it reached STA phase (see Section 2.2.1). It was then used to inoculate a second tube that was grown into STA phase and then used to inoculate a third. For each transfer, samples were collected for cell counts for comparison with the STA-phase fluorescence.

2.2.5. Effect of solvent and autoclaving on P forms in WP solutions

An abiotic experiment was conducted to analyze P speciation in WP solutions with autoclaving. Two WP solutions were prepared and autoclaved, one using 1 M NaOH as the solvent and the other using E-pure water as the solvent. Particulate P was measured before and after autoclaving by filtering the solutions on 25 mm GF/F filters and analyzing them according to Solórzano and Sharp (1980). Dissolved P was measured from the filtrate using the same method. The total P detected was calculated as the sum of the particulate and dissolved concentrations.

2.2.6. Effect of aging on algal growth in WP-amended media

The growth of *T. suecica* was tested in aged WP from three different time points, autoclaved once or twice in Pyrex bottles. The WP solutions were prepared as described in Section 2.2.1. The test media were fresh (0-month-old: mo) WP autoclaved once, 0 mo WP autoclaved twice, 7 mo WP, and 16 mo WP solutions. The aged-WP solutions were autoclaved once after preparation and were stored until use at 4 °C. The media were prepared as described in Section 2.2.1, except that nitrate was added at 880 µM. Control media had 36.2 µM phosphate instead of the amendment. Cultures were grown in 24-well plates placed inside C-boxes and were monitored for fluorescence until STA phase. On harvest, samples were taken for cell counts and Chla concentration measurements (see above).

2.2.7. Effect of visible light on WP-amended media on algal growth

The growth of *T. suecica* was tested in WP media that had been partially bleached by exposure to visible light. The medium was prepared as described in Section 2.2.4. The media-filled 40-mL borosilicate tubes were exposed to continuous illumination at 80 µmol photon m^{-2} s^{-1} on a light table for a duration of 5 days. One tube was harvested each day to measure absorbance, particulate C, N, P, and dissolved P.

Absorbance spectra were measured on the whole media from 250 to 750 nm, and absorption coefficients were obtained per Equation 2.4. For particulate C and N analyses, media samples were filtered onto pre-combusted Whatman GF/F filters (21 mm diameter), rinsed with 10 mL of 0.22 µm-filtered seawater, and subsequently dried in an oven at 60 °C (Fisher Scientific; Isotemp). The dried samples were then pelleted into combustion foils. Particulate C and N masses were determined following combustion using a Costech ECS 4010 analyzer (Costech Analytical Technologies Inc.). The standard curve was prepared using acetanilide (Sigma 112933). Particulate and total dissolved phosphorus were determined using the method of Solorzano and Sharp (1980).

2.2.8. Effect of headspace in closed tubes for gas exchange on algal growth

The final experiment focused on the effect of gas exchanges on algal mixotrophic growth. A WP-NaOH solution was prepared as described in Section 2.2.4. A culture of *Chroomonas mesostigmatica* CCMP1168 was inoculated into two 60-mL borosilicate closed tubes. One tube was filled with 60 mL of media without any headspace, while the other was filled with 55 mL of media, leaving approximately 7 mL of headspace. Algae were added in a proportionate volume to the media in both tubes. Growth was monitored through fluorescence measurements, and samples were collected for cell counts once the culture reached STA phase.

2.2.9. Data and statistical analyses

Growth curves were constructed by fitting daily measurements of chlorophyll fluorescence with the modified Blackman model (Eq. 2.2a,b). To test for significant differences, analyses of variance (ANOVA) were performed using a significance level of $p = 0.05$ in Microsoft Excel. Post-hoc Tukey HDS tests were used to compare between treatments. One- and two-way ANOVA tests, as appropriate, were used to test for differences in pH, F_{max}, μ_{max}, Chla concentration, and fluorescence per cell. The results presented are averages of biological replicates and standard deviations (SD).

2.3. Results

2.3.1. Effect of solvent (NaOH) concentration in WP solutions on algal growth

Different concentrations of the alkaline solvent NaOH were tested to dissolve WP powder prior to its use as a substrate for algal growth. The solutions were prepared with 50 g WP L^{-1} into 100, 180, 300, 560, 1000, and 3000 mM NaOH. The variation in pH of each WP-NaOH solution is shown at each step of media preparation (Figure 2.1). Prior to autoclaving, the pH was high across all treatments, with an estimated average of 12.9 ± 0.5. Note that this was obtained by extrapolation as the pH meter was calibrated with two buffers at pH 7 and 10. After autoclaving, a significant drop in pH was observed for the three least alkaline treatments (100-, 180-, and 300-mM NaOH), averaging 7.14 ± 0.73. In contrast, the three most alkaline treatments (560-, 1000-, and 3000-mM NaOH) showed no change, with an average pH of 13.3 ± 0.3, which was much higher compared to the least alkaline treatments ($p < 0.001$). This dissimilarity in pH measurements between low- and high-NaOH treatments persisted when the WP solutions were added to seawater media. Low-NaOH treatments had a low pH of 7.05 ± 0.1, while high-NaOH treatments decreased to a pH of 9.98 ± 0.43 but were still significantly higher than for low-NaOH treatments ($p < 0.001$).

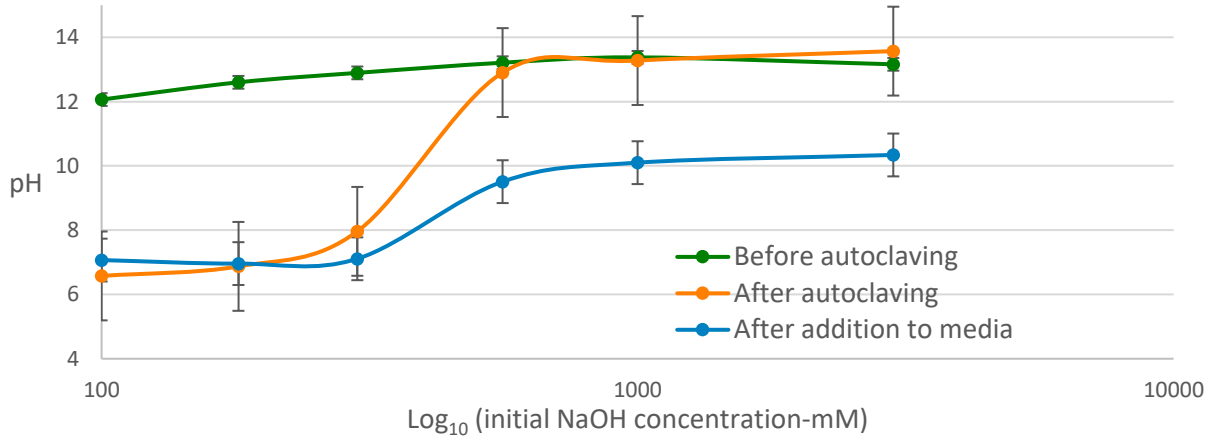

Figure 2.1. pH measurements (mean ± SD; n = 3) of WP solutions (50 g L^{-1}) dissolved in different NaOH concentration before and after autoclaving the solutions and following addition to seawater media at 1 %.

After autoclaving, all solutions developed a deep black colour with orange tinges, and the colour was more pronounced with higher NaOH concentration. The absorbance spectra from 250 to 750 nm of WP-NaOH solutions are shown in Figure 2.2-A. Spectra have been normalized to the mean value over the full range to emphasize differences in the position of peaks. In the three low-NaOH treatments, a dominant absorbance peak was observed at 267 nm, with a smaller feature around 340 nm. The three high-NaOH

treatments also had high absorption at 267 nm but had a second overlapping peak at about 285 nm. The absorption coefficient, a proxy for the height of the absorption peak at different NaOH concentrations, is shown in Figure 2.2-B. There is an observed increase in the 267-nm peak with increased NaOH concentration. There is also a shift to a higher peak (285 nm) in the high-NaOH solutions.

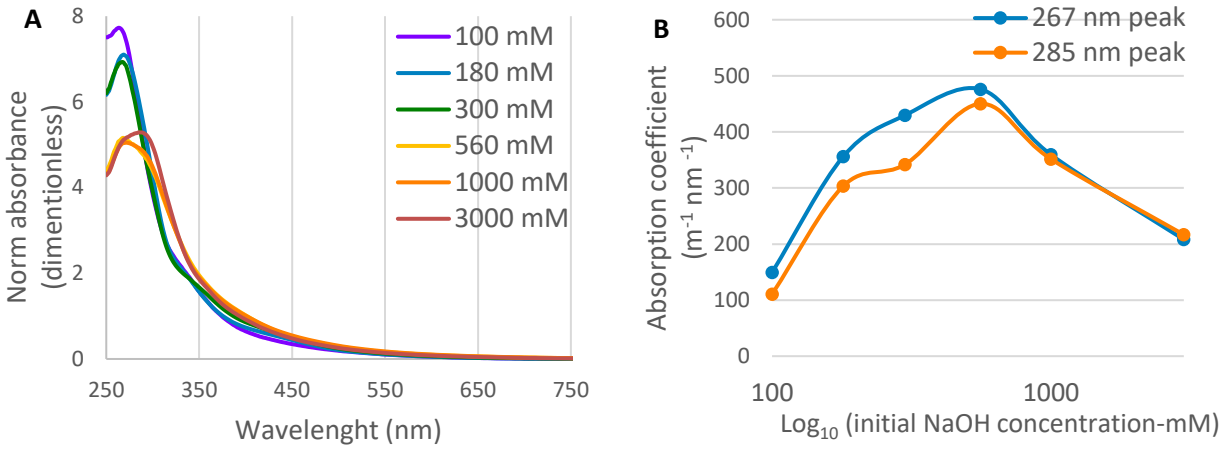

Figure 2.2. Normalized absorbance spectra from 250 to 750 nm (A) and absorption coefficient at peaks 267 nm and 285 nm (B) of autoclaved WP solutions (50 g L^{-1}) dissolved in different concentrations of NaOH (mM).

Nutrient analyses were performed on 1 % diluted WP-NaOH solutions for the 100-, 300-, and 1000-mM treatments before autoclaving, as well as for all treatments after autoclaving. The measured nutrients included phosphate and nitrogen species, specifically nitrite, nitrate, and ammonium. As shown in Figure 2.3, phosphate concentrations before autoclaving showed an increasing trend, increasing by almost 10 µM over the range of NaOH concentrations. Nitrite and nitrate were below the limit of detection (data not shown), and ammonium was low but consistent across concentrations before autoclaving. All nitrogen speciation was low but detectable after autoclaving. Samples of 3000 mM intended for phosphate analyses after autoclaving were compromised, and results were omitted.

After autoclaving, both phosphate and ammonium showed a similar pattern, where the nutrient concentrations of the low-NaOH treatments decreased with increasing NaOH to 300 mM and then showed an increase. Phosphate and ammonium concentrations were significantly higher for the high-NaOH compared with the low-NaOH treatments ($p < 0.01$). Phosphate did not exceed the pre-autoclaving concentrations at high NaOH, but ammonium concentrations did (Figure 2.3).

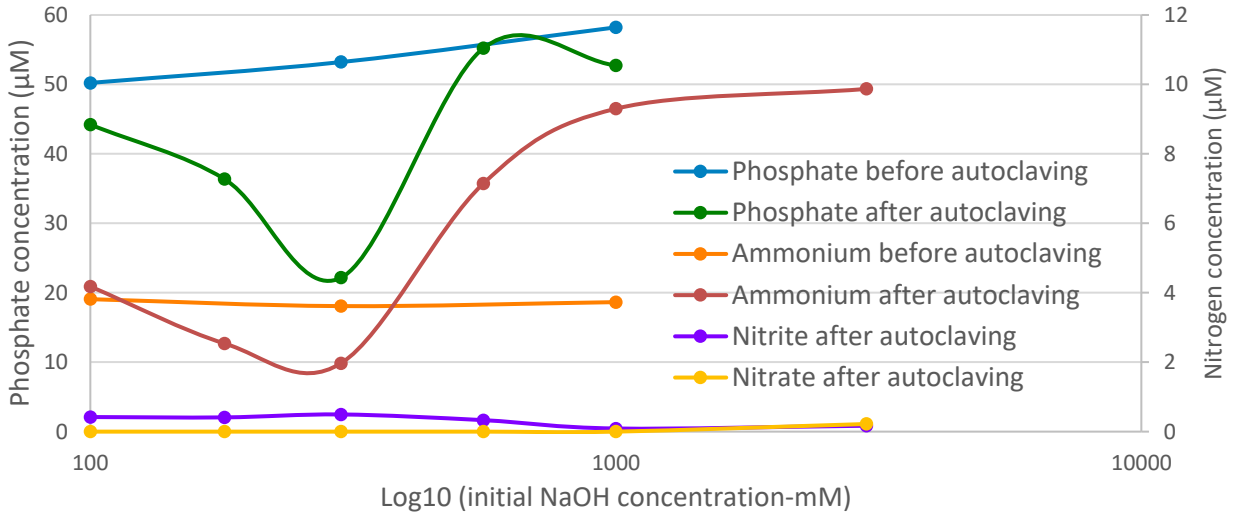

Figure 2.3. Nutrient concentrations (mean ± SD; n = 2) of dissolved phosphate and nitrogen species (nitrite, nitrate, ammonium) in WP solutions (0.5 g L^{-1}) dissolved in different NaOH concentrations before and after autoclaving.

The fluorescence-based growth curves for *T. suecica* batch cultures in control and WP media prepared using 100 mM and 1 M NaOH, the lowest and second-highest concentrations tested above, are shown in Figure 2.4. There were clear differences in fluorescence-based final yields, F_{max}, and reduced apparent maximum growth rates, μ_{max}, in cultures grown in WP-amended media. When compared across cultures, the patterns in both F_{max} and μ_{max} were broadly consistent with differences in absorption at 285 nm and nutrient concentrations in the media. Both parameters were low at 100-300 mM NaOH and then rose at higher concentrations (Figure 2.5-A-B). The control cultures had the highest μ_{max} at 1.55 d^{-1} ($p < 0.01$), followed by the 560- and 3000-mM treatments, which grew at rates of 0.94 and 0.89 d^{-1}, respectively ($p < 0.001$). Treatments 100-, 180-, 300-, and 1000-mM had slower apparent growth rates ($p < 0.01$), with μ_{max} values from 0.09 to 0.68 d^{-1}.

Consistent with the fluorescence-based estimates for yield, WP-amended cultures with 1 M NaOH had a higher final cell concentration than control cultures ($p < 0.05$), and they were both significantly higher than all other treatments ($p < 0.01$; Figure 2.5-C). There was no strong agreement between the two estimates of yield because fluorescence per cell was found to be higher in WP cultures with 1 M NaOH than in the other treatments ($p < 0.01$), although not significantly higher than controls ($p > 0.05$; Figure 2.5-D). These findings highlight the significant effect of NaOH concentration on the growth of *T. suecica* in WP media, with 1 M NaOH being the optimal concentration for achieving high biomass yield.

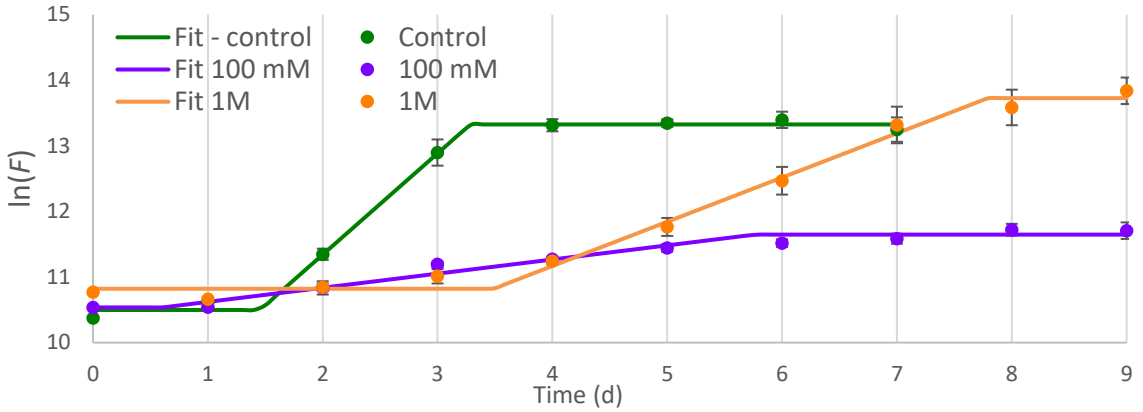

Figure 2.4. Growth curves, as ln-transformed fluorescence, showing data points (•; mean ± SD; n = 3) and fits to Equation 2.2 (–), of batch cultures of *T. suecica* grown in 24-well plates in control (without NaOH) and WP-amended media (0.5 g L^{-1}) prepared with 100 mM and 1 M NaOH.

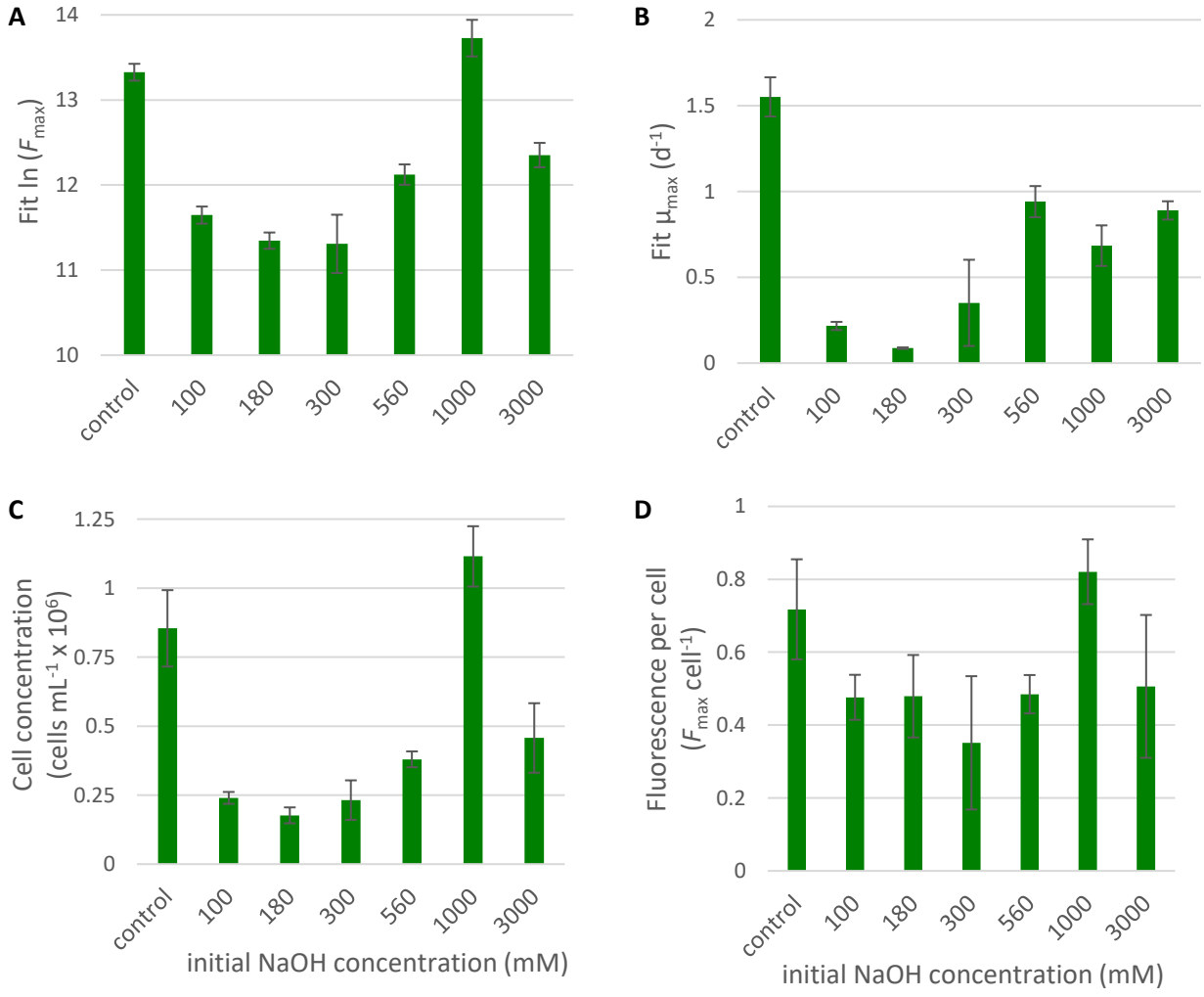

Figure 2.5. Fitted values of F_{max} (A) and μ_{max} (B) from Equation 2.2, final cell concentration (C), and final fluorescence per cell (D) (mean ± SD; n = 3) of batch cultures of *T. suecica* grown in 24-well plates in control and WP media (0.5 g L^{-1}) prepared with different NaOH concentrations.

2.3.2. Effect of pH-adjusted WP-amended media on algal growth

The effect of the initial pH of the media on batch culture growth of *T. suecica* was investigated in both control and WP media prepared with 100 mM and 1 M NaOH. The fitted fluorescence-based growth curves of the cultures at pH 10 are shown in Figure 2.6. Apparent yields were reduced in the WP-amended media. Control cultures reached a higher F_{max} compared to WP cultures across all treatments, except for cultures in the 1 M treatment at pH 7, which had the highest F_{max} ($p < 0.001$; Figure 2.7-A). Cultures in WP media with 1 M NaOH had a higher F_{max} compared with those with 100 mM ($p < 0.001$), consistent with higher nutrient availability at the higher concentrations (Section 2.3.1). Maximum fluorescence did not have significant variation across pH for both control and 100 mM treatments ($p > 0.05$). Similarly, no significant variations in F_{max} were observed for the 1 M treatment at pH 8, 9, and 10 ($p > 0.05$).

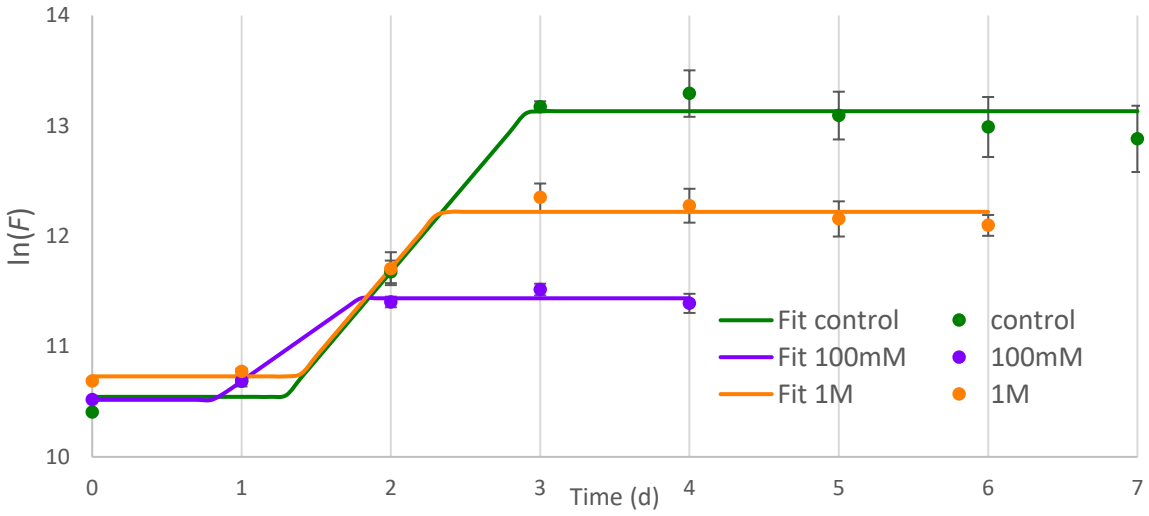

Figure 2.6. Growth curves, as ln-transformed fluorescence, showing data point (●; mean ± SD; n = 4) and fits to Equation 2.2 (–), of batch cultures of *T. suecica* grown in 24-well plates in control and WP media (0.5 g L^{-1}) prepared with 100 mM and 1 M NaOH at initial pH of 10.

The apparent maximum growth rate (μ_{max}) was higher for the control and 1 M treatment, with fitted values above 1.1 d^{-1}, while the 100 mM treatment had growth rates below 1 d^{-1} ($p < 0.001$; Figure 2.7-B). Among the different pH levels, cultures in the control media at pH 10 had faster growth ($p < 0.05$), as did cultures in the 100 mM media at pH 9 and 10 ($p < 0.01$). No significant differences in growth rate were observed across pH levels for the 1 M treatment ($p > 0.05$). It is important to note that the growth rates for WP cultures are based on two data points since they reached STA phase in approximately one day. Therefore, estimated growth rates are poorly resolved and might have been under- or over-estimated, especially in WP-amended cultures.

When harvested in STA phase, the cell concentration showed a similar trend as F_{max} (Figure 2.7-C). The cell concentration was significantly higher for the control and WP with 1 M NaOH treatments adjusted to pH 7 ($p < 0.01$). Additionally, final cell concentration was higher for the 1-M NaOH treatment at pH 10 than pH 9, and higher than at all pH levels in the 100-mM treatment ($p < 0.01$). The similarities in trends are consistent with the relatively low variability in per-cell fluorescence in STA phase (Figure 2.7-D) in all cultures except the cultures in WP media with 1 M NaOH adjusted to pH 7 ($p < 0.01$). All other treatments showed similar and lower fluorescence per cell ($p > 0.05$). These findings suggest that the NaOH concentration used to prepare the WP amendment has a higher impact on the growth of *T. suecica* than the pH to which the media are adjusted following the addition of the amendment.

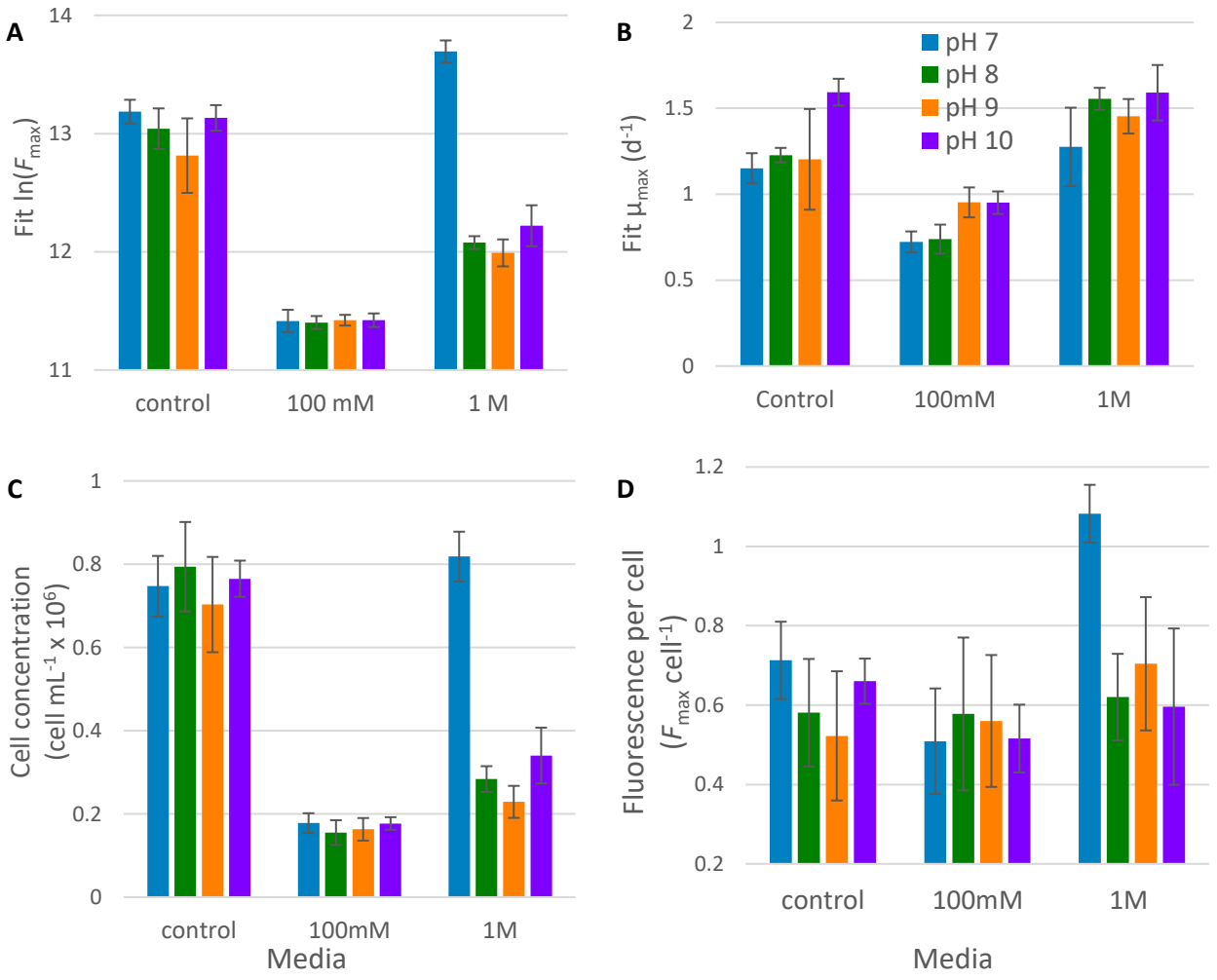

Figure 2.7. Fitted values of F_{max} (A) and μ_{max} (B) from Equation 2.2, final cell concentration (C), and final fluorescence per cell (D) (mean ± SD; n = 4) of batch cultures of *T. suecica* grown in 24-well plates in control and WP media (0.5 g L^{-1}) prepared with 100 mM and 1 M NaOH adjusted to pH 7, 8, 9, and 10 after autoclaving.

2.3.3. Effect of pH-adjusted lactose- and WP-amended media on growth of *T. suecica* and bacteria

To gain further insights on the influence of pH on cultures, an experiment was conducted with pH adjustments to 8, 9, and 10 in control, purified lactose- and WP-amended media. The lactose source, serving as the organic C component alone, was either autoclaved in solution or dry-autoclaved and then put into solution. The primary objective of this experiment was to assess the capacity of *T. suecica* and its bacterial community, independently and with the algal culture, to utilize lactose in each media. Figure 2.8 presents the absorption coefficient spectra from 200 to 700 nm of lactose before and after autoclaving, for comparison with WP solution diluted 0.1 % in E-pure water. All solutions show an absorbance peak around 275-285 nm, with minimal absorption observed for lactose in solution before autoclaving. In contrast, for the three other solutions, the peak was significant. Additionally, lactose solutions after autoclaving show another peak around 230 nm, which is not present in the WP solution.

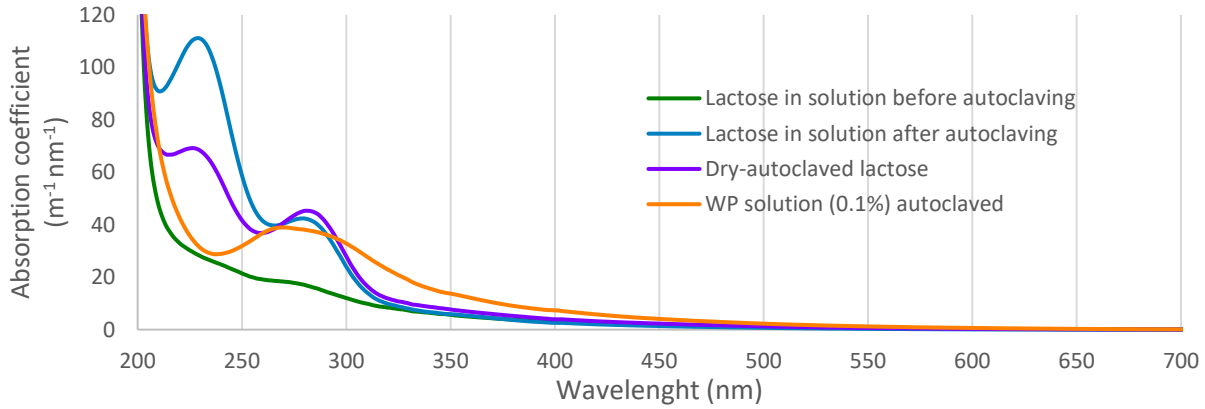

Figure 2.8. Absorption coefficient spectra of purified lactose and WP solutions (50 g L^{-1}): Lactose in E-pure before autoclaving, lactose in E-pure after autoclaving, lactose autoclaved dry, and WP in NaOH autoclaved diluted 0.1 % into E-pure.

Fluorescence-based growth curves of *T. suecica* in control, lactose autoclaved in solution, dry-autoclaved lactose, and WP-amended media, all adjusted to pH 10, are shown in Figure 2.9. Cultures in control media, media with lactose autoclaved in solution, and WP had high and similar F_{max} values across the pH to which the media were adjusted ($p > 0.05$; Figure 2.10-A). In contrast, the cultures amended with dry-autoclaved lactose media showed lower F_{max} in STA phase, particularly at pH 8 ($p < 0.01$). The apparent growth rates for control cultures and cultures in media amended with lactose autoclaved in solution or with WP were similar ($p > 0.05$), with fitted μ_{max} values ranging from 1 to 1.5 d^{-1} (Figure 2.10-B). However, the estimated μ_{max} was significantly lower for dry-autoclaved cultures at pH 8 ($p < 0.01$).

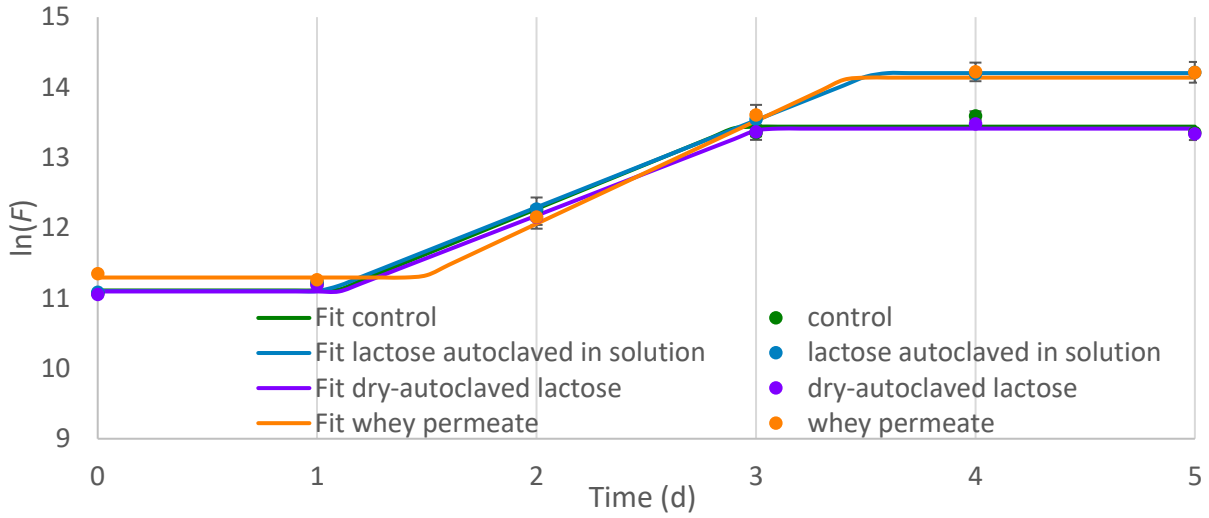

Figure 2.9. Growth curves, as ln-transformed fluorescence, showing data points (•; mean ± SD; n = 3) and fits to Equation 2.2 (–), of batch cultures of *T. suecica* grown in 24-well plates in control medium, medium amended with lactose autoclaved in solution or dry-autoclaved lactose, and WP-amended medium (0.5 g L^{-1}) at initial pH of 10.

The Chla concentration of *T. suecica*, shown in Figure 2.10-D, followed a trend similar to F_{max}. No significant differences were observed in Chla concentration across pH for control, lactose autoclaved in solution and WP treatments ($p > 0.05$). For dry-autoclaved lactose cultures, the Chla concentration was low at pH 8 and increased at higher pH levels ($p < 0.01$).

Algal cell concentrations in STA phase are shown in Figure 2.10-C. The trends are similar to those for F_{max} and Chla content. Control cultures had higher cell concentration at pH 9 than at pH 10 ($p < 0.05$). Cultures in lactose autoclaved in solution displayed higher cell concentrations at pH 8 and 9 compared to pH 10 ($p < 0.05$). For cultures in dry-autoclaved lactose, cell concentrations at pH 9 and 10 were similar to those in other treatments and much higher than at pH 8 ($p < 0.01$). No cell counts are available for *T. suecica* grown in the WP-amended media because clumping prevented accurate estimation with the flow cytometer (see below).

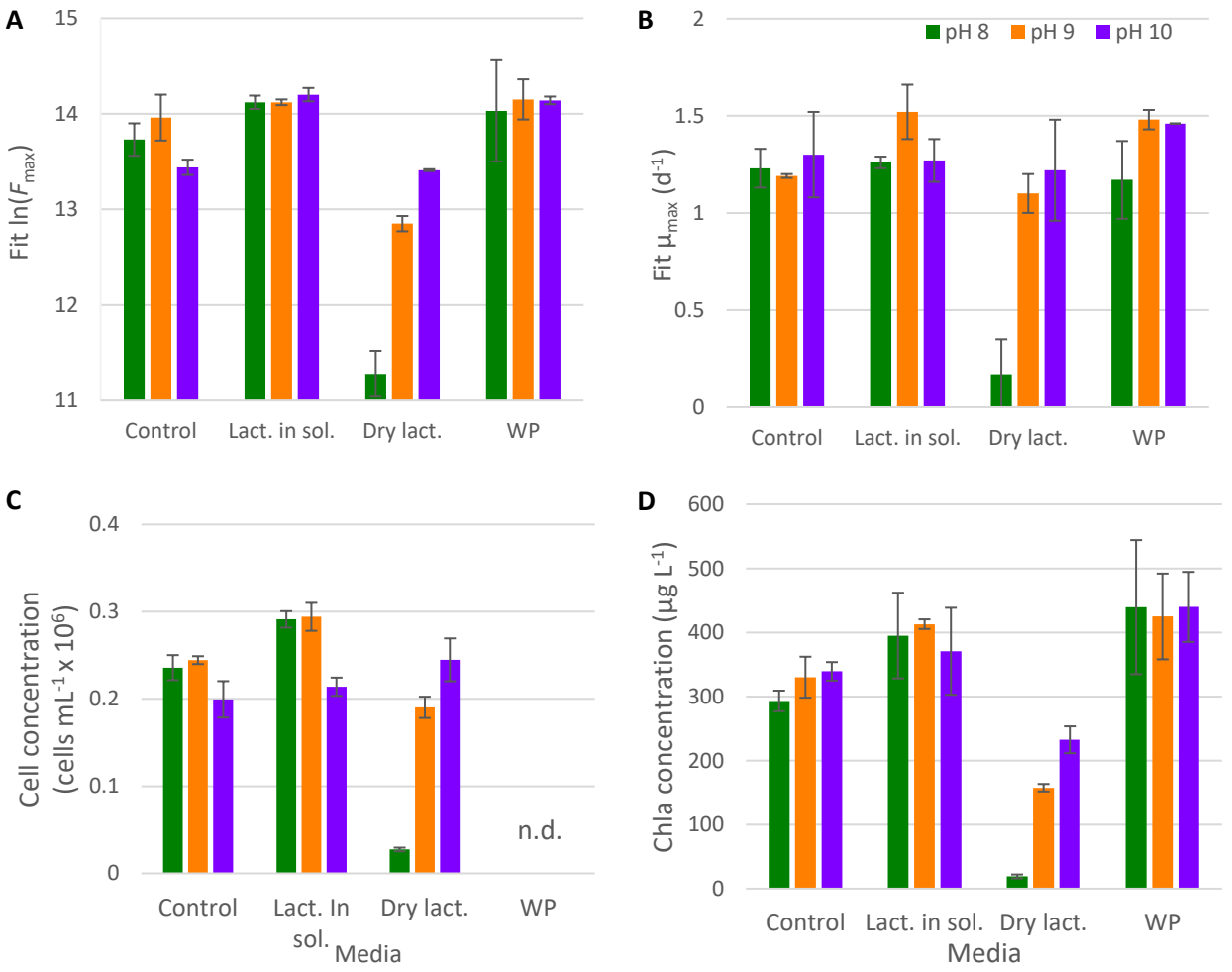

Figure 2.10. Fitted values of Fmax (A) and µmax (B) from Equation 2.2, final cell concentration (C), and final Chla concentrations (D) (mean ± SD; n = 3) of batch cultures of T. suecica grown in 24-well plates in control medium, medium amended with lactose autoclaved in solution or dry-autoclaved lactose, and WP-amended medium (0.5 g L-1) at initial pH of 8, 9, and 10. n.d. is no data collected.

Bacterial monitoring using absorbance at 600 nm did not reveal any measurable growth as the absorbance values were below the limit of detection of the instrument. The final bacterial cell concentrations in the different treatments are shown in Figure 2.11: (A) bacteria in co-culture with *T. suecica*, and (B) bacteria in culture alone, cultured after selective removal of the algae by filtration. Bacterial counts were higher in co-culture with the algae compared to bacterial cultures alone. Concentrations were higher at pH 10 than at other pH levels for bacteria growing with algae ($p < 0.05$). Cultures in dry-autoclaved lactose had higher final bacterial concentrations when growing with algae than in isolation ($p < 0.05$). The *T. suecica* to bacteria ratio was higher for the control at pH 9 than in other treatments (Figure 2.12). Dry-autoclaved lactose cultures showed a significantly lower ratio ($p < 0.05$). Cell concentrations could not be determined accurately for cultures in WP-amended media

because of the formation of aggregates of varying sizes. Cultures of *T. suecica* and bacteria at pH 8 in control media appear to be smaller in size compared to those in media with lactose autoclaved in solution (Figure 2.13). The presence of organic amendment in the culture tends to enhance cell clumping.

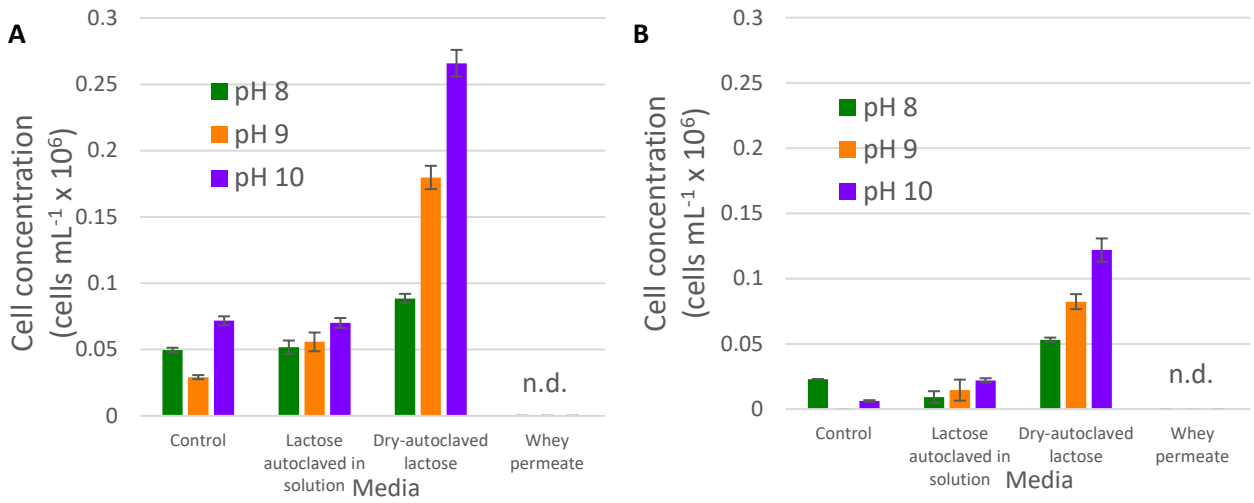

Figure 2.11. Final bacterial cell concentration (mean ± SD; n = 3) in STA phase batch cultures of (A) *T. suecica* plus bacteria and (B) bacteria alone after separation of the algae by filtration. Cultures were grown in 24-well plates in control medium, medium amended with lactose autoclaved in solution or dry-autoclaved lactose, and WP-amended medium (0.5 g L-1) at initial pH of 8, 9, and 10. n.d. is no data collected.

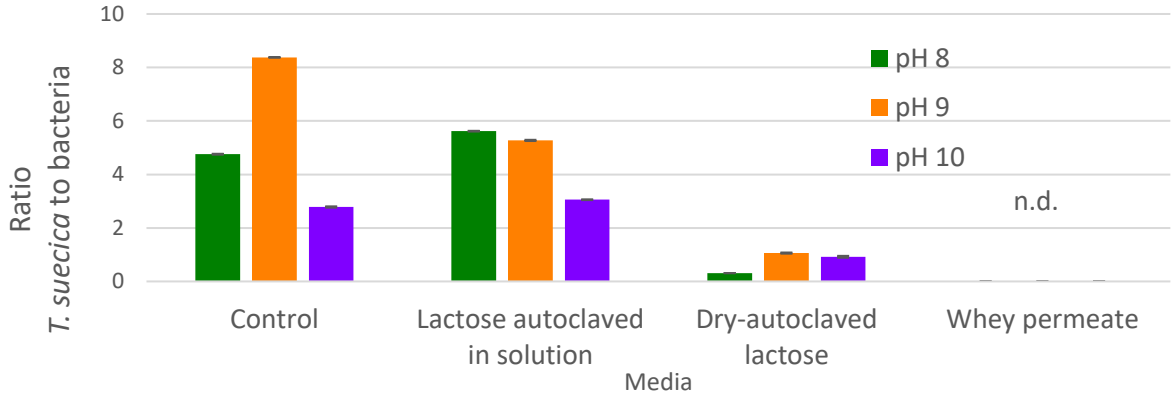

Figure 2.12. Ratio (mean ± SD; n = 3) of *T. suecica* to bacteria cell concentrations in STA phase batch cultures grown in 24-well plates in control medium, medium amended with lactose autoclaved in solution or dry-autoclaved lactose, and WP-amended medium (0.5 g L^{-1}) at initial pH of 8, 9, and 10.

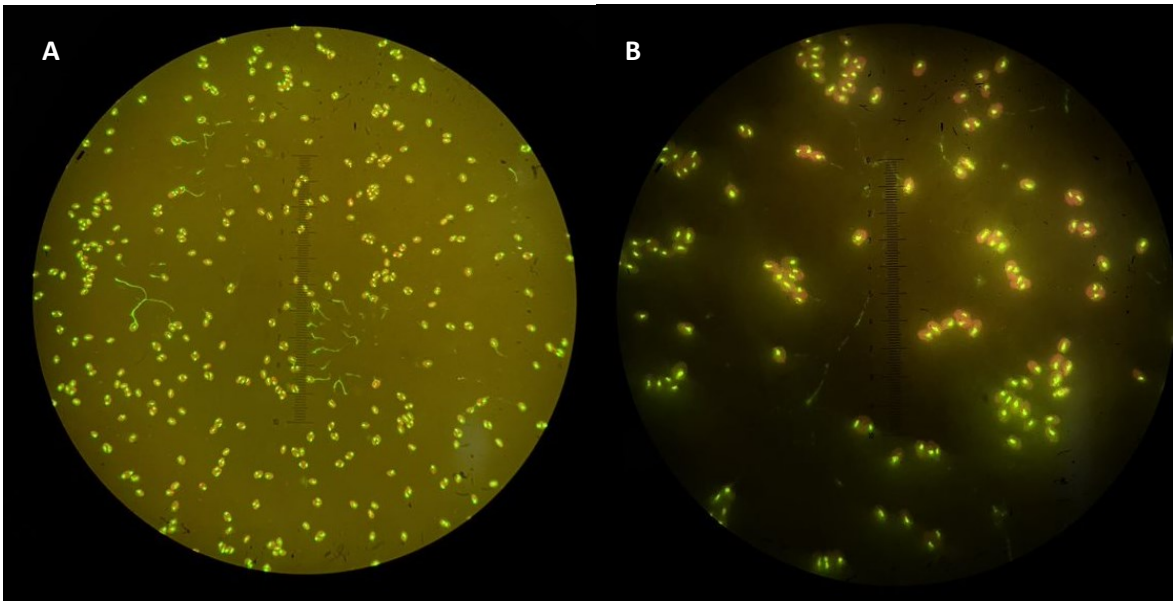

Figure 2.13. Epifluorescence micrograph (200X) pictures of SYBR Green dyed cultures of *T. suecica* and bacteria in STA phase batch cultures with a starting pH of 8 in control media (A) and medium amended with lactose autoclaved in solution (B). Note clumping of cells in the organic-enriched medium.

2.3.4. Testing algal growth in WP media in successive cultivation

This experiment explored the mixotrophic growth of *T. suecica* in WP media (0.5 g L^{-1}) in 1 M NaOH. Cultures were grown in closed 40-mL tubes with minimal headspace (about 2 mL) for gas exchange and were not replicated. Growth curves for three successive transfers in WP-amended media, starting from a culture acclimated to control media, are shown in Figure 2.14. The estimate of F_{max}, obtained from Equation 2.2, was higher for the first than for successive transfers. The first and second transfers reached STA phase in three and two days, respectively, while the third culture took six days to reach STA phase. There was a reduction in the maximum growth rate in the second and third transfers. The fit parameters, F_{max} and μ_{max}, and the final cell concentration of the three transfers are shown in Figure 2.15. All parameters showed a decline between the first and the second transfer. The progressive reductions in growth rate and yield in successive transfers of *T. suecica* in WP-amended medium were consistent with nutrient limitation.

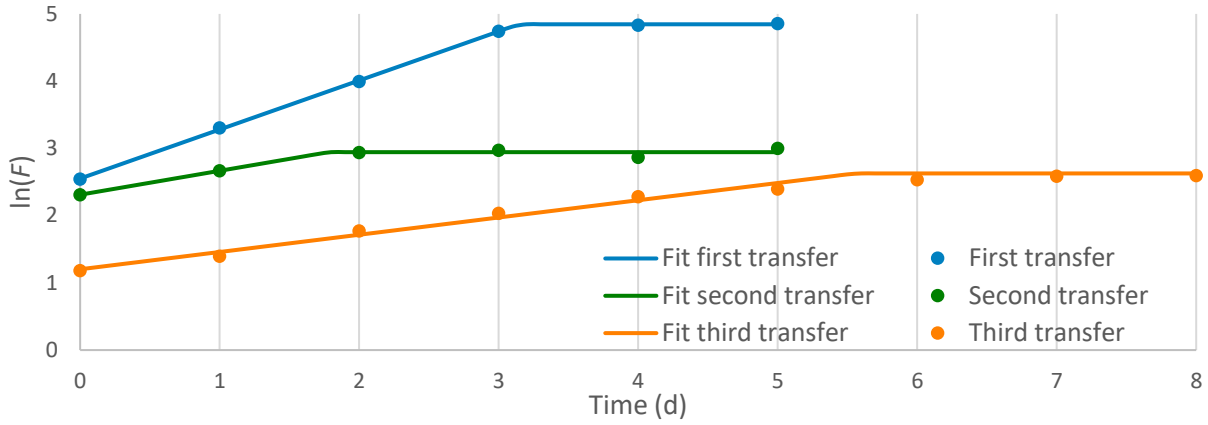

Figure 2.14. Growth curves, as ln-transformed fluorescence, showing data points (•; not replicated) and fit to Equation 2.2 (–), of successive transfers of batch cultures of *T. suecica* grown in WP-amended media (0.5 g L^{-1}) in 40-mL tubes.

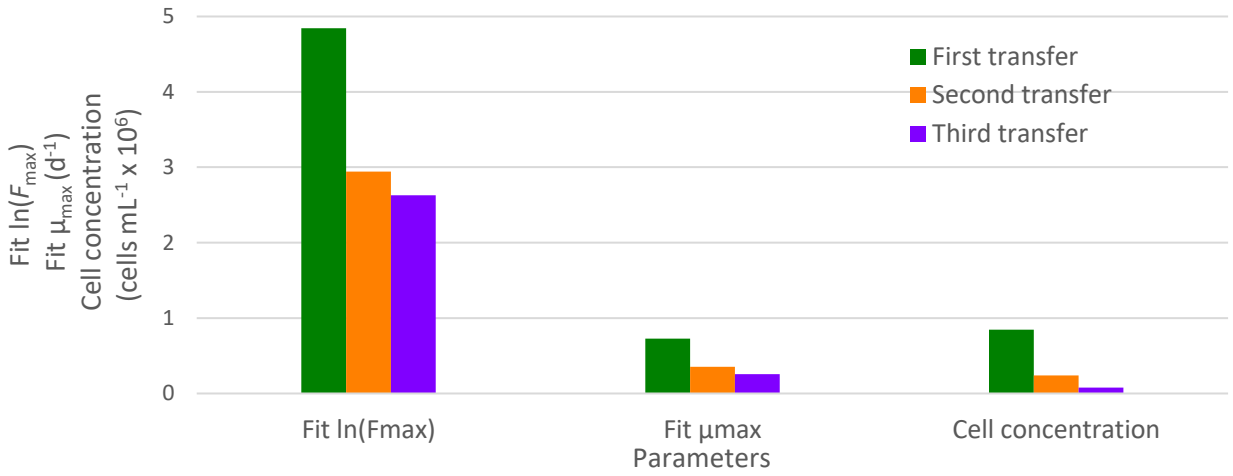

Figure 2.15. Fitted values of maximum fluorescence (F_{max}) and maximum growth rate (μ_{max}) from Equation 2.2, and final cell concentration from successive transfers of *T. suecica* grown 40-mL tubes in WP-amended media (0.5 g L^{-1}).

2.3.5. Effect of solvent and autoclaving on P forms in WP solutions

In this abiotic experiment, the concentrations of particulate and dissolved P were examined in WP solutions prepared using 1 M NaOH versus E-pure water (without NaOH), both analysed before and after autoclaving. The solutions prepared with NaOH had higher concentrations of particulate P compared to those prepared with E-pure ($p < 0.001$; Figure 2.16). Both NaOH and E-pure solutions had an increase in particulate P post-autoclaving compared to pre-autoclaving ($p < 0.001$). Dissolved P content (organic and inorganic) was slightly higher for solutions prepared with NaOH before autoclaving than after ($p < 0.05$). The dissolved P was much higher for solutions prepared with E-pure water as

solvent compared to NaOH ($p < 0.001$). When the particulate and dissolved pools were summed, there was a deficit in the solutions prepared in NaOH, resulting in lower expected total P for the NaOH-based solutions compared to the E-pure-based solutions. The difference indicates a non-reactive pool of P in samples prepared in NaOH. The deficit was reduced by autoclaving but still accounted for only 57 % of the total P pool.

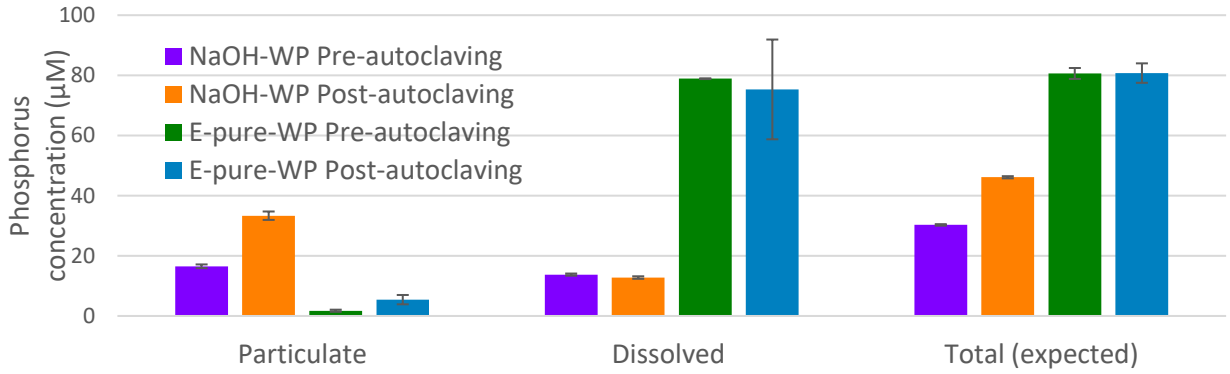

Figure 2.16. Particulate, dissolved, and total (particulate + dissolved) phosphorus (mean ± SD; n = 3) in WP solutions prepared with 1 M NaOH and E-pure water pre- and post-autoclaving.

2.3.6. Effect of aging on algal growth in WP-amended media

Growth was tested in batch cultures of *T. suecica* grown in 24-well plates, using control media and three different WP-amended media of varying ages (Figure 2.17). All cultures reached a similar F_{max} across the treatments ($p > 0.1$; Figure 2.18-A). There was an increase in μ_{max} from 0 to 7 mo WP-amended media, then a decline for 16 mo media. The cultures in 7 mo WP media had a higher μ_{max} compared to all other treatments ($p < 0.05$; Figure 2.18-B). It appears that autoclaving the WP solution twice did not affect the growth of *T. suecica* in comparison to autoclaving once (F_{max} $p > 0.1$; μ_{max} $p > 0.1$).

The final cell concentration, presented in Figure 2.18-C, was higher for all treatments than for cultures in 16 mo WP ($p < 0.001$), inconsistent with the apparent maximum yield (F_{max}). Cell quotas of Chla concentration were higher for 16 mo WP-amended than for younger WP media ($p < 0.05$; Figure 2.18-D), which explains the inconsistent F_{max} and cell concentration results. *T. suecica* showed enhanced growth in aged WP media. However, there was a threshold beyond which cell concentration and growth rates began to decline, particularly noticeable in the 16-mo treatment.

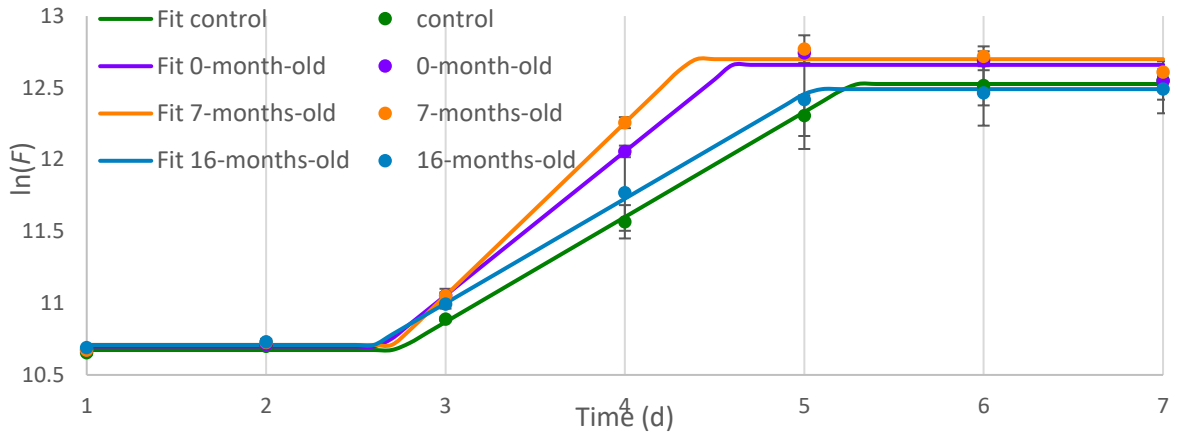

Figure 2.17. Growth curves, as ln-transformed fluorescence, showing data points (•; mean ± SD; n = 4) and fits to Equation 2.2 (–), of batch cultures of *T. suecica* grown 24-well plates in control and WP-amended media (0.5 g L^{-1}) of different age.

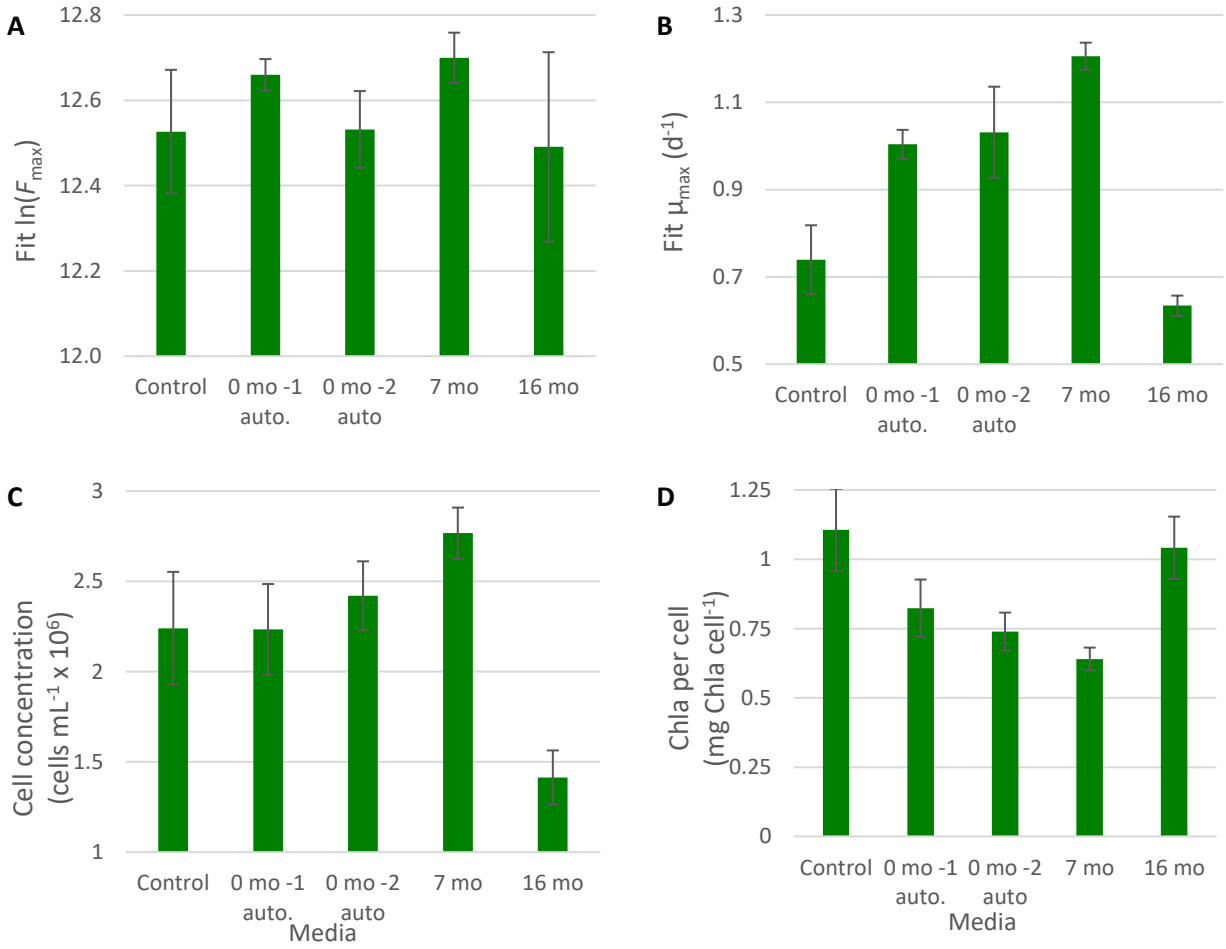

Figure 2.18. Fitted values of maximum fluorescence (A) and maximum growth rates (B) from Equation 2.2, final cell concentration (C), and final Chla per cell (mean ± SD; n = 4) of batch cultures of *T. suecica* grown in 24-well plates in control and different aged WP media (0.5 g L^{-1}): 0-month-old being autoclaved once (0 mo -1 auto), and twice (0 mo -2 auto), 7 mo and 16 mo WP media.

2.3.7. Effect of visible light on WP-amended media on algal growth

To investigate the potential factors contributing to the successful growth of algal cultures in aged WP media, an abiotic experiment was conducted to test the effect of visible light exposure (80 µmol photons m^{-2} s^{-1}; the growth irradiance for the cultures) on the media and its nutrient concentration. The WP-amended media's absorption coefficient spectra from 250 to 750 nm show a decrease across all wavelengths over five days on the light table (Figure 2.19), consistent with the colour of the media getting lighter. One peak was observed in the WP media's spectra around 265 nm.

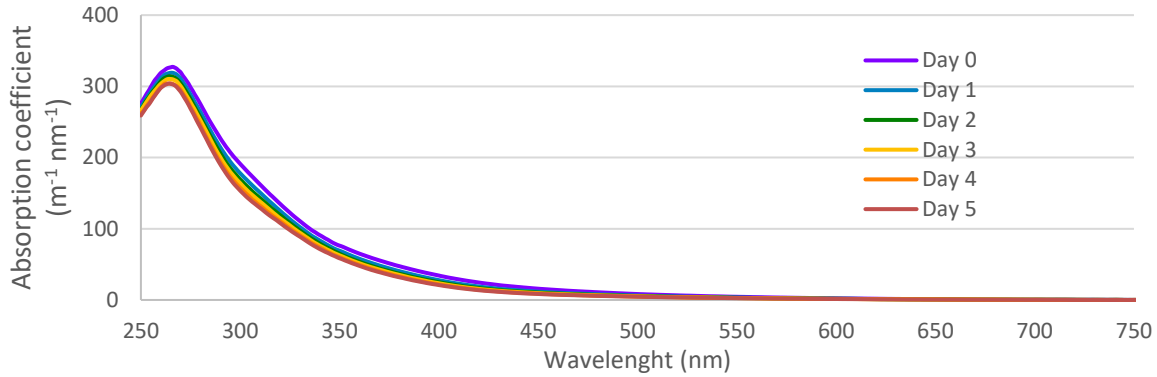

Figure 2.19. Absorption coefficient spectra from 250 to 750 nm of WP media (50 g L^{-1}) from day 0 to 5 of exposition to an 80 µmol photons m^{-2} s^{-1} light.

Particulate carbon, nitrogen, and phosphorus concentrations were measured, as well as dissolved and total P concentrations, as shown in Figure 2.20. Most of the P in the WP media was in particulate form (mean 87.5 ± 7.3 µM), with the remainder in dissolved form (mean 28.5 ± 6.9 µM). While no statistical linear trend was detected in the concentrations of different forms of P over light exposure time, there was an increasing trend in dissolved P, a decreasing trend of particulate P, and an overall 15 % increase in detected total P throughout the exposition period. The particulate C concentration in the abiotic WP media tubes followed the same trend observed for total P, with values ranging from 666 to 888 µM. Particulate N exhibited an irregular trend with fluctuations of 20 µM N per day due to the limited precision of the estimates as the samples were near or below the limit of detection.

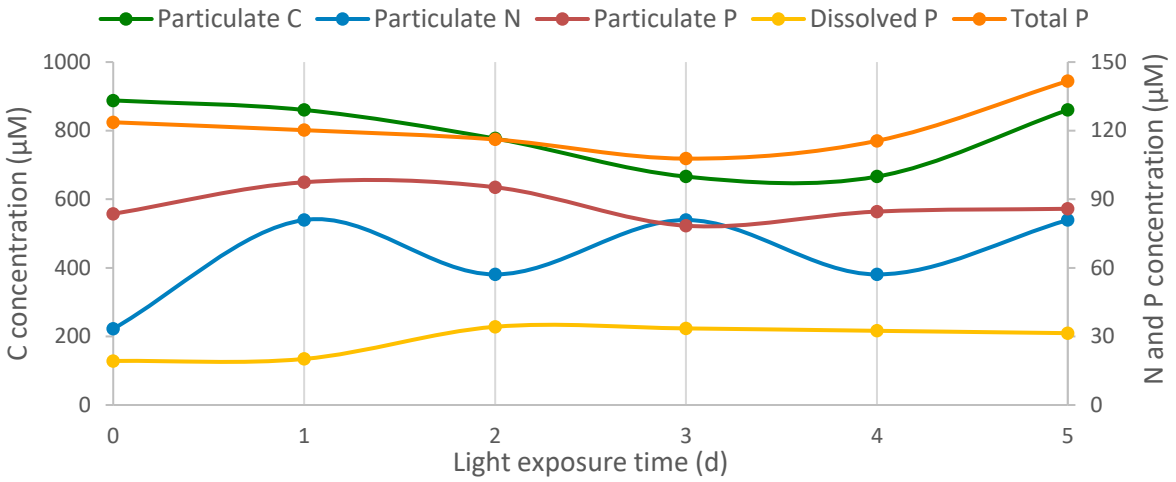

Figure 2.20. Carbon, nitrogen, and phosphorus concentrations (mean ± SD; n = 2) in WP media (50 g L^{-1}) from day 0 to 5 of exposition to an 80 µmol photons m^{-2} s^{-1} light.

2.3.8. Effect of headspace in closed tubes for gas exchange on algal growth

This experiment aimed to investigate the influence of gas exchanges in closed tubes. Growth curves for the cryptophyte *Chroomonas mesostigmatica* in 60-mL closed tubes, comparing cultures with and without headspace in WP-amended media, are shown in Figure 2.21. The culture with a headspace had a higher apparent final yield, F_{max}, and a higher maximum growth rate (1.06 versus 0.55 d^{-1}) than the culture without a headspace.

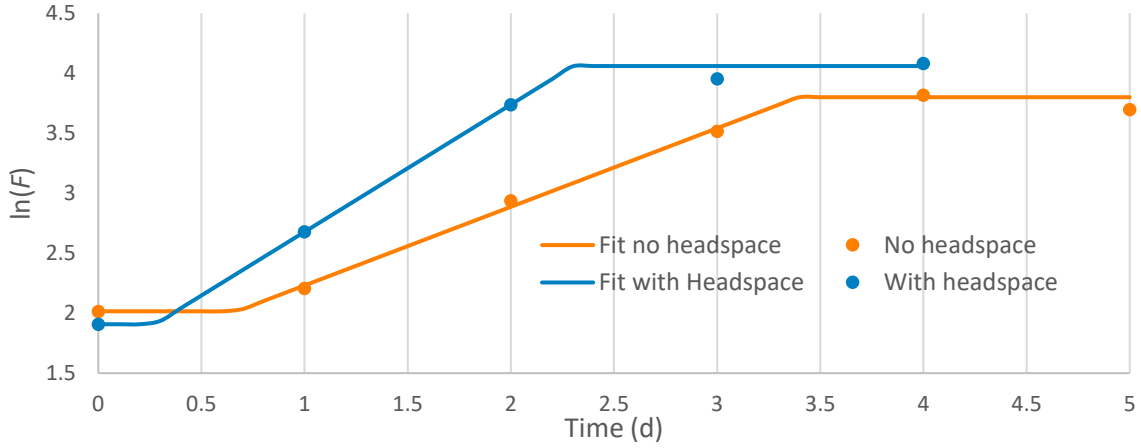

Figure 2.21. Growth curves, as ln-transformed fluorescence, showing data points (•; no replication) and fit to Equation 2.2 (–), of batch cultures of *C. mesostigmatica*. Cultures were grown in 60-mL closed tubes in WP media (0.15 g L^{-1}) with (55 mL media) and without (60 mL media) headspace in the culture tube.

2.4. Discussion

2.4.1. Extent of browning of WP solutions with NaOH concentration

The interactions taking place within the autoclave between the components of WP and NaOH under heat can induce substantial alterations in the chemical structure of the dairy by- product (Aktag et al. 2019). The observed browning suggests the possible occurrence of caramelization, the Maillard reaction, or both. For the scope of this study, the complete analytical characterization of the solutions post-autoclaving was not conducted thereby limiting the ability to definitively attribute the process to caramelization or Maillard.

Observations revealed that WP solutions had increased browning with higher NaOH levels. This suggests that the solutions underwent similar reactions, possibly the Maillard reaction, but were at different stages after autoclaving. The specific focus of this reaction involves reducing sugars and the ε-amino groups of amino acids, predominantly found in casein, the primary protein in bovine milk (Turner et al. 1978; Ulrich and Cerami 2001; Davoodi et al. 2016; Aktag et al. 2019). Important intermediates in this reaction include Schiff bases and Amadori and Heyns rearrangements, with the formation of melanoidin as a stable final product responsible for characteristic browning (Lund and Ray 2017; Ulrich and Cerami 2001; Cui et al. 2021). Lower browning in low-NaOH solutions might result from reduced melanoidin formation.

The presence of NaOH can intensify glucose and galactose availability for the Maillard reaction by speeding up lactose fragmentation into monosaccharides (Ajandouz et al. 2001; Rajakala and Selvi 2006). Alkaline conditions favour the formation of Schiff bases, and pH significantly influences the reactivity of amino groups in amino acids and the stability of reaction intermediates (Davidek et al. 2002; Cui et al. 2021). Additionally, the presence of phosphate has been found to accelerate the reaction process, which is particularly relevant considering the abundant phosphate content in WP (Davidek et al., 2002).

The variation in post-autoclaving pH between low-NaOH (100, 180, and 300 mM) and high-NaOH (560, 1000, 3000 mM) concentrations observed in Figure 2.1 suggest different reaction extents corresponding to NaOH levels. The near-neutral pH observed in low-NaOH solutions post-autoclaving could be attributed to the complete utilization of NaOH during the reactions, leading to a pH decrease to 7. In contrast, the high-NaOH solutions maintained their alkaline pH after autoclaving, likely due to the

presence of unreacted NaOH. The normalized absorption pattern in Figure 2.2 indicates a transition from substances primarily absorbing at 267 nm in the case of low-NaOH solutions to those with a peak absorption at 285 nm in the high-NaOH solutions. This shift in absorption could represent different intermediates and/or products of browning reactions, which all highly absorb in the UV domain (Hodge 1953; Ajandouz et al. 2001).

The extent of browning with NaOH concentrations influenced the availability of inorganic N and P. Interestingly, before autoclaving, there was an increasing trend in the concentration of P detected as orthophosphate with higher NaOH concentration, indicating that NaOH was already solubilizing P. The anticipated outcome of the autoclaving process was a reduction in available P as NaOH concentration increased, likely due to calcium phosphate precipitation within the autoclave (Fairbrother 1991). However, this trend was evident only in the case of low-NaOH solutions, as high-NaOH solutions increased P concentration.

Among the various NaOH concentrations tested, the treatment that used 1 M NaOH as the initial concentration to dissolved WP had the most favourable growth results. Compared to other treatments, *T. suecica* yielded enhanced fluorescence (F_{max}) and cell concentration. This suggests that the WP stock solution were subjected to NaOH-dependent reactions within the autoclave, which allowed higher nutrient solubilisation in the solutions. This resulted in efficient nutrient assimilation by the algae, similar to the nutrient availability in control cultures, in spite of the high pH caused by high NaOH. A pH above 9, which was observed in the media prepared with high NaOH, would favour the conversion of bicarbonate, which is available for uptake through a carbon concentrating mechanism (Raven et al. 2008), to insoluble carbonate. As a result, the 1 M NaOH concentration in the preparation of WP stock solution was kept as the most promising for this study even though its elevated level greatly influenced the pH of the media.

2.4.2. Effect of purified lactose- and WP-amended media on algal growth

Algal growth was assessed in media amended with WP and purified lactose. WP was dissolved in NaOH, while lactose was dissolved in E-pure water. The initial appearance of the WP solution was slightly opaque and creamy white, turning a deep black with orange tinges after autoclaving. The lactose solution, in contrast, was transparent initially and became slightly pale straw-coloured after autoclaving.

The colour changes and absorption coefficient spectra of these solutions suggest potential variations in the reactions they undergo.

The significant browning in WP solutions after autoclaving is likely a result of the Maillard reaction and the formation of melanoidin, potentially accompanied by lactose caramelization (Lund and Ray 2017). The broad peak of WP solutions observed in Figure 2.8 might be attributed to the presence of other oxidation products. Furthermore, it is reasonable to assume that the intensity of reactions in the autoclave is more pronounced in WP compared to lactose solutions due to the diverse composition of WP.

Lactose was sterilized by autoclaving using two methods: directly in solution in E-pure water or as a dry powder subsequently dissolved in E-pure. The lactose in solution before autoclaving showed a small peak at 280 nm, much lower than in post-autoclaving solutions. This indicates that the distinctive peaks at 235 and 280 nm in Figure 2.8, observed following autoclaving, correspond to compounds generated during the autoclaving process. Since both solutions of lactose had those absorbance peaks, it can be assumed that both solutions underwent analogous reactions within the autoclave, but to varying extents. The lactose autoclaved in solution had a slight colour change after the autoclave, hinting at the possibility of browning reactions taking place, as these reactions often produce intermediate compounds with a pale-yellow colour (Ajandouz et al. 2001). The reaction is not likely to have involved residual proteins, thereby pointing to the caramelization of lactose at elevated heat being responsible for the browning. Autoclaving the dry lactose powder involved subjecting it to steam within the autoclave, potentially triggering chemical reactions. The outcome had a firm texture resembling a cookie, suggesting some changes in the chemical composition, such as possible particle cross-polymerization or lactose crystallization (Durham 2009). The dissimilar peak intensities might be attributed to the increased water content for lactose in solution, most likely enhancing the reaction (Cui et al. 2021).

Algal growth was examined in cultures amended with WP and purified lactose. Lactose was expected to support superior algal growth due to the potential constraints posed by impurities and other elements in WP on nutrient assimilation by algae (Durham 2009). Contrarily, cultures of *T. suecica* amended with WP and lactose autoclaved in solution had comparable fluorescence in STA phase (F_{max}) and growth rates (μ_{max}), as shown in Figure 2.10-A-B. Unfortunately, due to time constraints with sonication tests to

disperse cell clumps in WP cultures, cell count samples were not processed through the flow cytometer. Despite this, the findings highlight the promising potential of utilizing WP to provide organic C for algal growth. Whey permeate itself did not exhibit any signs of growth inhibition or adverse effects when compared to commercially purchased purified organic C (lactose) in media formulations. This implies that WP could serve as a low-cost nutrient supply for algal cultures due to its status as a waste product.

2.4.3. Effect of pH in WP media on algal and bacterial cultures

The initial pH of a culture medium plays a crucial role in algal cultivation due to its potential impact on various biological and chemical processes. It can directly influence algal cell behaviour, including growth rates, metabolism, and overall health (Taraldsvik and Myklestad 2000). Moreover, pH also affects the availability of CO_2 within the culture medium (Henderson 1908). In the context of xenic cultures, the pH level could potentially shape the bacterial population associated with *T. suecica* culture, consequently influencing algal growth and biomass. *T. suecica* has displayed adaptability to a broad pH range (Almutairi and Toulibah 2017).

The first pH experiment in this study investigated algal growth within pH-adjusted media from 7 to 10. It aimed to assess the influence of incorporating a WP solution with 1 M NaOH into seawater culture media, without needing to lower the initial pH, as it naturally reached a pH of 10. Minimal discrepancies were observed in F_{max}, μ_{max}, cell concentration and fluorescence per cell between pH 8, 9 and 10 for both control and WP cultures, as shown in Figure 2.7. At pH 7, WP cultures with 1 M NaOH yielded higher F_{max}, cell concentration, and fluorescence per cell than at other pH. This improved yield at pH 7 might be attributed to the high solubility of CO_2 produced by the C-box. At pH 7, seawater readily absorbs atmospheric CO_2, enabling efficient utilization for photosynthesis by algae. However, at higher pH levels, bicarbonate formation is favoured, although the CO_2 absorption is still efficient (Borowitzka and Larkum 1987; Hansen et al. 2007). Similar results were obtained by Kassim and Meng (2017), where *T. suecica* yielded higher final biomass at pH 7 than other pH values.

The limited availability of CO_2 at pH 8, similar to the ocean's pH, presents a potential C-limitation challenge for marine organisms. As a countermeasure, many microalgae have evolved carbon concentrating mechanisms (CCMs) that enhance carbon uptake from the surrounding seawater (Badger et al. 1998; Hansen et al. 2007). The green algae *Tetraselmis gracilis* and *Chlorella vulgaris* demonstrated the capacity to assimilate bicarbonate (HCO_3^-) through external carbonic anhydrase (Rigobello-Masini et

al. 2003). This adaptation and the possibility of assimilating bicarbonate could account for the growth observed at pH 8, 9, and 10 for *T. suecica*. However, converting bicarbonate to CO_2 for photosynthesis involves a significant energy cost, likely leading to reduced yields compared to cultures in pH 7 (Raven 1997; Moheimani and Borowitzka 2011). Nevertheless, under non-equilibrium conditions such as in C-boxes, the pH 8 environment offers more room for CO_2 absorption due to the transformation of most CO_2 into bicarbonate, leading to a decrease in the partial pressure of CO_2 and a potentially increased CO_2 intake to the culture medium.

In the second pH experiment, algal biomass, including F_{max}, Chla, and cell concentration, did not vary significantly across pH levels, except for the dry-autoclaved lactose treatment, as shown in Figures 2.10-A-C-D. Dry-autoclaved lactose cultures had increased biomass and growth rates with rising pH levels from 8 to 10. Intriguingly, at pH 8, cell growth was minimal, and this was not attributed to high bacterial concentration, as the same trend was observed for bacterial cell concentrations (Figure 2.11), however, the underlying reason remains unclear. Given the favourable growth observed in lactose autoclaved in solution, particularly at pH 8, the reduced growth observed in the dry-autoclaved lactose treatment could potentially attributed to different extent of the browning reaction happening within the autoclave when in solution versus the dry powder alone.

Various mechanisms have been identified by which bacteria can stimulate algal growth, such as hormone production, P solubilization, carbohydrate degradation, and more (Liu et al., 2020). It is plausible that the bacterial community associated with *T. suecica* consists of growth-promoting bacteria capable of aiding lactose degradation from the media into monosaccharides (Arora et al., 2012). Interestingly, bacteria cell concentrations were significantly lower when cultivated alone compared to when cultivated with alga, as illustrated in Figure 2.11-B. If bacterial cells were limited by organic C availability, the higher bacterial count in the presence of algae suggests potential access to extracellular organic components from the algae (Wiliams 1981). There is a possibility that bacteria derive nutrients by feeding on *T. suecica* cell wall polysaccharides like glucans, galactans, and pectins (Arora et al. 2012). It is also plausible that bacteria cultivated alone were oxygen limited in C-boxes and that algae supplied both carbohydrates and oxygen, resulting in higher bacterial concentration when cultivated in co-culture.

2.4.4. Aged and light-exposed WP, effect on algal growth

An interesting observation indicated that storing WP media for approximately seven months in a refrigerator in the dark seemed to enhance both growth rate and final yield in *T. suecica*, as illustrated in Figure 2.18-B-C. Notably, cultures amended with seven mo WP had lower Chla per cell, as shown in Figure 2.18-D, consistent with mixotrophic growth or an amplified down-regulation of Chla in STA phase in response to nutrient starvation triggered by accelerated growth. One explanation for enhanced growth in aged media could be associated with chemical composition alterations in the WP media over time, likely involving the breakdown of detrimental constituents or the potential resolubilization of essential nutrients. The autoclaving process can induce calcium-phosphate precipitation, which might lead to a decline in P available for algal growth (Fairbrother 1991; Mondal et al. 2016). Moreover, the addition of the WP-NaOH solution to the seawater media can induce precipitation of struvite ($MgNH_4PO_4 \cdot 6H_2O$), considering the ammonium and phosphate content of WP and magnesium present in seawater (Stancheva et al. 2021). One approach to test this would involve enriching the freshly prepared WP media with additional P to determine if a similar effect could be replicated.

Since the only source of P for the cultures is the WP, the passage of time could facilitate the solubilization of previously precipitated P, enhancing yields. Figure 2.16 illustrates the impact of solvent (NaOH versus E-pure water) and autoclaving on both particulate and dissolved forms of P. Notably, the addition of WP to NaOH have resulted in P precipitation, expressed as a loss of detectable orthophosphate, and this precipitation is further exacerbated by autoclaving. The non-reactive pool of P observed in solutions with NaOH could have been attributed to organically bound P or crystal precipitation of P that resisted the hydrolysis step of the method, and temperature from the autoclave might have reduced this deficit. Due to the substantial quantity of aged WP media at our disposal, it was selected as the preferred medium for conducting larger-scale cultures of *T. suecica*, aimed at biomass characterization (Chapter 3).

Recognizing the potential for time to expedite nutrient availability, the need arose for a means to accelerate WP degradation, given that it is impractical to retain large volumes of processed WP over extended periods for commercial purposes. Consequently, to accelerate the degradation of WP, an attempt was made to use visible light exposure on abiotic WP media over five days. Continuous exposure to light resulted in a gradual bleaching of the media colour each day. Nutrient analyses revealed non-significant but intriguing phosphorus and particulate carbon patterns in the abiotic WP-

amended media exposed to light over time. Particulate P decreased by 15 % during exposure, while dissolved P increased by 60 %. This is likely attributed to the resolubilization of phosphate from calcium-phosphate precipitation in the autoclave or from struvite precipitation induced by the incorporation of WP solution into seawater media. Particulate carbon concentrations in the abiotic WP media ranged from 660 to 890 µM and followed the same trend as particulate P. Given that the seawater, post-sterile filtration, should not contain any particulate C, the measured presence can be attributed to the WP itself. Considering the WP concentration at 0.5 g L^{-1} and an estimated 70 % lactose content in WP, the media is anticipated to contain approximately 12.27 mM organic C (i.e., 14-19x the measured particulate C). It is plausible that a portion of the lactose is dissolved in the media, while some remain undissolved in colloidal formations (Hunziker and Nissen 1926).

Additional experiments involving UVC-irradiation (at 254 nm using a custom-built/low-pressure collimated beam following Bolton and Lindon, 2003), testing for quicker WP degradation and potential use as a sterilization technique, were conducted using the original stock WP powder obtained four years prior. However, these experiments yielded inconclusive results and were consequently omitted from this study. The altered odour developed and increased solubility of the WP stock powder in E-pure water over time, contrasting with its original insolubility, may be linked to changes in its properties, possibly influencing the absence of algal growth. These shifts could be attributed to suboptimal storage conditions, a factor recognized in other studies (Nham et al. 2023; Espinosa-Gonzalez et al. 2014; Girard et al. 2017).

2.4.5. Cultures in closed tubes in WP media

As the scaling-up of cultures in WP media would be done within closed tubes, it was important to conduct preliminary tests to assess algal growth under these conditions. Figure 2.15 demonstrates a decline in biomass yield (F_{max} and cell concentration) and μ_{max} after three transfers in WP media. This observation prompted the hypothesis that WP components might adsorb a micronutrient from the media. Vitamins and trace metals, vital for microalgal cells, could potentially bind with unknown WP components, rendering them unavailable in WP media. When cultures were initially inoculated in WP media, some essential micronutrients from the original control media may have remained available to the culture. However, subsequent transfers may have led to reduced growth due to decreased availability. Additional tests were conducted, but the results were inconclusive.

An assessment of the growth of *C. mesostigmatica* in closed tubes using WP media (0.15 g L^{-1}) before progressing to larger volumes was conducted. Figure 2.21 indicated that the algal culture had higher μ_{max} and F_{max} when a headspace was introduced to the culture tube. This implies that the air within the headspace provided a critical element for mixotrophic metabolism, most likely oxygen required for heterotrophic growth. The ratio of oxygen, essential for heterotrophic metabolism, to CO_2, vital for phototrophic metabolism, is fundamentally unbalanced in ambient air. This leads to the hypothesis that oxygen produced through photosynthesis might not be sufficient or readily available to support maximal heterotrophic growth like it could in certain close systems studied (Abiusi et al., 2020). The improved growth rate and biomass from increased gas exchange within the culture reinforced the adoption of headspaces for *C. mesostigmatica* cultures when characterizing biomass (Chapter 3).

2.5. Conclusion

In conclusion, this series of experiments shed light on the dynamics of algal growth in response to the formulation of WP-amended media. The browning reactions occurring during the autoclaving of WP dissolved in NaOH solution have indicated that algal growth thrives, with enhanced outcomes observed when employing 1 M NaOH as the solvent. The pH-adjustment experiments underscored the significance of pH levels on algal performance, with WP cultures at pH 7 displaying the highest biomass and dry-autoclaved lactose treatment displaying the least growth, especially at pH 8. Furthermore, storing WP media for approximately seven months improved *T. suecica*'s growth, possibly due to the resolubilization of calcium-phosphate or struvite precipitation. It was found that using NaOH as a solvent for WP solutions in the autoclaving process influenced P availability. Additionally, light exposition over a period of five days was tested for accelerated WP degradation. Finally, examining *C. mesostigmatica* growth in WP media with a headspace showed higher growth rates, emphasizing the importance of gas exchange for optimal growth in closed systems.

These results collectively highlight the interplay of nutrient availability, pH, aging, and gas exchange on algal growth. This series of experiments establishes a foundation for a better understanding of the dairy substrate, providing essential insights before progressing to medium-scale cultivation for biomass characterization in Chapter 3. Further exploration is imperative to gain an understanding of the interactions occurring in the autoclave involving WP and NaOH within the culture media and during algal growth. This knowledge is crucial for optimizing growth conditions in WP powder-based media.

Chapter 3: Effect of WP amendments and DIC on microalgae in exponential- and stationary-phases: characterization of photosynthetic apparatus, nutrients, fatty acids, and biomass productivity

Abstract

Microalgae, with their ability to synthesize valuable compounds like proteins and fatty acids (FAs), are subjects of extensive study for diverse applications, such as in pharmaceutical, biofuel, and aquaculture feed markets. Identifying optimal species and growth methods is crucial for maximizing biomass yields and minimizing production costs. This study explores the utilization of dairy waste whey permeate (WP) as a nutrient substitute in growth media and the addition of $NaHCO_3$ to address carbon limitation. It characterizes the biomass of four algal species cultivated in closed systems grown in different media: control (CTRL), control with $NaHCO_3$ (CTRL+DIC), WP, and WP+DIC media, harvested during exponential and stationary phases of growth. Results indicated signs of mixotrophic growth in diatom *Chaetoceros muelleri* and green alga *Tetraselmis suecica*, potentially assimilating lactose (organic carbon) from WP. The pinguiophyte *Pinguiococcus pyrenoidosus* had comparable eicosapentaenoic acid (EPA) productivity rates in WP media during exponential phase compared to CTRL cultures. *C. muelleri* displayed a significant accumulation of FAs in stationary phase when grown in WP media, suggesting its suitability for biofuel production. *T. suecica* and the cryptophyte *Chroomonas mesostigmatica*, with high N content in exponential phase, emerged as promising candidates for protein production. *C. muelleri* and *C. mesostigmatica* exhibited luxury phosphorus uptake in WP media, indicating the potential for remediation of wastes with high phosphorus content like WP. This work lays a foundation for identifying promising strains and conditions for large-scale algal production of valuable compounds, focusing on utilizing dairy waste WP as a growth substrate.

3.1. Introduction

3.1.1. Nutritional compounds from algae

The expanding global population and escalating demand for food production have essentialized the exploration of sustainable approaches to food production and consumption. There is an urgent need to enhance food quality and reduce waste along supply chains, a concern highlighted by the United Nations Sustainable Development Goals (SDGs) (The Global Goals 2023).

Microalgae are a promising solution, with applications across various sectors such as food supplements, aquaculture feed, pharmaceuticals, biofuels, and energy sources (Ummalyma and Sukumaran 2014; Cardozo et al. 2017; Garcia et al. 2017). Algal cells offer a large variety of vital nutrients essential for both human and aquaculture animal consumption, such as essential fatty acids (FAs), amino acids, proteins, vitamins, minerals, and pigments. These could serve as a food source but also contribute to human health by producing of pharmaceutically active compounds, offering potential prevention of various diseases and disorders (Garcia et al. 2017).

Microalgae have a notable potential as an alternative source of protein, offering high-quality products in powdered form, suitable for human consumption or as animal feeds (Becker 2007). Additionally, polyunsaturated fatty acids (PUFAs) have been utilized to prevent various diseases such as arthritis, cardiovascular disorders, cancer, diabetes, and inflammatory conditions, while also enhancing brain function (Garcia et al. 2017; Harwood 2019). Plants and algae have the ability to synthesize PUFAs that are not commonly abundant in our diets, such as omega-3s (Pulz and gross 2004; Harwood 2019). The existing market primarily relies on fish and fish oil products for omega-3s, such as eicosapentaenoic acid (EPA). However, concerns about overfishing and bioaccumulation of toxins in fish have increased interest in microalgae as an alternative source of PUFAs (Garcia et al. 2017).

Algae present multiple advantages over land-based agriculture to feed tomorrow's populations, including minimal land usage, avoidance of freshwater utilization (given the nutritional excellence of many marine species), rapid growth rates (Olguín 2003), and the ability to efficiently utilize nutrients, almost up to 100% efficiency (Tredici 2010). Microalgae continue to be extensively researched with the aim of increasing production rates of nutritious and valuable biomass. Despite all these advantages, algal cultivation remains expensive due to the high energy costs for lighting, nutrients, and aeration to mitigate C limitation (Acién et al. 2012).

3.1.2. Means to reduce biomass production costs

In this study, we explore approaches to reduce the costs of algal biomass production, including $NaHCO_3$ additions as a supply of dissolved inorganic carbon (DIC), mixotrophic cultivation, and providing essential nutrients from dairy waste whey permeate (WP).

Increasing DIC with bicarbonate addition

The primary limitation in cultivation media is likely to be carbon availability because of the high concentrations of the macronutrients nitrogen and phosphorus. The use of air bubbling significantly enhances CO_2 availability but can be extremely expensive when scaling up to commercial cultures. Supplementation with $NaHCO_3$ was proposed as a cost-effective alternative to air bubbling (Ratomski et al. 2021). Increased carbon availability for the cultures is likely to increase Calvin cycle activity and overall photosynthesis, resulting in an up-regulation of Chlorophyll-*a* (Chla) content (Salbitani et al. 2020). Studies have demonstrated increased cell density and lipid accumulation when adding $NaHCO_3$ to C-limited cultures (Guihéneuf et al. 2011; Nunez and Quigg 2015; Ratomski et al. 2021).

Utilizing mixotrophic cultivation

Another limitation of algal cultivation is the cost of energy associated with sustaining a light source for photoautotrophic organisms, those assimilating only inorganic forms of C using light energy. In the presence of labile organic compounds, certain species can transition from photoautotrophic to mixotrophic growth – a combination of photosynthesis and heterotrophy – and, less commonly, heterotrophic growth (Ceron Garcia et al. 2006). During mixotrophic metabolism, these organisms exploit both light and organic C simultaneously. Mixotrophic cultures have demonstrated elevated biomass productivity. For many species, mixotrophic cultivation increased the cellular content of valuable metabolites like proteins and PUFAs or promoted oil accumulation when compared with photoautotrophic controls (Ceron Garcia et al. 2006; Heredia-Arroyo et al. 2010; Ummalyma and Sukumaran 2014; Bashir et al. 2019; Baldisserotto et al. 2021).

Mixotrophic cultures often recalibrate their photosynthetic architecture, leading to potential reductions in fluorescence and Chla content per unit biomass (Lewitus and Kana 1994; Ogbonna et al. 1997). Alterations in other parameters might be observed when growing algal cultures mixotrophically, such as a reduction in variable fluorescence (F_v), in the ratio of variable to maximum dark-acclimated Chla fluorescence (F_v/F_m), and sigma (σ). These correspond to the number of functional photosystem II (PSII)

reaction centers, the proportion of PSII reaction centers that are functional, and the photosynthetic cross-section – a measurement of Chla antenna for light harvesting – (Oxborough et al. 2000; Gorbunov and Falkowski 2004). This is consistent with acclimative pigment regulation, a process that involves a continuous adjustment of the photosynthetic system to the environmental conditions until balanced growth is achieved, where the culture is fully acclimated to the substrate (Wood et al. 2005). Changes in the metabolic strategies of the algal cells likely induce this shift in the extent of the photosynthetic system. Leveraging organic compounds to stimulate mixotrophic growth in microalgal cultures presents a feasible approach for decreasing biomass production costs by minimizing light intensity in mixotrophic cultures.

Using waste to subsidize nutrients

Using waste effluents to supplement nutrients in microalgal growth media also represents an excellent strategy for cost reduction in commercial algal biomass production. Various industrial, food-grade, or wastewater sources have been explored for their nutrient-rich content, whether inorganic or organic, which microalgae can effectively remediate. This approach not only aids in reducing the expenses associated with algal biomass production but also decreases pollution loads.

Whey permeate, generated as a by-product of cheese production, must undergo significant waste treatment prior to disposal (Marwaha and Kennedy 1988; Zall 1992; Tsakali et al. 2010). It contains organic C, primarily in the form of lactose, along with significant concentrations of phosphate. These constituents represent fundamental macronutrients for algal growth. The objective here is to investigate whether WP is a potential substitute for DIC, N, and P in microalgal culture media. When introduced in small concentrations to the culture medium, WP and whey products have commonly resulted in an increase in cellular lipid and protein contents, along with enhanced biomass yields, compared to control cultures (Abreu et al. 2012; Espinosa-Gonzalez et al. 2014; Borges et al. 2016; Vieira Salla et al. 2016; Salati et al. 2017).

3.1.3. Algae and nutrient kinetics

For efficient algal biomass production and remediation of waste effluents such as WP, understanding the kinetics of nutrient and biomass dynamics within the culture is essential. A strategic decision must be made regarding harvesting during the exponential (EXP) or stationary (STA) phases of growth. The variation in up- or down-regulation of valuable compounds during EXP phase or the transition between

EXP and STA phase may lead to distinct optima for production in different species. The kinetics of algal biomass (X) produced through EXP and into STA phase and the concentration of nutrient X in the medium are shown in Figure 3.1. The limiting nutrient will be fully depleted during the STA phase of growth, corresponding with the highest biomass in terms of that nutrient as biomass X. However, the instantaneous productivity rate of biomass X, which is the product of biomass and growth rate, peaks in late EXP phase of growth, when nutrient concentrations are still relatively high.

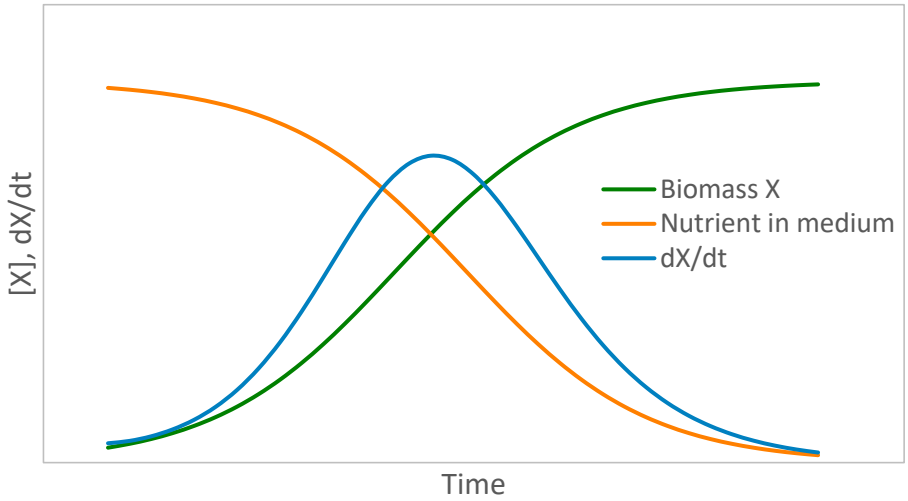

Figure 3.1. Modeled batch culture showing increasing biomass X (green), decreasing nutrient X in the medium (orange), and biomass X productivity rate – dX/dt – (blue). The curves area based on a Gompertz model (Eq. 3.4).

3.1.4. Subject of the study

Given the prospective acceptance of algal biomass as a food or feed in emerging markets due to high nutritional value, particularly in long-chain PUFAs, like EPA, and proteins, it is crucial to dig deeper into algal biomass characterization to identify strains with optimal profiles. A promising avenue for commercial algal biomass production involves utilizing a waste stream as a nutrient source, potentially promoting mixotrophic growth.

This study characterized algal biomass cultivated in dairy waste WP-amended media using four different strains of microalgae: *Pinguiococcus pyrenoidosus* (Heterokontophyta, Pinguiophyceae), *Chaetoceros muelleri* (Heterokontophyta, Bacillariophyceae), *Tetraselmis suecica* (Chlorophyta), and *Chroomonas mesostigmatica* (Cryptophyta). The cultures were grown in closed systems using control, control + DIC, WP-amended, and WP + DIC (specifically for *P. pyrenoidosus*) media and harvested in EXP and STA phases. Analyzing photosynthetic parameters during the grown outs revealed potential metabolic shifts

in response to the organic content in WP for those species capable of mixotrophic growth. Each species' nutrient uptake (C, N, P) was evaluated and compared with the initial concentrations in the growth media, alongside a detailed characterization of FA allocations for each species. Additionally, the productivity rates of total FA, EPA, and particulate N (as a proxy for proteins) were analyzed to identify the optimal growth phase for harvesting these compounds. Last, a synthesis of strategies adopted by the four species concerning their media and harvested phase is presented.

This study aimed to identify and characterize strains suitable for large-scale culturing using WP as a growth substrate. Accompanying this goal is exploring an intermediate-scale screening method for characterizing algal biomass and nutrient uptake from waste effluents. Cultivating in closed systems seeks to minimize bacterial proliferation by limiting oxygen availability as well as facilitating daily fluorescence monitoring. Additionally, trying mixotrophic cultivation in closed systems, where the oxygen generated from photosynthesis could support heterotrophy and CO_2 from heterotrophy could sustain photosynthesis, might serve as an effective means to assess cultures' performance in WP-amended media.

3.2. Material & Methods

3.2.1. Strain selection

In this study, four microalgal strains representing diverse phyla were tested: *Pinguiococcus pyrenoidosus* CCMP2078, a lesser-known strain with significant potential for omega-3 fatty acid production, *Chaetoceros muelleri* CCMP1316 and *Tetraselmis suecica* CCMP906, a diatom and a green alga commonly employed in aquaculture feeds, and *Chroomonas mesostigmatica* CCMP1168, a cryptophyte known for producing the high-value pigment phycocyanin. These strains were acquired from the National Center for Marine Algae and Microbiota (NCMA), East Boothbay, ME, USA.

3.2.2. Pre-experiment conditions

The cultures were maintained in 6-mL borosilicate closed tubes placed horizontally on light tables. *P. pyrenoidosus* was grown at a light intensity of 190 µmol photons m^{-2} s^{-1}, while the other three species experienced a light intensity of 80 µmol photons m^{-2} s^{-1}. The cultures were subjected to continuous light at a constant temperature of 18 °C, using their preferred media (as denoted by NCMA). Before initiating

the experiments (screening and grow-ups to harvest), all cultures were cultivated in seawater media without organic amendment (control). *P. pyrenoidosus* was grown in modified L1 media (Guillard and Hargraves 1993) with reduced concentrations of N and P (166 µM of NH_4Cl, 10 µM of NaH_2PO_4), with N added as ammonium instead of nitrate and no silicate. *T. suecica* and *C. mesostigmatica* were also cultured in modified L1 media with nitrate (220.5 µM $NaNO_3$). *C. muelleri* was cultured in f/2 media (Guillard and Ryther 1962) with reduced N and P (220.5 µM $NaNO_3$, 9.05 µM KH_2PO_4). Macronutrient concentrations were reduced to decrease the degree of carbon limitation in the media, as the base seawater, tangential flow-filtered seawater from NRC Ketch Harbour, contained about 2 mM DIC.

The cultures were monitored daily, using chlorophyll fluorescence as a proxy for abundance, with a Turner Designs 10-005R fluorometer (Turner Designs, SanJose, CA, USA) and a Satlantic Fluorescence Induction and Relaxation (FIRe) system (Satlantic; formerly, Halifax, NS). Single-turnover induction curves (Huot and Babin 2011) collected with the FIRe were fitted with Fireworx (Audrey Barnett: https://sourceforge.net/projects/fireworx/) to estimate minimum and maximum fluorescence (F_0 and F_m, rhodamine Eq. L^{-1}), the derived dimensionless parameter F_v/F_m (=[F_m-F_0]/F_m), and the photosynthetic cross-section, σ ($Å^2$). The fluorescence ratio, F_v/F_m, the quantum yield of electron transport at PSII, is a measure of the proportion of functional reaction PSII centers. The photosynthetic cross-section is a measurement of the size of the PSII antennas.

To ensure the microalgae remained nutrient-replete and in balanced growth, they were maintained in semi-continuous culture (MacIntyre and Cullen 2005), with an inoculum transferred into fresh media when *F* reached approximately 50 % of their maximum value obtained in STA phase batch culture (F_{max}). Cultures were considered suitable for inoculating experiments when the regression of dilution-corrected *F* on time over 10 generations had an R^2 value exceeding 0.995 (MacIntyre and Cullen 2016) and when F_v/F_m remained stable (coefficient of variation < 10 %).

3.2.3. WP concentration screening

Cultures were screened for growth on WP-amended media using 24-well culture plates covered with a porous membrane and placed within a CO_2-generating system (C-box; see Chapter 2, section 2.2). Yamamoto (2023) previously evaluated WP concentrations of 0.05, 0.15, 0.5, and 1.5 g L^{-1} while cultivating *P. pyrenoidosus* and *T. suecica*. The present study tested the growth of *C. muelleri* and *C. mesostigmatica* in media amended with 0.15, 0.25, 0.4, and 0.5 g WP L^{-1}.

3.2.4. Treatments and grow-up experiments

Larger-scale experiments were conducted on batch cultures of microalgae grown in 60-mL borosilicate closed tubes at light intensities described above. For each species, cultures were inoculated from a parent maintained in balanced growth in control or WP-amended media. The "+DIC" treatments involved the addition of 2 mM $NaHCO_3$ to the control and/or WP media, effectively doubling the dissolved inorganic carbon (DIC) concentration. The following abbreviations are used:

- CTRL: Control media (i.e., not amended with WP);
- CTRL+DIC: Control media with 2 mM $NaHCO_3$;
- WP: WP-amended media, concentration specific to each species and described below;
- WP+DIC: WP-amended media with 2 mM $NaHCO_3$ – (for *P. pyrenoidosus* only).

The WP-amended media was prepared by dissolving WP powder (Agropur, Lot# 321190702-22; collected on August 22nd, 2019) in 1 M NaOH at a concentration of 50 g L^{-1}. The solution was then autoclaved in a Pyrex bottle for 45 minutes at 121 °C and a pressure of about 100 kPa (15 PSI) using a vacuum steam sterilizer (Lancer LSS 275). After cooling, the WP solution was added to CTRL seawater media described above, modified by excluding phosphate. The WP concentrations added to the media for each species were as follows: 0.05 g L^{-1} for *P. pyrenoidosus*, 0.5 g L^{-1} for *T. suecica* and *C. muelleri*, and 0.15 g L^{-1} for *C. mesostigmatica*. Each WP media resulted in different pH levels, where *P. pyrenoidosus* was cultivated at pH 7.5, *C. muelleri* and *T. suecica* were cultivated at a pH level of 9.6, and *C. mesostigmatica* was cultivated at pH 8.3.

The cultures underwent two growth cycles: first to reach STA phase and second to reach late EXP phase, both terminated by harvesting for biomass characterization. First, *F* was monitored daily, and cultures were tracked until they had been in STA phase for the equivalent of three generations (measured with the maximum growth rate determined in EXP phase), where the generation time (t_{gen}) was calculated using Equation 3.1 (Wood et al. 2005). The maximum growth rate (μ_{max}) was obtained by fitting the daily measurements of *F* to a modified Gompertz model (Zwietering et al. 1990), further modified with a non-zero intercept to account for varying initial values of *F* (Equation 3.2).

$$t_{gen} = \frac{\ln(2)}{\mu_{max}} \quad \text{(Eq. 3.1)}$$

$$F_t = \left[F_{max} \cdot e\left(-e^{\frac{\mu_{max} \cdot e}{F_{max}}(\lambda - t) + 1}\right)\right] + F_{init} \quad \text{(Eq. 3.2)}$$

where F_t is the time-dependent value of ln-transformed *F*, F_{max} is the maximum ln-transformed value of *F*, F_{init} is the initial ln-transformed value of *F*, λ is the duration of the lag phase (d), and *t* is time (d). The growth rates presented in the result section for STA cultures are the values of μ_{max} from Equation 3.2, as this model is widely used for exponentially grown organisms. To facilitate the determination of the onset of STA phase, a modified Blackman model was also used to fit the daily *F* data (Equation 3.3) as in MacIntyre et al. (2018). The Blackman model is an extreme simplification of the models that describe saturating kinetics (Jones et al. 2014).

$$F = F_{init} \text{ for } t \leq \lambda \quad \text{(Eq. 3.3a)}$$

$$F_t = \frac{(F_{max} - F_{init}) \times (t-\lambda) + t_{sat} - |(t-\lambda) - t_{sat}|}{2 \times t_{sat}} + F_{init} \text{ for } t > \lambda \quad \text{(Eq. 3.3b)}$$

where, t_{sat} is the time (d) to saturation (duration of the growth from λ to STA phase).

The second set of cultures was grown until late EXP phase, after which they were harvested. The target *F* for the EXP harvest was established based on the highest calculated value of fluorescence productivity rates (d*F*/dt; Equation 3.4), computed from the time-dependence of *F* values of the STA-harvested cultures, as modelled from the fits to Gompertz' model (Equation 3.2).

$$\frac{dF}{dt} = F_t * \mu \quad \text{(Eq. 3.4)}$$

where

$$\mu = \frac{F_x - F_{x-1}}{t_x - t_{x-1}} \quad \text{(Eq. 3.5)}$$

where d*F*/dt is the fluorescence productivity rate, F_t is the time-dependent specific fluorescence from the model, and μ is the time-dependent/specific fluorescence-based growth rate calculated by Equation 3.5. The growth rates presented for EXP cultures were determined by fitting daily ln-transformed *F* in EXP to a linear regression, where the slope of this regression represented μ_{max}.

3.2.5. Culture harvest & sample characterisation

The cultures were harvested to characterize biomass composition in EXP and STA phases across treatments. Samples of whole culture were collected to measure cell and chlorophyll-*a* (Chla) concentrations. Additionally, cultures were collected on Whatman GF/F filters to measure particulate C,

N, P, and FAs. All equipment employed during harvests, such as glass pipettes, funnels, scintillation vials, and filters, had been previously subjected to baking at 400 °C in a muffle furnace for two hours to eliminate any organic contaminants.

Duplicate samples were collected in cryovials, preserved by adding 0.4 % (final concentration) of glutaraldehyde, and flash-freezing in liquid nitrogen. Cells were counted using a hemocytometer (Bright-Line™; Lot# 3110) and a microscope (Leitz dialux 20 EB) at 125 X magnification. Chla concentration was quantified following Welshmeyer (1994) using dimethylsulfoxide: 90 % Acetone (3:2) as the extraction solvent. Calibration of the fluorometer (Turner designs 10-005R) was performed using purified Chla (Sigma C6144).

Samples for measurements of particulate C and N were filtered onto pre-combusted 21 mm diameter GF/F filters. These were rinsed with 10 mL of 0.22 µm-filtered seawater following collection and dried in a 60 °C oven (Fisher Scientific; Isotemp). The dried samples were pelleted into combustion foils. Particulate C and N were quantified with a Costech ECS 4010 analyzer (Costech Analytical Technologies Inc.), determined by thermal conductivity after separation by gas chromatography, employing acetanilide standards. Parallel samples were collected on pre-combusted 25 mm GF/F filters for particulate P analyses. The filters were rinsed twice with 2 mL of 0.17 M Na_2SO_4 and soaked with 2 mL of 0.017 M $MgSO_4$ while being dried at 90 °C. The dried filters were combusted, hydrolyzed, and phosphate determined calorimetrically, following Solórzano and Sharp (1980).

To prepare samples for FA analyses, cultures were filtered onto pre-combusted GF/F filters (47 mm diameter) followed by rinsing with 10 mL of 0.22 µm-filtered boiling seawater. Fatty acid analyses were conducted by the Marine Lipids Laboratory, supervised by Professor Suzanne Budge at the Department of Process Engineering and Applied Science, Dalhousie University. The analysis employed a modified Folch, Lees, and Sloane Stanley (1957) method, as described by Parrish (1999).

3.2.6. Data and statistical analyses

The particulate N concentration, fluorescence-based growth rates, nutrient concentrations, and productivity rates were averaged across three biological replicates, and standard deviations (SD) were calculated for treatment variability. To assess significant differences, one- and two-way analyses of variance (ANOVA) were conducted using a significance level of 0.05, employing Microsoft Excel. Post-

hoc Tuckey HDS tests were applied to compare different treatments: CTRL, CTRL+DIC, WP, WP+DIC (for *P. pyrenoidosus* only). Biomass productivity rates were calculated differently for EXP and STA cultures. In EXP cultures, production rates (dX/dt) were calculated as the product of the biomass component (X) concentrations and maximum growth rates in the cultures, following Equation 3.4 by replacing *F* with biomass component X. As for STA cultures, yield rates were calculated from the change in concentration of the biomass component (X) over the interval between the peak biomass productivity measured in EXP phase and the time of the STA harvest using Equation 3.6.

$$dX/dt_{STA} = \frac{X_{STA} - X_{EXP}}{t_{STA} - t_{EXP}} \quad \text{(Eq. 3.6)}$$

where X is the valuable biomass.

Multivariate statistical analyses were performed using PRIMER 7 software (Plymouth Routines In Multivariate Ecological Research, Primer-E), comparing the culture's responses in different growth media. The first analysis was to compare photosynthesis-related characteristics in EXP phase – F_v/Chla, Chla/cell, F_v/F_m, and sigma (σ) – where variables were standardized to the total in the software before the analysis. A resemblance matrix was created based on Euclidean distances between samples for each species individually. One-way analyses of similarity (ANOSIM) were conducted to test for treatment differences. Subsequently, cluster analyses at Euclidean distances 1, 2, and 3 were performed and overlayed onto two-dimensional metric multidimensional scaling (MDS) plots, illustrating distinctions among samples. Following this, analyses of similarity percentage (SIMPER) were executed to identify the variables most responsible for these differences.

The fatty acid dataset quantified 68 FAs, of which the 17 most abundant FAs across all species, collectively accounting for 80-85% of the total FA concentration, were included in the comparison. This reduction was achieved using a matrix display wizard in PRIMER, generating heat maps showing the top 10 most abundant FAs for each species, which ultimately resulted in a set of 17 FAs common to all species. The data was normalized to particulate C, and outliers were removed from the analyses. The data is presented using heat maps of each species' 17 most abundant FAs, displaying clusters of FAs and variables. Two-way crossed ANOSIM tests were carried out to compare growth phases and treatments, and SIMPER analyses were conducted to identify FAs contributing the most to the observed differences.

3.3. Results

3.3.1. WP concentration screening

In prior screening trials, small-scale grow-up experiments were conducted with WP concentrations of 0.05, 0.15, 0.5, and 1.5 g L^{-1}, assessing the growth of *P. pyrenoidosus* and *T. suecica*. It was concluded that *P. pyrenoidosus* thrived in media with 0.05 g L^{-1}, while *T. suecica* exhibited optimal growth at 0.5 g L^{-1} WP (Yamamoto, 2023). In line with the favourable conditions for *T. suecica*, *C. muelleri* was also cultivated using a WP concentration of 0.5 g L^{-1}. Preliminary findings indicated higher yield and growth rates for *C. mesostigmatica* with 0.15 g L^{-1} of WP (data not presented).

3.3.2. Biomass in particulate N

Following the determination of optimal WP concentrations for each species, larger-scale cultures intended for harvests in both EXP and STA phases for biomass characterization were set up. Each treatment and species' daily *F* were fitted to Gompertz and Blackman models. Fluorescence and biomass data are presented in Appendix 5.3, Table 5.13, and the fit parameters are in Appendix 5.4, Table 5.14.

The concentration particulate N was selected as the parameter to present the biomass of the cultures. It was chosen because dissolved inorganic N is more likely the limiting nutrient due to its decreased concentration and considering the elevated levels of C and P in WP. Within this section, comparisons of N concentrations were made between treatments and growth phases. The particulate N concentration of all four species, with the dashed line indicating the initial N concentration in the media, is shown in Figure 3.2.

Nitrogen concentrations of *P. pyrenoidosus* remained consistent across treatments in STA cultures ($p > 0.05$). In contrast, EXP culture displayed a varied trend, where CTRL ± DIC treatments exhibited significantly lower N concentration in EXP ($p < 0.01$), while WP ± DIC treatments had similar N concentration compared to STA cultures ($p > 0.05$). In *C. muelleri*, the N concentrations remained consistent between EXP and STA cultures within each treatment ($p > 0.05$). However, the N in WP cultures was significantly higher ($p < 0.01$), approximately twice as high as CTRL ± DIC treatments. For *T. suecica*, N concentration in STA cultures across treatments showed similarity ($p > 0.05$), while CTRL ± DIC cultures had lower N compared to cultures in WP in EXP phase ($p < 0.01$). In *C. mesostigmatica*, the N concentration of STA cultures in CTRL was significantly higher than in WP ($p < 0.01$). Additionally, EXP

cultures in CTRL + DIC treatment showed significantly higher N concentration than in WP and CTRL treatments ($p < 0.01$). Cultures of C. mesostigmatica in STA phase in CTRL + DIC treatment displayed an unexpectedly high N concentration, approximately double the concentration added to the media. This discrepancy was likely due to an error during the filtration process at harvest. These doubled values were divided by two for better accuracy in the nutrient-uptake analyses below.

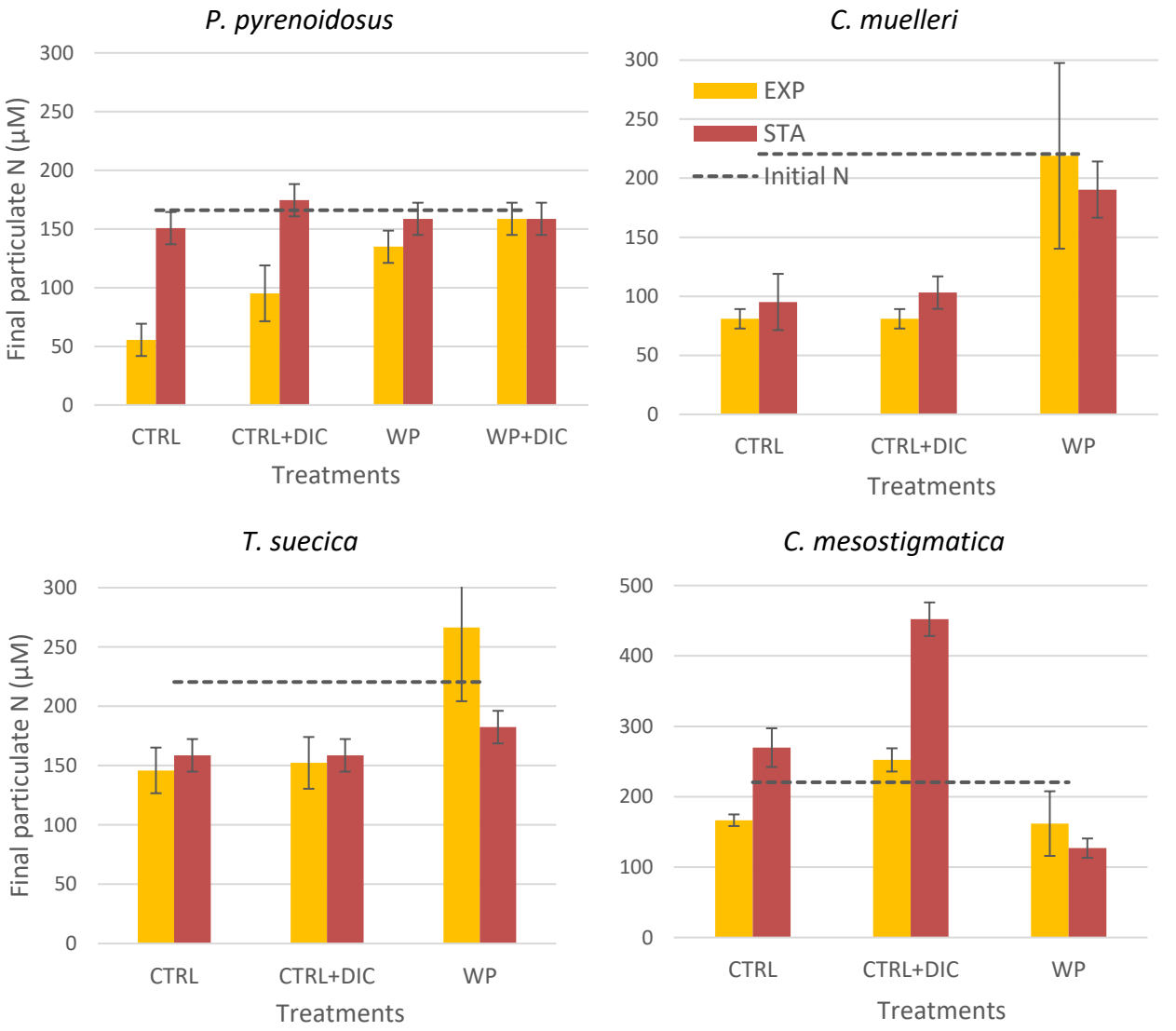

Figure 3.2. Particulate N concentrations (mean + SD; n = 3) of EXP and STA harvested cultures of *P. pyrenoidosus*, *C. muelleri*, *T. suecica*, and *C. mesostigmatica* grown in 60-mL closed tubes in CTRL, CTRL+DIC, WP, and WP+DIC media. Dashed line are initial dissolved inorganic N concentrations in the media: 166 µM NH_4^+ for *P. pyrenoidosus* and 220.5 µM NO_3^- for the three other species.

3.3.3. Fluorescence and photosynthetic system

Fluorescence-based growth rates

The fluorescence-based growth rates of STA- and EXP-phase harvested cultures were determined using distinct methods. The maximum growth rates (μ_{max}) for STA cultures were obtained by fitting the STA ln(*F*) data to a modified Blackman model (Equation 3.3), while μ_{max} for EXP cultures were determined by fitting the EXP ln(*F*) data with a linear regression. In STA cultures, there were no differences in μ_{max} between CTRL and CTRL+DIC for all species, except for *C. muelleri*, where μ_{max} was slightly higher in CTRL+DIC ($p < 0.05$; Figure 3.3). However, WP cultures had lower apparent growth rates with reductions ranging from 10 to 20 % for *P. pyrenoidosus* in WP+DIC, *T. suecica* and *C. mesostigmatica* in WP to about 85 % for *C. muelleri* in WP media ($p < 0.01$). The same pattern was observed in maximum growth rates in EXP cultures for *C. muelleri* and *T. suecica*, where reductions of 55 and 47 % were observed in WP media (Figure 3.4). EXP cultures of *P. pyrenoidosus* showed reduced growth rates in WP ± DIC compared to CTRL ± DIC treatments ($p < 0.05$).

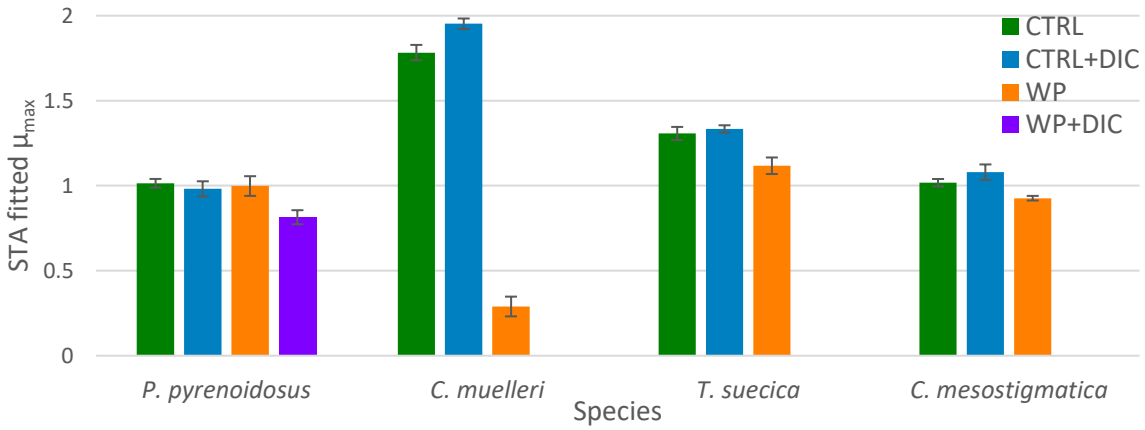

Figure 3.3. Fluorescence-based μ_{max} (mean + SD; n = 3) of STA cultures of *P. pyrenoidosus*, *C. muelleri*, *T. suecica*, and *C. mesostigmatica* grown in 60-mL closed tubes in CTRL, CTRL+DIC, WP, and WP+DIC media. Ln(*F*) data were fitted to a modified Blackman model (Equation 3.3).

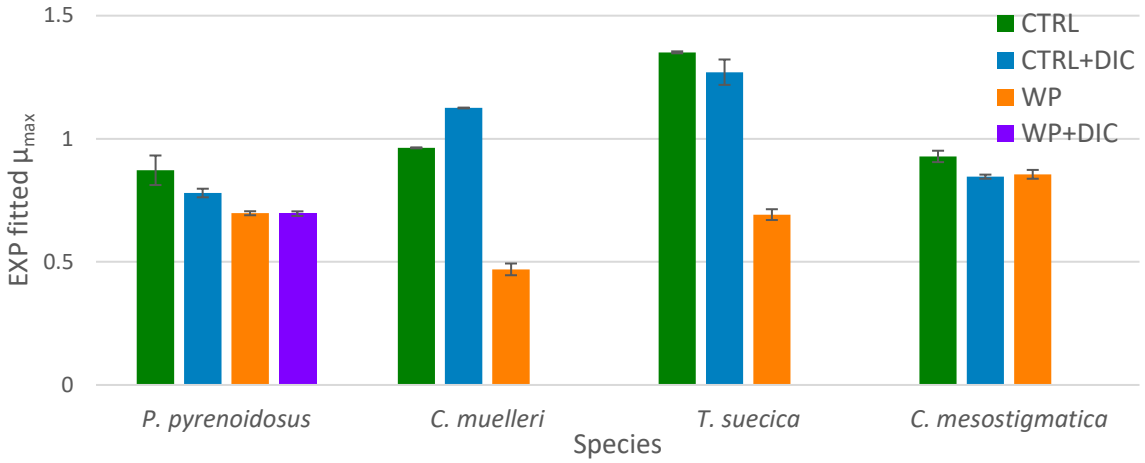

Figure 3.4. Fluorescence-based μ_{max} (mean + SD; n = 3) of EXP cultures of *P. pyrenoidosus*, *C. muelleri*, *T. suecica*, and *C. mesostigmatica* grown in 60-mL closed tubes in CTRL, CTRL+DIC, WP, and WP+DIC media. Ln(*F*) data were fitted to a linear regression.

Photosynthetic response characteristics

Patterns in photosynthetic response variables were compared to further investigate treatments' effect on the cultures and to evaluate the metabolic "strategies" within them. Data from EXP cultures grown in CTRL, CTRL+DIC, WP, and WP+DIC were used for these analyses. Multivariate comparisons were conducted using biomass-independent variables: F_v/F_m, F_v/Chla, Chla/cell, and σ. Matrices of sample-to-sample resemblances (as Euclidian distance) for each species were generated in PRIMER. Significant treatment effects among samples were tested using one-way ANOSIM, a non-parametric, multivariate analog of Analysis of Variance. The analysis compares within-treatment differences of all possible group-to-group comparisons of randomly paired samples to test for significance. Due to the limited number of permutations possible (10), the pairwise tests were constrained to a lower detectable significance level of 0.1. Cluster analyses, allowing more permutations, led to significance levels below 0.1. The clusters generated at Euclidean distances 1, 2, and 3 are overlayed on the MDS ordinations below. Last, SIMPER analyses were conducted to identify variables responsible for the observed differences (see Appendix 5.1, Table 5.1 for detailed results).

P. pyrenoidosus and *C. mesostigmatica* did not show any overall significant differences in the CLUSTER analyses, as shown in Figure 3.5. In both species, the samples clustered closely within a Euclidean distance of 1 or 2, indicating small differences between samples from the different experimental treatments. Repeating the analysis with *C. muelleri* and *T. suecica* revealed highly significant clustering, confirmed in ANOSIM between CTRL ± DIC and WP treatments ($p < 0.1$). This distinction is clearly

illustrated by the separations in Euclidean distances of 3 and 10 in Figure 3.6. SIMPER analyses showed that for *C. muelleri* cultures, approximately 55 % of the dissimilarity was influenced by higher σ values in WP, while around 33 % was due to lower F_v/Chla in WP treatment. Substantial differences observed in *T. suecica* cultures were predominantly driven by Chla/cell (>90% of dissimilarity), which were reduced by about 95 % in WP cultures. These results highlight the differences in photosynthetic parameters, likely explaining the reduced apparent growth rates in these two species cultivated in WP media.

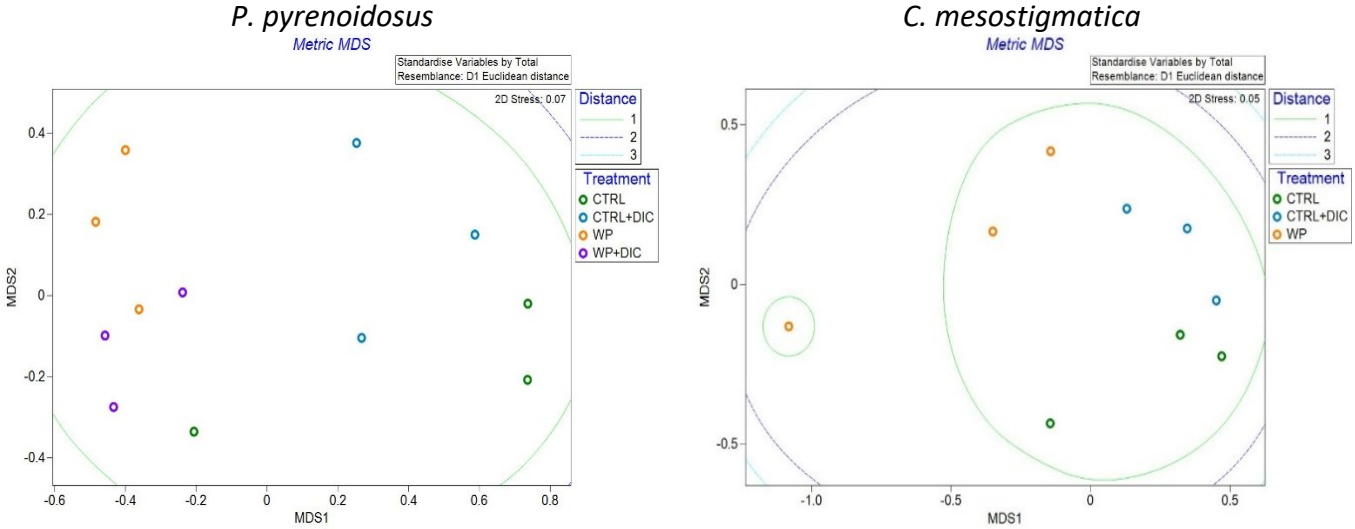

Figure 3.5. Metric MDS of photosynthesis-related biomass independent variables (F_v/F_m, F_v/Chla, Chla/cell, and σ): EXP cultures of *P. pyrenoidosus* and *C. mesostigmatica* grown in 60-mL closed tubes in CTRL, CTRL+DIC, WP, and WP+DIC (0.05 and 0.15 g WP L^{-1}, respectively) treatments.

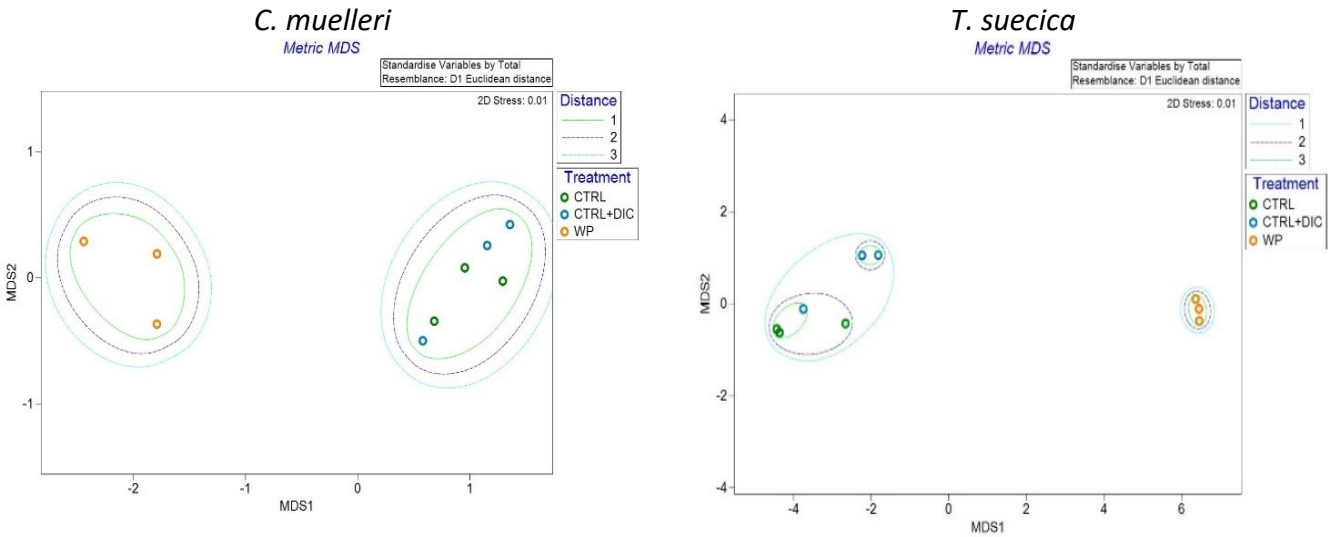

Figure 3.6. Metric MDS of photosynthesis-related biomass independent data variables (F_v/F_m, F_v/Chla, Chla/cell, and σ): EXP cultures of *C. muelleri* and *T. suecica* grown in 60-mL closed tubes in CTRL, CTRL+DIC, and WP (both 0.5 g WP L^{-1}) treatments. Note the coherent separation between CTRL ± DIC and WP treatments.

3.3.4. Nutrient uptake

This section assesses nutrient (C, N, P) uptake by comparing the particulate concentrations at the STA harvest with the initial dissolved inorganic nutrient media composition (Figures 3.7 to 3.9). All species showed significantly higher particulate C in CTRL+DIC compared to CTRL cultures, although this difference was small for *C. muelleri* ($p < 0.05$). *P. pyrenoidosus* exhibited no significant differences in C, N, or P concentrations between the CTRL and WP treatments ($p > 0.05$). As for *C. muelleri*, the intracellular concentrations of C, N, and P were all significantly higher in WP compared to CTRL treatment, where a slight increase in C-uptake for WP compared to CTRL ($p < 0.05$), a higher N-uptake and a massive P-uptake for WP compared to CTRL ± DIC treatments ($p < 0.01$) were observed. These patterns resulted in decreased C:P and C:N ratios in WP cultures. Despite the high N-uptake in WP treatment, the N:P ratio remained markedly lower than in CTRL ($p < 0.05$).

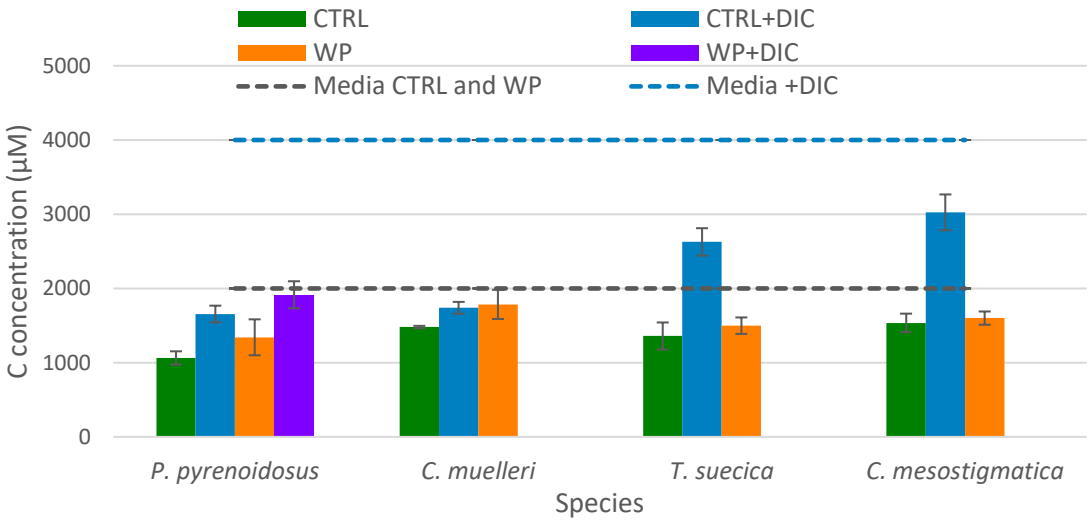

Figure 3.7. Particulate carbon concentration (µM) (mean + SD) on harvest in cultures of *P. pyrenoidosus*, *C. muelleri*, *T. suecica*, and *C. mesostigmatica* grown in CTRL, CTRL+DIC, WP, and WP+DIC media. Initial dissolved inorganic C in the media are the dotted lines.

For *T. suecica*, no significant differences were observed in C or N concentrations between WP and CTRL treatments ($p > 0.05$), but its P content was notably lower in WP ($p < 0.05$). There were no indications of luxury uptake of P in *T. suecica*, which appeared to be P-limited. The particulate P at harvest was significantly lower than the phosphate in the media. The N:P ratio of cultures in WP media was higher than in CTRL ($p < 0.05$). As for *C. mesostigmatica*, there was a significant increase in P-uptake with a simultaneous reduction in N-uptake for WP cultures compared to CTRL ± DIC treatments ($p < 0.05$).

Consequently, the C:P and N:P ratios for cultures in WP were lower than those in CTRL, while C:N was significantly higher due to the lower N-uptake ($p < 0.05$).

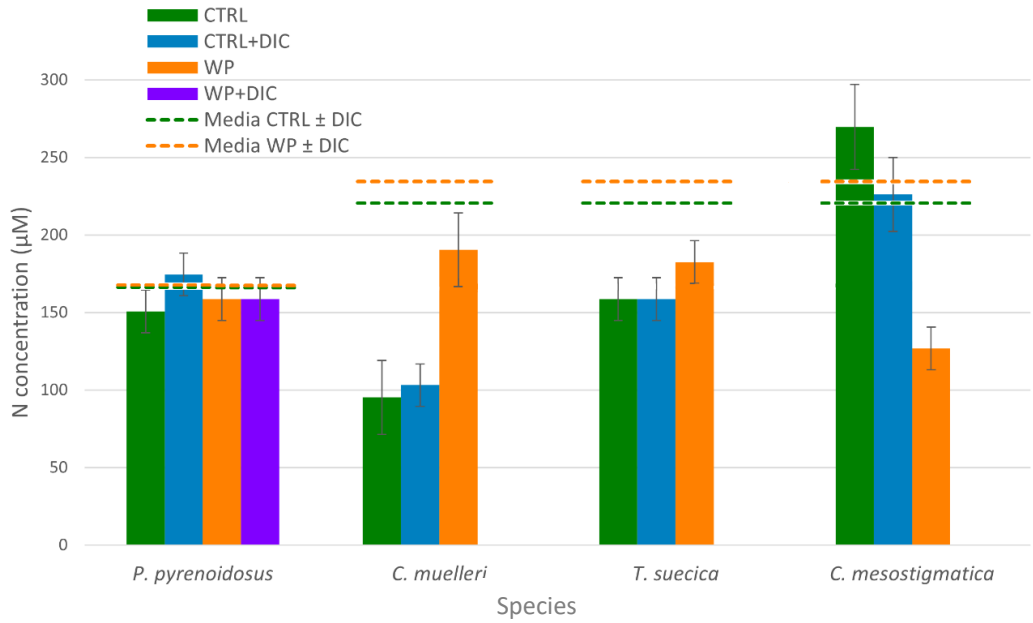

Figure 3.8. Particulate nitrogen concentration (µM) (mean + SD) on harvest in cultures of *P. pyrenoidosus*, *C. muelleri*, *T. suecica*, and *C. mesostigmatica* grown in CTRL, CTRL+DIC, WP, and WP+DIC media. Initial dissolved inorganic N concentrations in the media are the dotted lines.

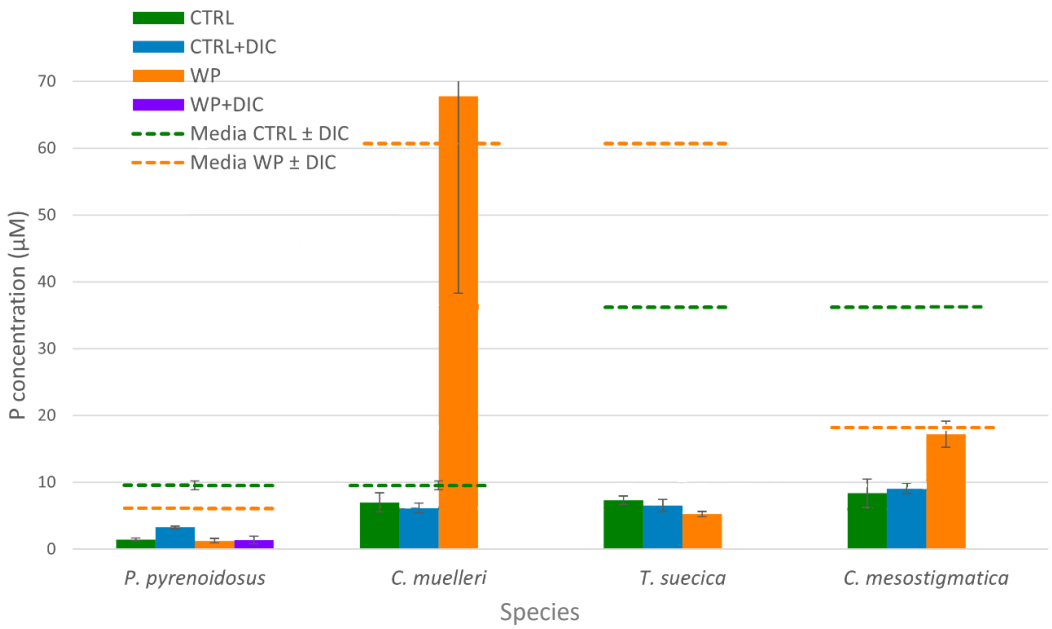

Figure 3.9. Particulate phosphorus concentration (µM) (mean + SD) on harvest in cultures of *P. pyrenoidosus*, *C. muelleri*, *T. suecica*, and *C. mesostigmatica* grown in CTRL, CTRL+DIC, WP, and WP+DIC media. Initial dissolved inorganic P concentrations in the media are the dotted lines.

3.3.5. Fatty acid allocation

The fatty acid composition was tested to assess differences within the four cultures across treatments and growth phases. From the initial extensive dataset of 68 FAs, a condensed set of the 17 most abundant was derived, collectively representing 80-85% of the overall FA content among all species. A cumulative plot of the relative abundance of the complete FA dataset is shown in Appendix 5.2.1, Figure 5.2. The detailed profiles of the 17 most abundant FAs in EXP and STA phases for the four species are shown in Appendix 5.2.2, Tables 5.3 to 5.6. FA data was normalized to C biomass, and outliers identified by the coherence plot wizard in PRIMER software were excluded from the analyses. A heat map displaying the FA composition of all four species in CTRL media in EXP and STA phases, offering an overview of the FA production by each species, is shown in Figure 3.10. Dendrograms of FA are shown in the y axis to provide information on the covariance of certain FAs, potentially within a same metabolic pathway. *P. pyrenoidosus* culture's most abundant FAs were 14:0 (myristic acid) and 20:5n-3 (EPA), while for *C. muelleri*, it was 16:1n-7 (palmitoleic acid) and 16:0 (palmitic acid). *T. suecica* produced more of 16:0, 18:3n-3 (alpha-linolenic acid), and 16:4n-3, while *C. mesostigmatica* had the highest concentrations of FAs 18:3n-3 and 18:4n-3 (stearidonic acid).

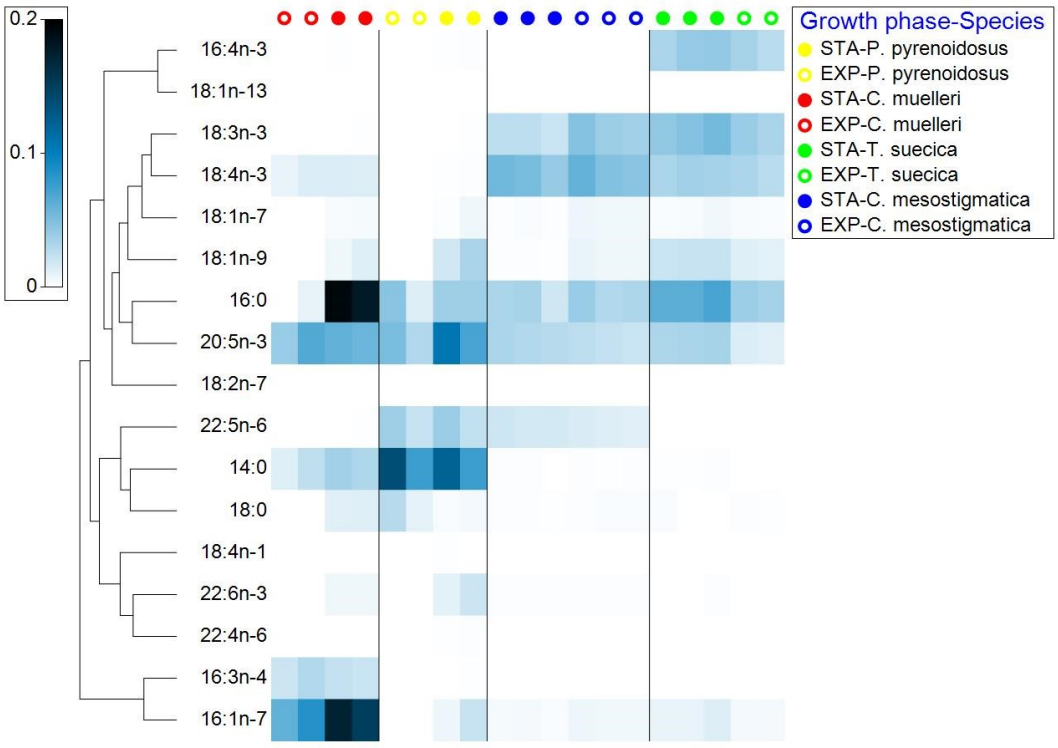

Figure 3.10. Heat map of relative abundance of fatty acids for CTRL cultures of *P. pyrenoidosus*, *C. muelleri*, *T. suecica*, and *C. mesostigmatica* in EXP and STA phases. Data have been normalized to C content and are presented as µg FA per µg of particulate C.

To compare between growth phases and treatments for each species, two-way crossed ANOSIM and SIMPER analyses were carried out, with detailed statistical outcomes provided in Appendix 5.2.3, Tables 5.7 and 5.8. Below, heat maps illustrate the relative abundance of FAs for each species, presenting dendrograms of FA clusters on the left of the figure. Growth phase/treatment clusters are displayed above the figure, where red dotted lines represent samples that are not statistically different ($p > 0.05$). Additionally, coherence plots of each FA cluster for all species are shown in Appendix 5.2.4, Figures 5.9 to 5.12.

The relative FA abundance of *P. pyrenoidosus* cultures shows the increased prevalence of FAs like 16:0, 20:5n-3, 22:5n-6 (docosahexaenoic acid; DHA), and 14:0. ANOSIM results indicated significant differences between growth rates and treatments ($p < 0.05$; Figure 3.11). The predominant FAs contributing to the variance between EXP and STA cultures were 14:0 (44% of cumulative dissimilarity) and 16:0 (30% of dissimilarity), with higher levels of both observed in STA phase. Significant differences emerged in pairwise tests between treatments CTRL ± DIC and WP+DIC ($p < 0.05$), primarily influenced by 14:0, 16:0, and 20:5n-3, with values generally higher in WP+DIC treatment.

There was a noticeable FA abundance separation between EXP and STA cultures for *C. muelleri*, primarily due to the elevated presence of 16:0 (71% of dissimilarity) during STA phase (Figure 3.12). Treatment analysis through ANOSIM indicated distinctions among CTRL+DIC and WP treatments ($p < 0.05$). The difference was due primarily to FA 16:0 (69% of dissimilarity), which was present at lower concentrations in the WP treatment.

The relative abundance of FAs in *T. suecica* cultures showed considerable divergence, especially between treatments CTRL ± DIC and WP ($p < 0.01$, Figure 3.13). SIMPER analyses confirmed this difference, primarily driven by 16:0 (23-25% of dissimilarity), 18:3n-3 (24-25% of dissimilarity), 16:4n-3 (18-20% of dissimilarity), and 18:4n-3 (12-14% of dissimilarity), which were much lower in WP and nearly absent. Although WP cultures largely down-regulated FA quotas, the cultures had higher concentrations of 18:1n-7 (cis-vaccenic acid), which was nearly absent in CTRL ± DIC cultures. Additionally, significant differences were observed between growth phases ($p < 0.05$), where FA 18:1n-9 (oleic acid, 33% of dissimilarity), 16:0 (33% of dissimilarity), and 18:4n-3 (13% of dissimilarity) were the main drivers. While the relative abundance of 18:1n-9 and 16:0 was lower in EXP phase, 18:4n-3 accounted for a higher proportion of the FAs during this phase.

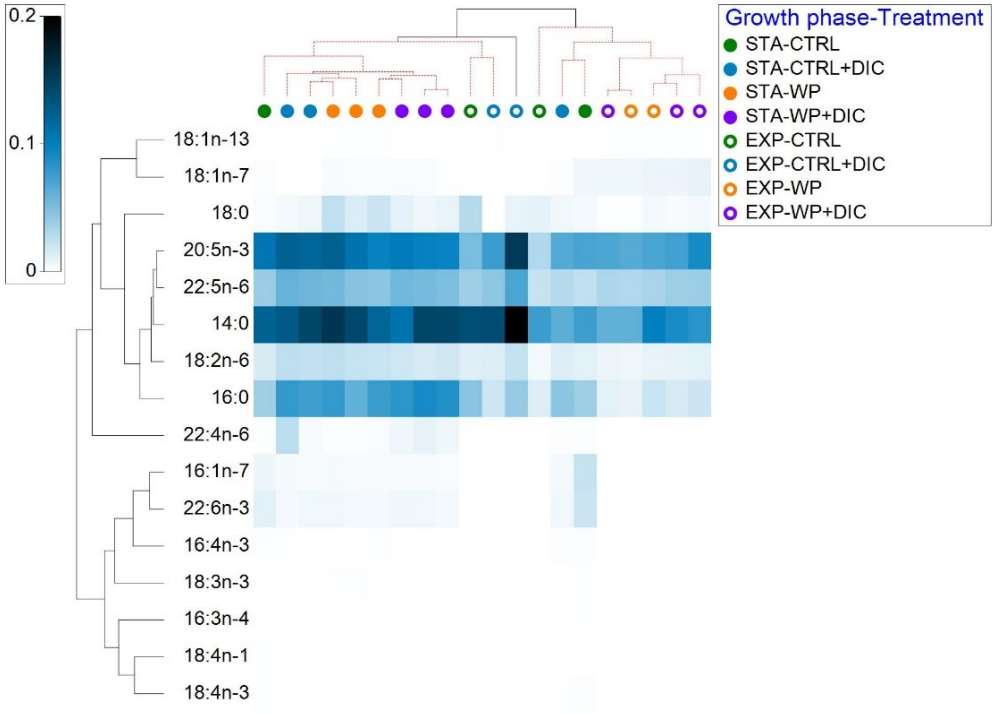

Figure 3.11. Heat map of relative abundance of fatty acid composition: EXP and STA cultures of *P. pyrenoidosus* grown in 60-mL closed-tube in CTRL, CTRL+DIC, WP (0.05 g L^{-1}), and WP+DIC treatments. Data have been normalized to C content and are presented as µg FA per µg of particulate C.

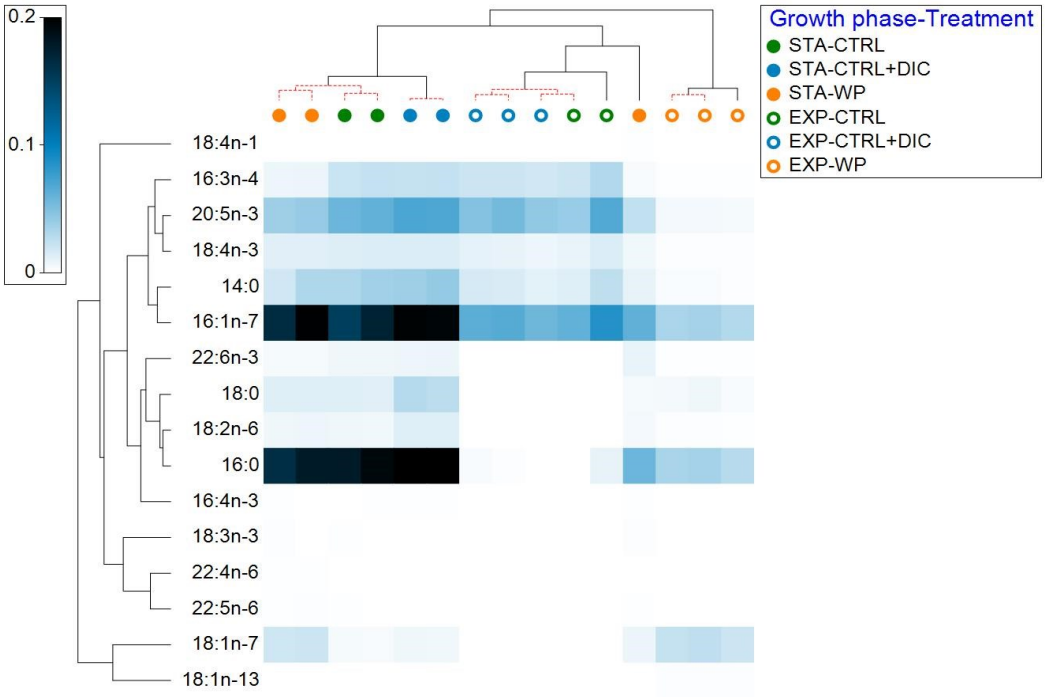

Figure 3.12. Heat map of relative abundance of fatty acid composition: EXP and STA cultures of *C. muelleri* grown in 60-mL closed-tube in CTRL, CTRL+DIC, and WP (0.5 g L^{-1}) treatments. Data have been normalized to C content and are presented as µg FA per µg of particulate C.

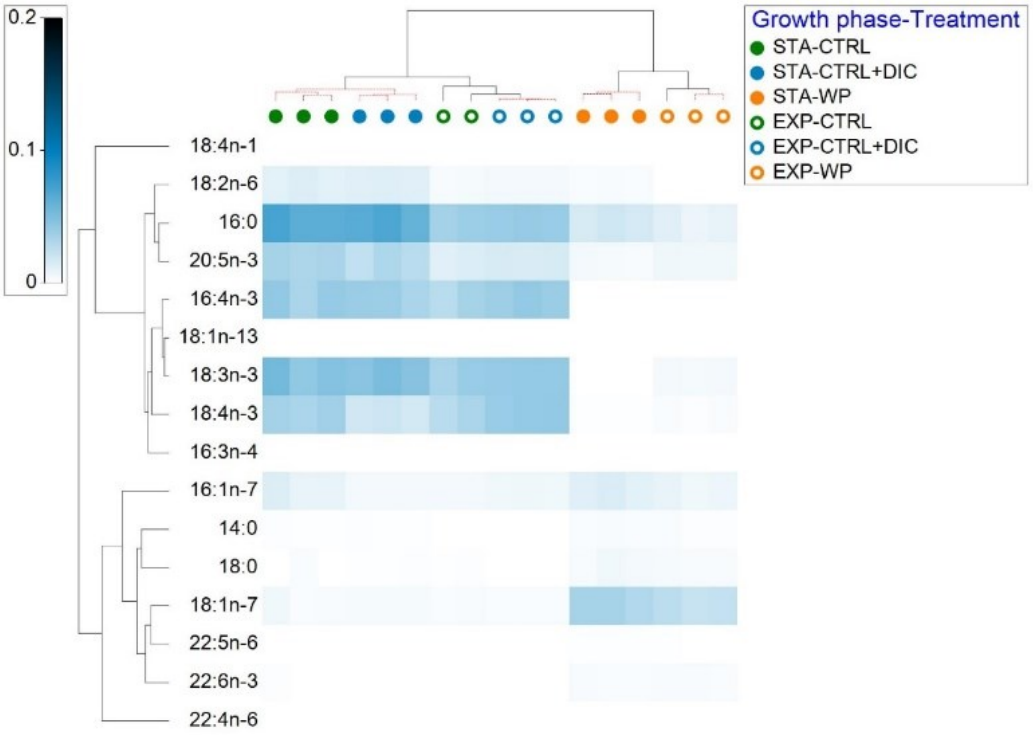

Figure 3.13. Heat map of relative abundance of fatty acid composition: EXP and STA cultures of *T. suecica* grown in 60-mL closed-tube in CTRL, CTRL+DIC, and WP (0.5 g L^{-1}) treatments. Data have been normalized to C content and are presented as µg FA per µg of particulate C.

In the last species, *C. mesostigmatica* displayed very distinct FA patterns, particularly in STA cultures in WP, compared to others (Figure 3.14). ANOSIM analysis indicated significant differences across growth phases and treatments ($p < 0.05$). The primary FAs contributing to the contrast between growth phases were 16:0 (50% of dissimilarity) and 18:3n-3 (30% of dissimilarity), having much higher concentrations in STA cultures in WP. As for differences between treatments, WP samples had notable distinctions compared to CTRL ± DIC treatments, predominantly driven by the elevated levels of 16:0 (39-45% of dissimilarity) and 18:3n-3 (23-29% of dissimilarity), which were nearly three times higher in WP samples than in CTRL ± DIC treatments.

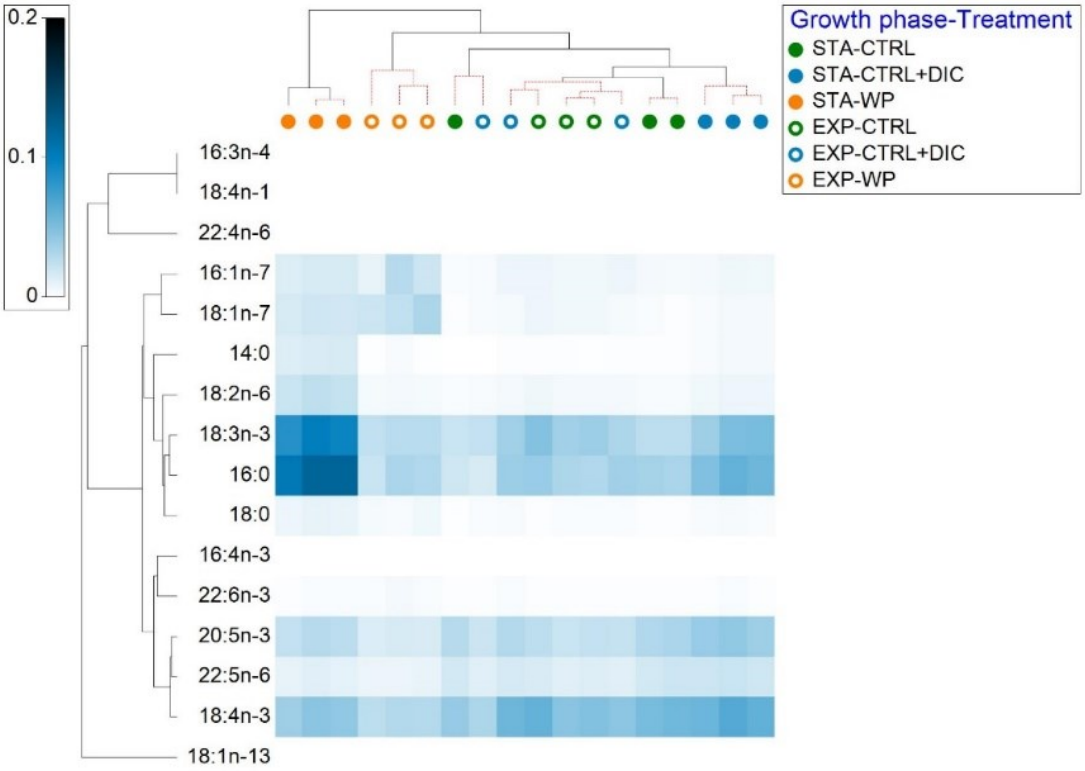

Figure 3.14. Heat map of relative abundance of fatty acid composition: EXP and STA cultures of *C. mesostigmatica* grown in 60-mL closed-tube in CTRL, CTRL+DIC, and WP (0.15 g L^{-1}) treatments. Data have been normalized to C content and are presented as µg FA per µg of particulate C.

3.3.6. Biomass productivity rates

To effectively cultivate microalgae on a large scale for commercial use, it is crucial to assess the production rates of the target products and pinpoint the optimal growth conditions for harvesting. This study analyzed the productivity rates (dX/dt) of different variables, such as total FA for biofuel production, EPA, an essential omega-3 FA for human and animal consumption, and particulate N as a proxy protein. The objective was to identify a species capable of generating significant quantities of these cellular compounds in WP-amended media. Production rates in EXP cultures were calculated as the product of the concentration of each target metabolite by EXP μ_{max}. Production rates for the transition from EXP to STA cultures followed Equation 3.6. Comparisons between species are not definitive due to variations in the media composition, distinct WP concentrations, and differences in light intensities under which they were cultivated.

Total fatty acids

Examining the production rates of total FA by each species could provide insights into potentially valuable FA like EPA but primarily indicates their potential in biofuel production. The total FA production rates (dFA/dt) across treatments and growth phases for each species are illustrated in Figure 3.15. *P. pyrenoidosus* had similar total FA production rates in EXP phase across treatments ($p > 0.05$) and notably higher rates in EXP compared to STA in WP ± DIC treatments ($p < 0.05$). In contrast, *C. muelleri* showed no significant differences between EXP and STA cultures in CTRL and WP treatments ($p > 0.05$). However, DIC enrichment of the control (CTRL+DIC) resulted in about 2x increase in FA production rate in STA phase ($p < 0.05$). For *T. suecica*, adding WP to the growth medium decreased the FA production rate in EXP phase by 67 % ($p < 0.05$). In STA phase, FA productivity rates were significantly lower across all treatments compared to EXP ($p < 0.05$). A similar pattern was observed in *C. mesostigmatica* in EXP phase, although the reduction with the addition of WP was less pronounced (about 34 %) but still significant ($p < 0.05$). As with *T. suecica*, FA production rates in STA cultures were lower than in EXP but were significantly higher in CTRL+DIC and WP treatments than in the CTRL ($p < 0.05$). Across cultures, the highest yield rates of total FAs were in DIC-enriched CTRL media and were highest in *P. pyrenoidosus*.

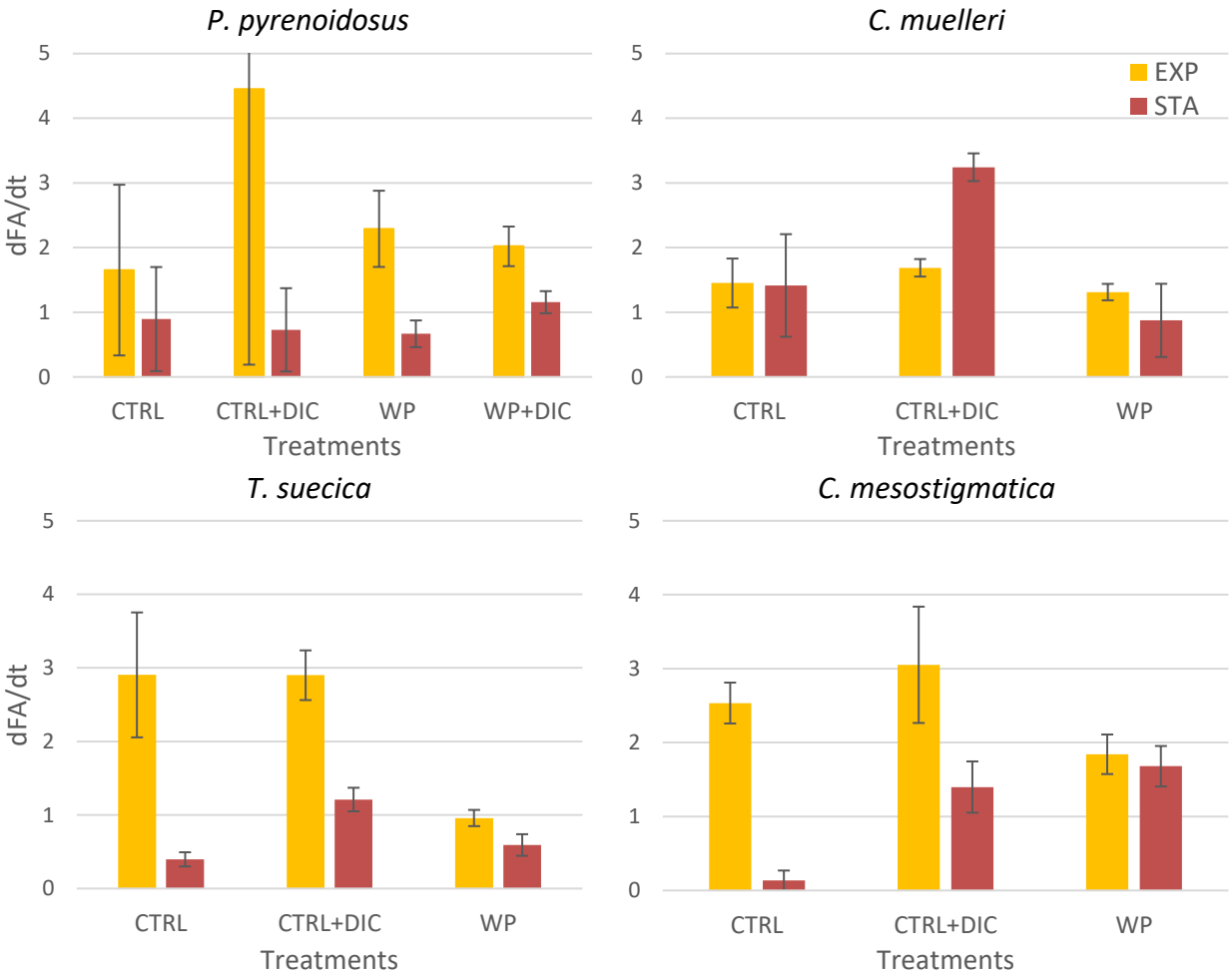

Figure 3.15. Productivity rates of total FA (dFA/dt) in mg of FA L^{-1} d^{-1} (mean + SD) of EXP and STA harvested cultures of *P. pyrenoidosus*, *C. muelleri*, *T. suecica*, and *C. mesostigmatica* grown in 60-mL closed tubes in CTRL, CTRL+DIC, WP, and WP+DIC media.

Eicosapentaenoic acid (EPA)

Production rates of the valuable fatty acid EPA (dEPA/dt) were assessed across treatments and growth phases (Figure 3.16). For *P. pyrenoidosus*, a notable disparity in EPA productivity rates was observed between EXP and STA cultures for all treatments except for CTRL ($p < 0.01$), with values reaching 0.5-0.6 mg EPA L^{-1} d^{-1} in EXP phase but only about 0.2 mg EPA L^{-1} d^{-1} in the transition from EXP to STA phase. The productivity rates of STA culture in WP+DIC exceeded those in WP ($p < 0.01$). In contrast, EPA production rates in WP treatment were significantly lower than in CTRL ± DIC treatments for the remaining three species in EXP cultures. The CTRL ± DIC culture of *C. muelleri* had high EPA productivity rates in EXP phase, comparable to those of *P. pyrenoidosus*, while the STA phase cultures again had significantly lower yield rates ($p < 0.05$). Alone among the test species, WP cultures of *C. muelleri* had higher EPA productivity rates in the EXP-to-STA transition than in EXP phase ($p < 0.01$).

The EPA production rates were much lower in *T. suecica* and *C. mesostigmatica* than in *P. pyrenoidosus* and *C. muelleri*. The trends in EPA productivity rates were otherwise similar, with EXP cultures consistently having higher values than STA cultures across all treatments ($p < 0.01$). EPA production in WP treatment was significantly lower than in CTRL ± DIC treatments for both species ($p < 0.01$). EPA production rates in the WP treatment were significantly lower than in CTRL ± DIC treatments for both *T. suecica* and *C. mesostigmatica* ($p < 0.01$).

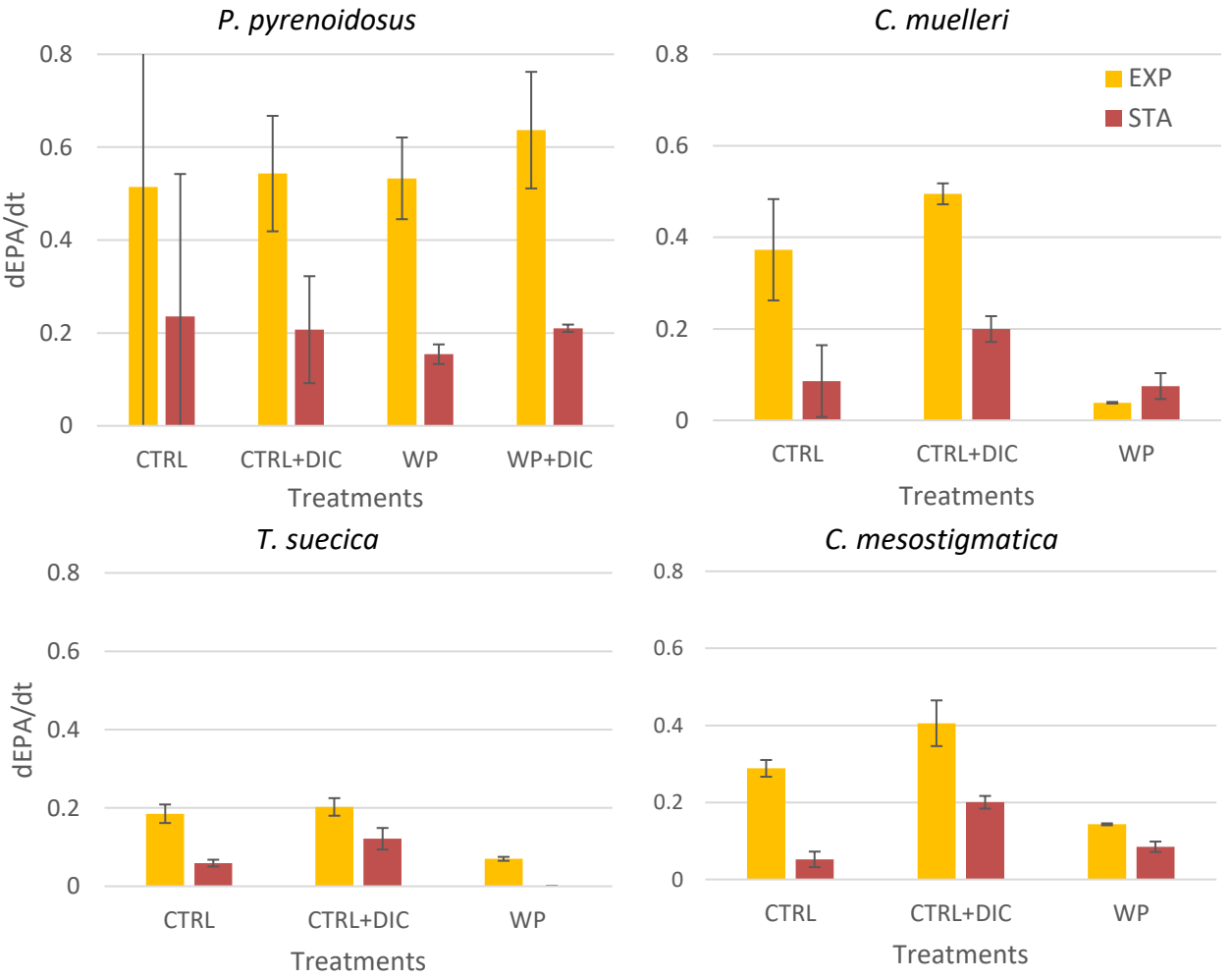

Figure 3.16. Productivity rates of EPA (dEPA/dt) in mg of EPA L^{-1} d^{-1} (mean + SD) of EXP and STA harvested cultures of *P. pyrenoidosus*, *C. muelleri*, *T. suecica*, and *C. mesostigmatica* grown in 60-mL closed tubes in CTRL, CTRL+DIC, WP, and WP+DIC media.

Nitrogen as a proxy for proteins

Most protein samples collected at harvests were below the assay's limit of detection or had high signal-to-noise ratios that complicated interpretation (data not presented). As proteins account for a

significant fraction of cellular N, particulate N was employed to estimate protein concentration within the cultures. N productivity rates (dN/dt) for each species were considerably higher in EXP cultures compared to STA cultures ($p < 0.05$), as shown in Figure 3.17. For *P. pyrenoidosus* and *C. muelleri*, N production rates were significantly higher in WP treatment compared to CTRL treatment ($p < 0.05$). In contrast, dN/dt remained similar across these treatments for cultures of *T. suecica* and *C. mesostigmatica* ($p > 0.05$). Furthermore, *C. mesostigmatica* cultures in CTRL+DIC treatment exhibited higher N productivity rates than other treatments ($p < 0.05$). In a comparison between species, the N productivity rates in EXP were inversely related to the FA production rate. The FA production rates were high in *P. pyrenoidosus* and *C. muelleri*, and N production rates were relatively low, while dFA/dt were low in *T. suecica* and *C. mesostigmatica*, and dN/dt were relatively high.

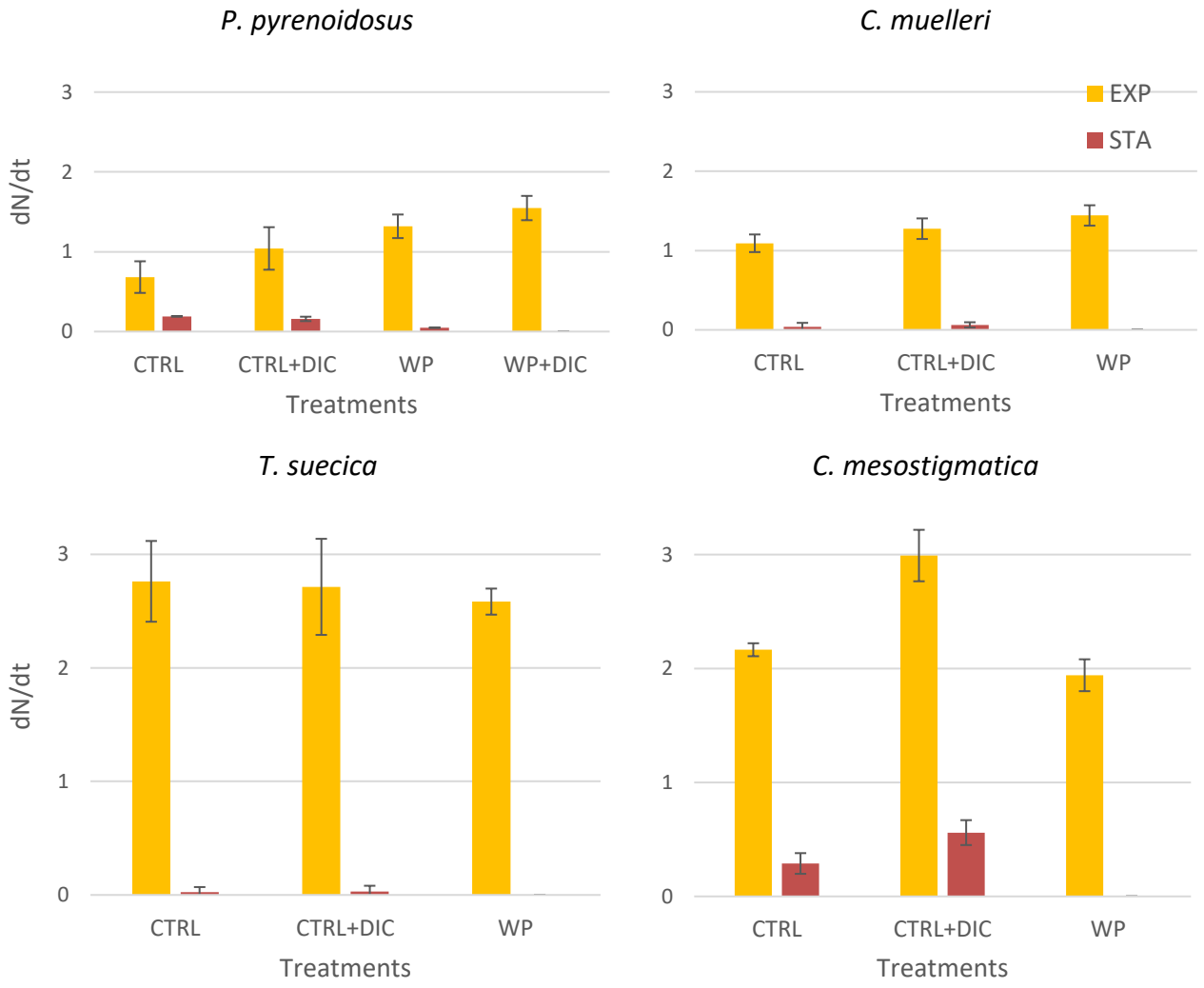

Figure 3.17. Productivity rates of particulate N (dN/dt) in mg of N L^{-1} d^{-1} (mean + SD) of EXP and STA harvested cultures of *P. pyrenoidosus*, *C. muelleri*, *T. suecica*, and *C. mesostigmatica* grown in 60-mL closed tubes in CTRL, CTRL+DIC, WP, and WP+DIC media.

3.3.7. Synthesis of the effect of WP on cultures

Each species had unique responses to the WP-amended media, synthesized below and in Table 3.18, offering insights into their metabolic mode and resource allocation. *P. pyrenoidosus*, cultivated using the lowest WP concentration (0.05 g L^{-1}), did not exhibit any indications of mixotrophic growth and showed consistent fluorescence and photosynthetic response characteristics comparable to CTRL treatment. No differences were observed in nutrient allocation or FA composition, and EPA was relatively high. This suggests that *P. pyrenoidosus* had access to the P present in WP but did not utilize the organic C. *P. pyrenoidosus* had high EPA production, with higher EPA levels observed in STA phase.

C. mesostigmatica was cultivated using a moderate WP concentration of 0.15 g L^{-1}, and with an increased headspace within the closed tubes to facilitate gas exchange. In the presence of WP-amended media, the cultures did not display major alterations in fluorescence, photosynthetic parameters, or fluorescence-based growth rates. Even so, the N concentration of WP cultures during STA phase was notably lower than observed in CTRL ± DIC treatments, while its P concentration was much higher, indicating a potential capacity for P remediation in WP. Cultures in WP had considerable enhancement in alpha-linolenic and palmitic acids in STA phase, resulting in higher total FA productivity rates for WP cultures compared to CTRL and similar to CTRL+DIC treatment. Moreover, *C. mesostigmatica* had good N (as a proxy for protein) productivity rates in WP, around 2 mg of N L^{-1} d^{-1}, similar to those in CTRL treatment.

C. muelleri and *T. suecica* were both cultivated using a higher concentration of 0.5 g L^{-1} WP. Both species showed a reduction in fluorescence-based growth rates in WP treatment, *C. muelleri* during both EXP and STA phases, and *T. suecica* during EXP phase. Both cultures showed a down-regulation of photosynthetic parameters and displayed fundamentally different structures compared to CTRL ± DIC cultures. *C. muelleri* had a very high P uptake from the WP and a notable increase in N compared to CTRL ± DIC cultures. Its FA quota was elevated, particularly in STA phase, although the WP treatment had lower levels than the CTRL+DIC treatment. Total FA productivity rates during STA phase in WP and CTRL treatments approached similar levels to those observed in the EXP phase. EPA productivity rates were reduced in WP cultures, while N productivity rates remained relatively consistent across treatments.

In *T. suecica* cultures grown with WP, no substantial differences in nutrient uptake were noted compared to the CTRL treatment. The FA composition was markedly different and significantly lower than in CTRL ± DIC treatments. The cultures up-regulated cis-vaccenic acid in WP, a component barely produced in other treatments. In WP media, *T. suecica* had similar total FA production rates during STA phase but much lower rates in EXP phase compared to CTRL ± DIC treatments. Additionally, it displayed reduced EPA production rates but had similar N assimilation, acting as a proxy for proteins.

Table 3.18. Summary of major differences between cultures of *P. pyrenoidosus*, *C. muelleri*, *T. suecica*, and *C. mesostigmatica* in WP-amended media compared to CTRL ± DIC harvested in EXP and STA phases.

Species	***P. pyrenoidosus***	***C. mesostigmatica***	***C. muelleri***	***T. suecica***
[WP]	0.05 g L^{-1}	0.15 g L^{-1}	0.5 g L^{-1}	0.5 g L^{-1}
F-based growth rates	Similar	Similar	↓ in WP in EXP and STA	↓ in WP in EXP
Inferred Mixotrophy	No	No	Yes. ↑ σ ↓ Fv/Chla	Yes. 20X ↓ Chla/cell
[Nutrient] and ratios in STA	Similar	Luxury uptake P ↑ P, ↓ N in WP ↓C:P, N:P ↑ C:N	Luxury uptake P ↑ P, N, C ↓ C:P, C:N, N:P	↓ P in WP ↑ N:P
FA overall	↑ in STA	3X ↑ 16:0 18:3n-3 in WP STA	↓ FA in WP 16:0, 16:7n-1 STA	Completely different FA composition in WP ↑ 18:1n-7 in WP
Valuable biomass	Similar EPA production	Proteins (N) in EXP ↓ EPA in WP	Similar total FA ↓ EPA in WP	Proteins (N) in EXP ↓ EPA
Conclusions	EPA producer	Remediation of P Proteins in EXP	Remediation of P Good for FA in STA	Proteins in EXP

3.4. Discussion

3.4.1. Cultivating algae in 60-mL tubes

This study is part of a broader research project conducted by the MicroAlgal Process and Evaluation Laboratory (Dalhousie University, Halifax, Canada) focused on characterizing algal biomass in media amended with food-grade wastes. One goal was to find a time-efficient method for cultivating various species, including recently isolated indigenous strains, and characterize their nutrient uptake and biomass composition. The biomass intended to be characterized included FAs, proteins, carbohydrates, particulate C, N, and P, particulate absorbance, Chla, fluorescence parameters, and cell counts, which all required a minimum volume for harvest. Flask cultures were tested in the initial stages even though sub-sampling for fluorescence measurements in the daily monitoring takes a long time. Initially, plastic

tissue-culture flasks were tried but were found to leak. Glassware flasks were then tested but proved impractical due to the extended time for monitoring (data not presented). Consequently, 60-mL borosilicate closed tubes were chosen. This choice facilitated daily monitoring using *F* and FIRe measurements until harvest and allowed for non-destructive measurements.

A limitation of the approach was that 60-mL volumes were insufficient for certain analyses, including proteins and carbohydrates. We attempted to assay proteins in this study using a protocol established by the Marine Microbial Proteomics and Trace Nutrient Biogeochemistry, supervised by Professor Erin Bertrand (Department of Biology, Dalhousie University) and based on a modified Lowry Protein Assay Kit with Pierce™ Bovine Gamma Globulin (BGG) standards. However, even when the samples collected for protein were combined with those intended for carbohydrate analysis, the results were very close to the assay's lower limit of detection (Miller and Miller 2005) and compromised by low signal-to-noise ratios.

The use of 60-mL tubes remains a feasible approach to screening diverse species at an intermediate scale for biomass characterization. However, the ease and speed of non-destructive daily monitoring with chlorophyll fluorescence is offset by the limits the volume imposes on characterizing the biomass. The approach would be improved by developing more sensitive assays, and efforts are underway to improve the protein method's sensitivity. A viable alternative could be to use larger tubes, perhaps 80-mL, that are still compatible with the fluorometers used for monitoring.

3.4.2. Metabolic modes

Photosynthetic characteristics

In vivo Chla fluorescence measurements have served as a proxy for biomass estimation and have been widely used in aquatic science since the introduction of the technique by Lorenzen in 1966 (Lorenzen 1966; Brand et al. 1981). This method offers the convenience of estimating biomass and growth rates without sub-sampling the culture, provided the tube where the culture is grown fits in the fluorometer. This technique heavily relies on a consistent Chla content within the cell and a constant quantum yield of fluorescence, requiring fully acclimated cultures (Brand et al. 1981; Wood et al. 2005). However, both pigment quotas and quantum yields vary in response to environmental stressors and potentially to the presence of organic substrates (e.g., Roth et al. 2019). This might have biased the fluorescence-based growth rates estimated in this study. In WP media, *C. muelleri* and *T. suecica* appeared to have notably reduced growth rates compared to CTRL ± DIC treatments despite exhibiting similar or higher C and N

uptakes in the WP medium. This observation strongly implies that these cultures' growth rates were underestimated in media amended with WP.

To investigate further into fluctuations in fluorescence-based growth rates among the cultures, multivariate statistical analyses were conducted for each species in EXP phase, incorporating physiological variables such as F_v/F_m, F_v/Chla, Chla/cell and σ. The analyses revealed distinct patterns, where *P. pyrenoidosus* and *C. mesostigmatica* displayed consistent parameters across treatments, and *C. muelleri* and *T. suecica* had substantial differences between the CTRL ± DIC treatments and WP treatment in these aspects. This suggests fundamental alterations in their photosynthetic systems and signifies that the cultures were either fully acclimated to the WP media by the harvest or were still acclimating but had significantly changed, depending on their growth rates.

Mixotrophic metabolism

In photoautotrophic conditions, cells assimilate inorganic forms of carbon and harness energy from absorbed light. However, when exposed to labile organic compounds like lactose in WP, some species can switch from photoautotrophic to mixotrophic growth, a combination of photosynthesis and heterotrophy, and, less commonly, to fully heterotrophic growth (Ceron Garcia et al., 2006).

The physiological data clearly indicates that *C. muelleri* and *T. suecica* were growing mixotrophically, in contrast to *P. pyrenoidosus* and *C. mesostigmatica*. Both species had reduced Chla, indicating a down-regulation of light harvesting in response to the available organic C in the WP media. Additionally, lower F_v/Chla ratios suggest a reduction in the number of functional reaction centers per unit Chla, while reduced F_v/F_m values imply a smaller proportion of functional reaction centers to the total. Moreover, estimates of σ were 40-60 % higher in WP-amended media, compared to CTRL ± DIC treatments, consistent with a "lake" model of Photosystem II connectivity, implying a redirection of energy from once-functional reaction centers to a reduced number of active ones (Laney et al. 2009). In mixotrophic cultures, the cells appear to reallocate their resources away from repairing non-functional reaction centers for sustaining photosynthesis (e.g., Roth et al. 2019), presumably toward assimilating organic C from WP. This strategy is notably pronounced in *C. muelleri* and *T. suecica*, indicating a substantial investment in mixotrophy. It is noteworthy that the two mixotrophic species had optimal WP concentration (0.5 g L^{-1}) compared to the two non-mixotrophic species (0.05 and 0.15 g WP L^{-1}), potentially enough to initiate mixotrophic growth.

Oxygen balanced mixotrophy

Cultivating microalgae mixotrophically in closed systems presents certain challenges regarding the absence of gas exchange, limiting the supply of additional CO_2 for photosynthesis and oxygen for heterotrophy. To address this, the concept of oxygen-balanced mixotrophy was explored, where the exchange between oxygen produced via photosynthesis and CO_2 from heterotrophy could support both processes simultaneously. This concept was implemented successfully in a previous study by Abiusi et al. (2020), doubling biomass yield compared to individual photoautotrophic or heterotrophic cultures. However, in the current study, this harmony between metabolic modes did not significantly enhance yields or productivity in the mixotrophic cultures, suggesting an imbalance between the two metabolic pathways. It is plausible that the oxygen levels in the closed tubes were lacking to support heterotrophic growth, and the oxygen generated through reduced photosynthesis (in mixotrophic cultures) might have also been insufficient. The oxygen consumption rate, likely due to heterotrophic growth, may exceed the rate of oxygen production by photosynthesis. Given the limited headspace in the closed system for *T. suecica* and *C. muelleri* and considering the approximate solubility of oxygen in seawater at about 0.3 mM, there might be insufficient oxygen in the tubes to meet the culture's demand. This is consistent with the observation that increasing the headspace in cultures of *C. mesostigmatica* (see section 2.4.5) increased both growth rates and final yields, which implies that without any gas exchanges, the cultures had less favourable growth in WP-amended media.

3.4.3. Nutrient uptake

The nutrient concentrations in the different media used varied significantly among species and treatments. N was reduced by a factor of 4 compared to regular L1 and F/2 media, resulting in concentrations around 200 µM. This led to a molar DIC:DIN (dissolved inorganic nitrogen) ratio of about 9 to minimize the likelihood of C limitation in the cultures. For *P. pyrenoidosus* and *C. muelleri*, the P concentration in the media was similarly reduced to 6-10 µM, with molar DIC:DIN:DIP of 180:20:1 to 300:33:1. It was increased for *T. suecica* and *C. mesostigmatica* to match the P concentration in WP better. The reported C concentration in WP media considered only inorganic forms; no analyses for dissolved organic carbon were conducted. However, concentrations of organic carbon from lactose in the WP amendments ranged from about 1.23 mM (0.05 g L^{-1} WP) to 12.27 mM (0.5 g L^{-1} WP), assuming the WP was 70 % lactose by weight. This is equivalent to 0.62 – 6.1x the DIC concentration. The substantial lactose concentration in WP makes in less probable that C is limiting in WP treatment,

provided it is available to the cultures. The different stoichiometry of the initial culture media limits the ability to detect a consistent trend across species.

Effect of DIC addition

The +DIC treatments explored the effect of bicarbonate on the growth of four species compared to treatments without added DIC. The use of bicarbonate presents some benefits as an alternative to the expensive method of air bubbling the cultures, and it eliminates the dependence on gas-liquid exchange of C, which is highly inefficient compared to using a dissolved form (Langley et al. 2012). It also has the advantage of minimizing the risk of bacterial contamination, which could be problematic in the WP-amended cultures.

Comparing the growth rates between CTRL and CTRL+DIC treatments across the four species, there were similarities within each species. *P. pyrenoidosus* and *C. muelleri* only slightly enhanced particulate C production in CTRL+DIC media. In contrast, *T. suecica* and *C. mesostigmatica* exhibited a substantial increase in particulate C concentration, nearly doubling the production seen in the CTRL treatment when exposed to CTRL+DIC conditions. This might be attributed to varying nutrient stoichiometry in different taxa. It was reported that Chlorophyta have a higher C:P than diatoms (Quigg et al. 2003). In this study, *T. suecica* (Chlorophyta) had a significant increase in particulate C concentration in the CTRL+DIC treatment, compared to CTRL without DIC. In contrast, cultures of *C. muelleri* (diatom) did not have a substantial increase in particulate C concentration in CTRL+DIC treatment compared to CTRL, possibly due to their lower C:P requirement (Quigg et al. 2003) and the nearly depleted P concentration in their media at harvest. The variations in elemental stoichiometry observed among taxa, particularly in cultures of *P. pyrenoidosus* and *C. mesostigmatica*, still need more clarity. To enhance understanding of the effect of DIC on the cultures, it would have been beneficial to maintain the initial N and P concentrations in L1 and f/2 media, providing a more specific indication of C-limitation in the CTRL cultures and facilitating a clearer interpretation of the observed effects.

Effect of organic C addition

Regarding the assimilation of organic C from the WP-amended media, besides the slight increase in C uptake observed in WP media compared to CTRL for *C. muelleri*, there is limited evidence suggesting greater C uptake in WP compared to CTRL media across other species. In the case of potentially non-mixotrophic species like *P. pyrenoidosus* and *C. mesostigmatica*, this implies a lack of utilization of

organic C, resulting in similar C concentrations in both CTRL and WP treatments. As for mixotrophic species such as *C. muelleri* and *T. suecica*, the carbon acquisition could potentially be in part organic C from WP, considering the down-regulation of photosynthesis. However, the overall C uptake did not increase significantly compared to CTRL treatments, indicating another limitation to mixotrophic growth, possibly oxygen levels (see Section 3.4.2).

Luxury uptake of P

C. muelleri and *C. mesostigmatica* displayed substantial P uptake from WP, effectively depleting it from the media. In contrast, the other two species did not exhibit significant variations in P-uptake compared to the CTRL ± DIC treatments. The concept of luxury uptake of non-limiting nutrients, such as P in WP, suggests that certain species develop internal pools of nutrients to buffer against environmental fluctuations (Leonardos and Geider 2004). This phenomenon has been extensively documented and studied, with observations spanning numerous phytoplankton phyla, demonstrating the storage of excess P in various forms, such as polyphosphate or surface-adsorbed inorganic P (Rhee 1978; Liefer et al. 2019). Studies specifically focusing on diatoms, and the genus *Chaetoceros* in particular, have highlighted their luxury uptake of P, predominantly storing it in the form of polyphosphate (Diaz et al. 2008; Bastos et al. 2022), which may explain the high P-uptake by *C. muelleri*.

3.4.4. Fatty acids allocation

The commercial potential of various algal species depends on their capacity to generate valuable or nutritional products. Among the main components of algae – such as proteins and carbohydrates – fatty acids hold significant value and are extensively researched for applications in producing triacylglycerols for biofuels or essential PUFAs like EPA (20:5n-3) intended for human consumption or aquaculture feeds. FAs with chains of 16-18 C are preferred for algae-based biofuel production due to their higher energy content and increased stability (Khethiwe et al. 2020). Saturated FAs like palmitic acid (16:0) and stearic acid (18:0), as well as monounsaturated FAs such as palmitoleic acid (16:1) and oleic acid (18:1) are good FA candidates for biofuel production (Khethiwe et al. 2020). PUFAs, synthesized mainly by microalgae and plants, play a vital role in the biological functions of animals and higher trophic levels. Given that alpha-linolenic acid (18:3n-3) and linoleic acid (18:2n-6) are precursors of long-chain PUFAs like EPA, and that animals and humans are inefficient at converting alpha-linolenic and linoleic acids into longer-chain PUFAs, their incorporation into our diets is essential (Taipale et al. 2020). The significance

of FA for biofuel production and the essential role of PUFAs underscores the importance of examining species-specific FA profiles.

P. pyrenoidosus, known for its high EPA – around 34% of its FA profile, as Sang et al. (2012) reported – has been a focus of previous studies. These indicate that approximately 27% of *P. pyrenoidosus* biomass consists of FA, predominantly EPA, myristic acid (14:0) and palmitic acid (Li et al. 2009; Sang et al. 2012). Sang et al. (2012) documented the highest concentrations of FA and EPA at a growth irradiance of 50 µmol photon m^{-2} s^{-1}, lower than in the current study, in which *P. pyrenoidosus* was cultivated at 190 µmol photon m^{-2} s^{-1}. No substantial variation in the FA signature was observed across different treatments. This stability is primarily attributed to the absence of mixotrophic growth, suggesting that WP in the media had minimal influence on the cultures beyond acting as a source of P.

Diatoms, including *C. muelleri*, are recognized for their elevated concentrations of FA with 16 C, notably palmitic and palmitoleic acids (Jónasdóttir 2019), which are the dominant FAs found in STA phase in this study. Both have potential for biofuel production. The substantial variance in FA allocation between EXP and STA phases supports findings in the literature indicating that when *C. muelleri* is cultivated under nutrient limitation, its total FA content increases significantly, up to 5-7 times higher compared to nutrient-repleted conditions (e.g., McGinnis et al. 1997). Moreover, diatoms typically produce around 10% of their total FA as long-chain EPA, a component present in our cultures during STA phase for all treatments and in EXP phase for CTRL ± DIC treatments.

Among the Chlorophyta, PUFAs are typically less abundant than other algal phyla (Jónasdóttir 2019). Chlorophyta commonly have a substantial proportion of their total FA in chains of 16 C (12-28%) and often display a high proportion of alpha-linolenic acid, a pattern observed in the FA profile of *T. suecica* for CTRL ± DIC cultures in this study. The culture contained some EPA, a valuable omega-3 for the pharmaceutical markets, which is consistent with previous studies (Jónasdóttir 2019) but was down-regulated in WP media. *T. suecica*'s FA profile significantly diverged when cultivated mixotrophically in WP-amended media, displaying a solid down-regulation of numerous FAs while showing an up-regulation of cis-vaccenic acid (18:1n-7).

Cryptophyta typically display a reduced presence of FAs with 16 C, as indicated by prior research (Jónasdóttir 2019). However, in *C. mesostigmatica*, palmitic acid constituted one of the predominant FA

across all treatments. Although EPA is present in its profile, its concentration in WP cultures is lower than in CTRL ± DIC treatments. Peltomaa et al. (2017) found that *C. mesostigmatica* efficiently produced alpha-linolenic acid, comprising 60% of the total omega-3 FA profile, and EPA production accounting for approximately 20%, aligning closely with observations in this study. Their research identifies *C. mesostigmatica* as the most promising strain for EPA production within the division Cryptophyta (Peltomaa et al. 2017). The addition of WP in the media substantially increased alpha-linolenic and palmitic acids concentrations in cultures during STA phase compared to CTRL ± DIC treatments.

The FAs were presented as FA allocation for the scope of this study due to its valuable aspect on a modeling perspective. Among the species studied, *P. pyrenoidosus* and *C. muelleri* had the highest FA quotas. *P. pyrenoidosus* maintained a consistent profile in WP media, resembling the CTRL ± DIC treatments, particularly rich in EPA, indicating the potential to use WP media as a P source for EPA production. *C. muelleri* had a similar FA profile across all treatments in STA phase, containing FA suitable for biofuel production, underscoring its viability for biofuel production under mixotrophic conditions in WP. However, *T. suecica* and *C. mesostigmatica* had lower FA allocation than the other species, and their FA profiles were notably altered in WP media, diminishing their suitability for commercial FA production. Curiously, across all species, the greatest abundance of cis-vaccenic acid was observed in WP ± DIC treatments, while it was almost absent in the CTRL ± DIC treatments. This notable occurrence could potentially be linked to the presence of high bacterial abundance in the cultures, as vaccenic acid is uncommon and has been reported to be linked with bacteria and other heterotrophic microorganisms (Awad et al. 1995; Bowen-Forbes and Goldson-Barnaby 2016). This FA is also a natural component of cow's milk and may be present in WP (AbuGhazaleh et al. 2003).

3.4.5. Cultivation modes

The final step in characterizing the four species cultivated involved assessing the productivity rates of specific compounds of interest. A strategy for the commercialization of STA phase compounds is cultivation in fed-batch mode. At harvest time, a portion of the culture would be withdrawn for commercial harvest, while the remaining would be replenished with fresh media, thereby facilitating further production (as shown by the red lines in Figure 3.19). As for EXP phase compounds, the cultures were intended to fully acclimate to the media at harvest using a semicontinuous mode (illustrated by the blue lines in Figure 3.19). Acclimation to new media or light intensity can require numerous

subsequent transfers to reach a steady state, where cell density and growth rates are constant (Wood et al. 2005).

In the scenario presented in Figure 3.19, if EXP phase harvests occur once a day, the production of a STA culture would take five days. Semicontinuous growth offers the advantage of achieving rapid biomass production, while the rationale behind fed-batch growth lies in the possible alteration of biomass composition in response to nutrient limitation in the transition between the EXP and STA phases. The selection of the cultivation mode depends on the specific compound targeted for commercialization. For instance, in scenarios where triacylglycerides are the desired product for biofuel production and are significantly up-regulated in STA phase, using fed-batch cultures could be advantageous as the reduction in growth rate could be offset by an increase in the cell quota.

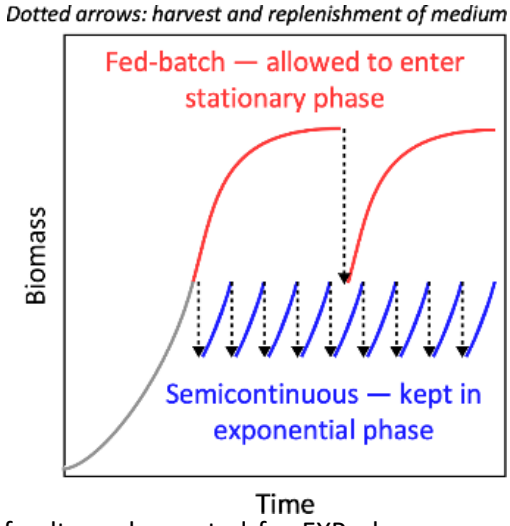

Figure 3.19. Growth kinetics of cultures harvested for EXP phase compounds kept in semi-continuous growth (bleu) or for STA phase compounds grown in fed-batch mode (red). Figure from MacIntyre et al, in prep.

Semicontinuous growth in WP media

In practice, achieving semicontinuous growth was not straightforward for all species in this study. Each species was grown under varying concentrations of WP, likely impacting their growth responses to the amendments. *P. pyrenoidosus*, cultivated with the lowest WP concentration (0.05 g L^{-1}), acclimated well to the media, enabling successful growth in semicontinuous mode. Similarly, *C. mesostigmatica*, cultivated with 0.15 g L^{-1} WP and inoculated with headspaces in the closed tubes for enhanced gas exchange, also demonstrated ease in acclimation and growing semi-consciously in WP media. These two species also did not show indications of mixotrophic growth or down-regulation of photosynthesis.

In contrast, there were challenges in acclimating *C. muelleri* and *T. suecica*, both cultivated with 0.5 g L^{-1} WP. On inoculation from CTRL cultures to WP-amended media, several distinct patterns emerged, complicating efforts to maintain these for semicontinuous growth:

- No increase in fluorescence or cell counts, indicating no growth.
- Increase in cell concentration without an increase in fluorescence.
- A rapid increase in fluorescence and cell concentration for one or two days, followed by a STA phase for one day, ultimately leading to culture decline the next day.
- A very slow increase in fluorescence and cell concentration, eventually reaching much higher yields than the previous scenario, then entering STA phase after more than ten days.

These inconsistent growth patterns posed challenges to acclimation in WP-amended media. Consequently, cultures of *C. muelleri* and *T. suecica* harvested in EXP phase were not fully acclimated and did not grow semi-continuously. The chosen WP concentration was based on a smaller-scale screening experiment using C-boxes, which allowed atmospheric CO_2 to enter the cultures, facilitating gas exchange. The inconsistent growth patterns observed in both species might be due to differences in gas exchange between cultures. They might also be due to age-dependant, growth-inhibiting compounds present in WP, such as calcium or chloride, which can impact enzymatic activity within the cells (Bentahar et al. 2019).

Certain preferences in culture conditions were identified through repeated cell counts of cultures in WP-amended media. For *C. muelleri*, inoculating a larger culture volume facilitated better growth, but still at a very slow rate. Semicontinuous growth was not achieved, and the cultures harvested were inoculated from a CTRL-acclimated culture. In the case of *T. suecica*, using a 7-month-old media possibly enabled the resolubilization of essential nutrients, such as P, trapped in calcium-phosphate or struvite precipitates (see section 2.4.4.). This aged media allowed some acclimation for *T. suecica*, where the culture had approximately three generations of acclimation in WP media before inoculating the experiment for harvest.

3.4.6. Effect of treatments on productivity rates

Calculating productivity rates (dX/dt) in STA cultures involved computing the biomass concentration difference between STA and EXP cultures divided by the time difference between their harvests (see Equation 3.5). Productivity rates for EXP phase harvested cultures were calculated as the product of the

biomass concentration and the maximum specific growth rate in EXP phase, μ_{max}. Due to the limited daily measurements beyond fluorescence during the growth experiments, the productivity rates determined in this study relied on fluorescence, which is decoupled from biomass production if the cellular composition is not inconsistent. Consequently, productivity rates might be underestimated for species like *C. muelleri* and *T. suecica*, which significantly down-regulated their photosynthetic apparatus during mixotrophic growth.

The total FA productivity rate (dFA/dt) served as an indicator of biofuel potential. In the CTRL+DIC treatment during STA phase, *C. muelleri* culture had the highest dFA/dt, averaging around 3 x 10^{-6} mg of total FA L^{-1} d^{-1}. Although *C. muelleri* showed similar FA quotas in WP-amended media, the growth rates in STA cultures were notably low, resulting in a lower apparent dFA/dt in the WP condition. Considering *C. muelleri*'s FA composition, primarily saturated and monosaturated FAs, along with substantial internal lipid concentrations, this species appears to hold significant potential for biofuel production (McGinnis et al. 1997; Wang et al. 2014).

A comparison of the EPA productivity rates (dEPA/dt) indicates that *P. pyrenoidosus* is a strong candidate for commercial production in EXP phase. Despite displaying a lower EPA allocation in EXP phase compared to STA phase, its dEPA/dt was significantly greater in EXP phase because of the rapid growth rate observed. The WP-amended culture had a dEPA/dt comparable to the CTRL ± DIC treatments, roughly 5 x 10^{-7} mg of EPA L^{-1} d^{-1}, which makes it well-suited for EPA production in EXP phase using WP-amended media.

As most of the protein samples obtained at harvest were beneath the limit of detection of the method, N concentration was used as a proxy for proteins in this study. The N productivity rates (dN/dt) in WP-amended media were highest in *T. suecica* and *C. mesostigmatica*, approximately 2-3 x 10^{-6} mg of N L^{-1} d^{-1}, similar to those in the CTRL media. This suggests that WP might serve as a suitable nutrient substrate for these cultures without altering the protein production rates. The N concentration of *T. suecica* in EXP phase in WP-amended media was similar to CTRL ± DIC treatments, while its fluorescence-based growth rate was considerably lower. However, the down-regulation of pigments may have led to underestimating the specific growth rate. If so, there is a strong possibility that *T. suecica* in WP has a much higher dN/dt than the CTRL ± DIC treatments. As for *C. mesostigmatica*, its fluorescence-base growth rate in EXP phase was likely more accurate as pigments were not down-regulated in WP media,

suggesting that the calculated dN/dt, which is similar between CTRL and WP treatments, is relatively accurate. When considering the commercial-scale production of proteins with *C. mesostigmatica* cultures, enhancing the medium with DIC might be more beneficial than WP, as dN/dt was notably higher in CTRL+DIC compared to CTRL and WP treatments.

3.5. Conclusion

The use of WP as a growth substrate for microalgae cultivation shows potential. However, the effectiveness and effect of WP media on the species studied varied significantly, influencing the metabolic pathways and altering the production of essential compounds like FAs, possibly proteins, and other nutrients, in some but not all. The investigation into mixotrophic growth revealed significant changes in metabolic pathways, particularly in *C. muelleri* and *T. suecica*, where the presence of organic compounds from WP led to changes in their physiology. These species exhibited a down-regulation of photosynthesis, a reallocation of resources, and a shift toward mixotrophic metabolism when exposed to WP.

P. pyrenoidosus had relatively high EPA production during the EXP phase when grown in WP media. In the case of *C. muelleri*, its considerable FA content in STA phase suggests the potential for biofuel production or as a lipid source. Both *T. suecica* and *C. mesostigmatica* had high N production in EXP phase in WP media, indicating the potential for them to function as a protein source in such media. The luxury uptake of P observed in *C. muelleri* and *C. mesostigmatica* indicates good candidates for WP remediation.

There were methodological limitations, such as challenges in measuring certain compounds (proteins and carbohydrates) and reliance on fluorescence for growth rate estimations, potentially affecting the accuracy of the assessments. Despite these challenges, exploring mixotrophic growth and the utilizing waste substrates like WP offer promising avenues for commercializing microalgal biomass. Further research focusing on better intermediate-scale cultivation methods and understanding metabolic shifts for different species growing in WP-amended media could significantly advance the potential for microalgal cultivation using the dairy waste as a substrate.

Chapter 4: Conclusion

In summary, microalga, rich in intracellular compounds like proteins, fatty acids, and omega-3s, offer a promising solution for future food needs, presenting nutritional quality and health benefits, as well as potential for other sectors sur as biofuel production. Their potential to address the growing population's nutritional needs and improve aquaculture feed sustainability is substantial. However, the challenge lies in the costs associated with mass algal culturing, encompassing nutrient supply, a carbon source, and energy for light sources. To mitigate these expenses, this study uses nutrient-rich waste to substitute the culture with essential nutrients (carbon, nitrogen, phosphorus). The presence of readily accessible organic compounds in waste, potentially inducing mixotrophic growth, may contribute to lowering algal production costs by enabling the cultivation facility to decrease its reliance on the light source required for photosynthesis.

In this study, whey permeate (WP), a by-product of cheese making, served as a substrate to amend the culture media. This dairy industry waste consists of lactose as an organic carbon source and a substantial quantity of phosphate, which are potentially beneficial for the culture. While various studies have explored algal growth in fresh and liquid WP, this study focuses on dehydrated WP, considering logistical challenges in transporting liquid WP to distant algal facilities.

Chapter 2 investigates the preparation of WP powder and its integration into culture media. Autoclaving the WP-NaOH solutions induced browning reactions, significantly supporting *T. suecica*'s growth, with optimal outcomes observed at 1 M NaOH. pH adjustments of the WP-amended media showed increased yields at pH 7 in CO_2-generating systems (C-boxes). Experiments comparing purified lactose with WP-amended media revealed higher yields in lactose autoclaved in solution, possibly due to increased browning reactions, and a 7-month storage period indicated enhanced growth rates for *T. suecica* cultures. The choice of NaOH as a solvent notably influenced phosphorus availability, and light exposure experiments offered valuable insights into WP degradation. Tests in closed tubes with *C. mesostigmatica* cultures in WP media with a headspace exhibited higher growth rates, emphasizing the pivotal role of gas exchange in closed systems.

Chapter 3 extends into larger-scale cultures, characterizing biomass from four algal species under diverse conditions. A primary goal was to identify a suitable screening method for algal cultures using

food-grade wastes that allowed fast and efficient monitoring and substantial volume to harvest. To meet this, 60-mL closed borosilicate tubes were chosen. Closed systems allowed testing CO_2 and oxygen exchange between photoautotrophic and heterotrophic metabolisms in a potential mixotrophic culture in WP-amended media. Growth of *P. pyrenoidosus*, *C. muelleri*, *T. suecica*, and *C. mesostigmatica* was tested in WP-amended media at various concentrations. Signs of mixotrophic growth were found for *C. muelleri* and *T. suecica* cultures, suggesting lactose assimilation from WP. *P. pyrenoidosus* showed promising EPA productivity rates in WP media during the exponential phase. *C. muelleri* displayed significant fatty acid accumulation in stationary phase with WP-amended media, hinting at its suitability for biofuel production. *T. suecica* and *C. mesostigmatica* emerged as potential candidates for protein production. *C. muelleri* and *C. mesostigmatica* seem suitable for WP remediation, given their luxury phosphorus uptake.

Further research is essential to optimize growth conditions in WP powder-based media, unlocking the full potential of using this dairy waste as a substrate for producing valuable algal-based compounds. This circular and sustainable solution addresses food challenges and revolutionizes waste management practices.

Bibliography

- Abiusi, F., Wijffels, R.H., and Janssen, M. (2020). Doubling of microalgae productivity by oxygen balanced mixotrophy. *ACS Sustainable Chemistry & Engineering*, 8: 6065-6074.
- Abreu, A.P., Fernandes, B., Vicente, A.A., Teixeira, J., and Dragone, G. (2012). Cultivation of *Chlorella vulgaris* using industrial dairy waste as organic carbon source. *Bioresource Technology*, 118: 61-66.
- AbuGhazaleh, A.A., Schingoethe, D.J., Hippen, A.R., and Kalscheur, K.F. (2003). Conjugated Linoleic Acid and Vaccenic Acid in Rumen, Plasma, and Milk of Cows Fed Fish Oil and Fats Differing in Saturation of 18 Carbon Fatty Acids. *Journal of dairy science*, 86(11): 3648-3660.
- Acién, F.G., Fernández, J.M., Magán, J.J., and Molina, E. (2012). Production cost of a real microalgae production plant and strategies to reduce it. *Biotechnology Advances*, 30(6), 1344–1353.
- Ahmed, P.M., Pajot, H.F., de Figueroa, L.I.C., and Gusils, C.H. (2018). Sustainable bioremediation of sugarcane vinasse using autochthonous macrofungi. *Journal of Environmental Chemical Engineering*, 6(4): 5177–5185.
- Ajandouz, E.H., Tchiakpe, L. S., Ore, F.D., Benajiba, A., and Puigserver, A. (2001). Effects of pH on Caramelization and Maillard Reaction Kinetics in Fructose-Lysine Model Systems. *Journal of Food Science*, 66(7): 926–931.
- Aktağ, I.G., Hamzalıoğlu, B.A., and Gökmen, V. (2019). Lactose hydrolysis and protein fortification pose an increased risk for the formation of Maillard reaction products in UHT treated milk products. *Journal of Food Composition and Analysis*, 103308.
- Almutairi, A.W. and Toulibah, H.E., (2017). Effect of Salinity and pH on Fatty Acid Profile of The Green Algae *Tetraselmis suecica*. *Journal of Petroleum & Environmental Biotechnology*, 7: 333.
- Arora, M., Anil, A.C., Delany, J., Rajarajan, N., Emami, K., and Mesbahi, E., (2012). Carbohydrate-degrading bacteria closely associated with *Tetraselmis indica*: influence on alga growth. *Aquatic Biology*, 15: 61-71.
- Awad, A.B., Herrmann, T., and Horvath, P.J. (1995). 18:1 n7 fatty acids inhibit growth and decrease inositol phosphate release in HT-29 cells compared to n9 fatty acids. *National Library of Medicine*, 91(1): 55-61.
- Badger, M.R., Andrews, T.J., Whitney, S. M., Ludwig, M., Yellowlees, D.C., Leggat, W., and Price, G.D. (1998). The diversity and coevolution of Rubisco, plastids, pyrenoids, and chloroplast-based CO2-concentrating mechanisms in algae. *Canadian Journal of Botany*, 76(6): 1052–1071.
- Baldisserotto, C., Sabia, A., Guerrini, A., Demaria, S., Maglie, M., Ferroni, L., and Pancaldi, S. (2021). Mixotrophic cultivation of *Thalassiosira pseudonana* with pure and crude glycerol: Impact on lipid profile. *Algal Research*, 54: 102194.
- Bashir, K.M.I., Mansoor, S., Kim, N.-R., Grohmann, F.R., Shah, A.A., and Cho, M.-G. (2019). Effect of organic carbon sources and environmental factors on cell growth and lipid content of *Pavlova lutheri*. *Annals of Microbiology*, 69: 353–368.
- Bastos, C.R.V., Maia, I.B., Pereira, H., Navalho, J., and Varela, J.C.S. (2022). Optimisation of Biomass Production and Nutritional Value of Two Marine Diatoms (Bacillariophyceae), *Skeletonema costatum* and *Chaetoceros calcitrans*. *Biology*, 11(4): 594.
- Becker, E.W. (2007). Micro-algae as a source of protein. *Biotechnology Advances*, 25(2): 207–210.
- Bentahar, J., Doyen, A., Beaulieu, L., and Deschênes, J.-S. (2019). Acid whey permeate: An alternative growth medium for microalgae *Tetradesmus obliquus* and production of β-galactosidase. *Algal Research*, 41: 101559.

- Bolton, J.R. and Linden, K.G. (2003). Standardization of methods for fluence (UV dose) determination in bench-scale UV experiments. *Journal of Environmental Engineering-ASCE 129*, (3): 209-215.
- Borges, W.d.S., Alves Araújo, B.S., Moura, L.G., Filho, U.C., de Resende, M.M., and Cardoso, V.L. (2016). Bio-oil production and removal of organic load by microalga *Scenedesmus* sp. using culture medium contaminated with different sugars, cheese whey and whey permeate. *Journal of Environnmental Management*, 173: 134-140.
- Borowitzka, M.A., and Larkum, A.W.D. (1987). Calcification in algae: Mechanisms and the role of metabolism. *Critical Reviews in Plant Sciences*, 6(1): 1–45.
- Bowen-Forbes, C.S and Goldson-Barnaby, A. (2016). Pharmacognosy Fundamentals, Applications and Strategy. London, United Kingdon: *Academic Press*. Chapter 21.
- Boyd, C.E., D'Abramo, L.R., Glencross, B.D., Huyben, D.C., Juarez, L.M., Lockwood, G.S., Valenti, W.C. (2020). Achieving sustainable aquaculture: Historical and current perspectives and future needs and challenges. *Journal of the World Aquaculture Society*, 51(3): 578–633.
- Brand, L.E., Guillard, R.R.L., and Murphy, L.S. (1981). A method for the rapid and precise determination of acclimated phytoplankton reproduction rates. *Journal of Plankton Research*, 3(2): 193–201.
- Brown, M.R. (1991). The amino-acid and sugar composition of 16 species of microalgae used in mariculture. *Journal of Experimental Marine Biology and Ecology*, 145(1): 79–99.
- Cardozo, K.H.M., Guaratini, T., Barros, M.P., Falcão, V.R., Tonon, A.P., Lopes, N.P., Campos, S., Torres, M.A., Souza, A.O., Colepicolo, P., and Pinto, E. (2007). Metabolites from algae with economical impact. *Comparative Biochemistry and Physiology Part C: Toxicology & Pharmacology*, 146(1-2): 60–78.
- Ceron Garcia, M.C., Garcia, C.F., Sanchez, M.A., Fernandez, S.J.M., Chistri, Y., and Molina, G.E. (2006). Mixotrophic Production of Marine Microalga Phaeodactylum tricornutum on Various Carbon Sources. *Journal of Microbiology and Biotechnology*, 16(5): 689-694.
- Colman, B., Huertas, E., Bhatti, S., and Dason, J., (2002). The diversity of inorganic carbon acquisition mechanisms in eukaryotic microalgae. *Functional Plant Biology*, 29: 261-270.
- Confectionery Production. (2016, April 6). The next step for whey permeate. https://www.confectioneryproduction.com/feature/15608/next-step-whey-permeate/
- Coopérative Agropur. (May 19, 2021). Whey/Dairy Proteins. https://www.agropur.com/us/ingredients/specialty-ingredients/whey-dairy-proteins
- Cui, H., Yu, J., Zhai, Y., Feng, L., Chen, P., Hayat, K., and Ho, C.-T. (2021). Formation and fate of Amadori rearrangement products in Maillard reaction. *Trends in Food Science & Technology*, 115: 391–408.
- Danalewich, J.R., Papagiannis, T.G., Belyea, R.L., Tumbleson, M.E., and Raskin, L. (1998). Characterization of dairy waste streams, current treatment practices, and potential for biological nutrient removal. *Water Research*, 32(12): 3555–3568.
- Davidek, T., Clety, N., Aubin, S., and Blank, I. (2002). Degradation of the Amadori Compound N-(1-Deoxy-d-fructos-1-yl) glycine in Aqueous Model Systems. *Journal of Agricultural and Food Chemistry*, 50(19): 5472–5479.
- Davoodi, S.H., Shahbazi, R., Esmaeili, S., Sohrabvandi, S., Mortazavian, A.M., Jazayeri, S., and Taslimi, A. (2016). Health-Related Aspects of Milk Proteins. *Iranian Journal of Pharmaceutical Research*, 15(3): 573-591.
- Diaz, J., Ingall, E., Benitez-Nelson, C., Paterson, D., de Jonge, M.D., McNulty, I. and Brandes, J.A. (2008). Marine polyphosphate: a key player in geologic phosphorus sequestration. *Science*, 320(5876): 652-655.

- Diaz, R.J. and Rosenberg, R. (2008). Spreading dead zones and consequences for marine ecosystems. *Science*, 321 (5891):926-929.
- Domínguez-Niño, A., Cantú-Lozano, D., Ragazzo-Sanchez, J.A., Andrade-González, I., and Luna-Solano, G. (2017). Energy requirements and production cost of the spray drying process of cheese whey. *Drying Technology*, 36(5): 597–608.
- Durham, R.J. (2009). Modern approaches to lactose production. *Dairy-Derived Ingredients*, 103–144.
- España-Gamboa, E., Mijangos-Cortes, J., Barahona-Perez, L., Dominguez-Maldonado, J., Hernández-Zarate, G., and Alzate-Gaviria, L. (2011). Vinasses: characterization and treatments. *Waste Management & Research*, 29(12): 1235–1250.
- Espinosa-Gonzalez, I., Parashar, A., and Bressler, D.C. (2014). Heterotrophic growth and lipid accumulation of Chlorella protothecoides in whey permeate, a dairy by-product stream, for biofuel production. *Bioresource Technology*, 155: 170-176.
- Fairbrother, P., (1991). The fermentation of cheese whey by Lactobacillus helyeticus. [PhD thesis]. *The Polytechnic of Whales*. 151 p.
- FAO (2022). The State of World Fisheries and Aquaculture. Towards Blue Transformation. Rome, Italy: FAO. https://doi.org/10.4060/cc0461en
- Folch, J., Lees, M., and Sloane Stanley, G.H. (1957). A simple method for the isolation and purification of total lipids from animal tissues. *Journal of Biological Chemistry*, 226(1): 497-509.
- Fry, J.P., Love, D.C., MacDonald, G.K., West, P.C., Engstrom, P.M., Nachman, K.E., and Lawrence, R.S. (2016). Environmental health impacts of feeding crops to farmed fish. *Environment International*, 91: 201–214.
- García, J.L., de Vicente, M., and Galán, B. (2017). Microalgae, old sustainable food and fashion nutraceuticals. *Microbial Biotechnology*, 10(5), 1017–1024.
- Gasol, J.M. and Del Giorgio, P.A. (2000). Using flow cytometry for counting natural planktonic bacteria and understanding the structure of planktonic bacterial communities. *Scientia Marina*, 64 (2):197-224.
- Girard, J.-M., Roy, M.-L., Hafsa, M.B., Gagnon, J., Faucheux, N., Heitz, M., Temblay, R., and Deschênes, J.-S. (2014). Mixotrophic cultivation of green microalgae *Scenedesmus obliquus* on cheese whey permeate for biodiesel production. *Algal Research*, 5: 241–248.
- Girard, J.-M., Tremblay, R., Faucheux, N., Heitz, M., and Deschênes, J.-S. (2017). Phycoremediation of cheese whey permeate using directed commensalism between *Scenedesmus obliquus* and *Chlorella protothecoides*. *Algal Research*, 22: 122–126.
- Glibert, P.M., Al-Azri, A., Icarus Allen, J., Bouwman, A.F., Beusen, A.H.W., Burford, M.A., Harrison, P.J., and Zhou, M. (2018). Key Questions and Recent Research Advances on Harmful Algal Blooms in Relation to Nutrients and Eutrophication. *Springer International Publishing*, Cham, pp. 229-259.
- Global Footprint Network (2023). Earth Overshoot Day. America's Global Footprint Network; [accessed 2023 Oct 22]. https://www.overshootday.org/
- Gorbunov, M.Y. and Falkowski, G. (2004). Fluorescence induction and relaxation (FIRe) technique and instrumentation for monitoring photosynthetic processes and primary production in aquatic ecosystems. In: Bruce D, van der Est A (eds) Fundamental Aspects to Global Perspectives. *Allen Press*, Montreal, pp 1029–1031.
- Guihéneuf, F., Ulmann, L., Tremblin, G., and Mimouni, V. (2011). Light-dependent utilization of two radio labelled carbon sources, sodium bicarbonate and sodium acetate, and relationships with long chain polyunsaturated fatty acid synthesis in the microalga *Pavlova lutheri* (Haptophyta). *European Journal of Phycology*, 46(2): 143–152.

- Guillard, R.R.L., and Hargraves, P.E. (1993). *Stichochrysis immobilis* is a diatom, not a chrysophyte. *Phycologia*, 32(3): 234–236.
- Guillard, R.R.L., and Ryther, J.H. (1962). Studies of marine planktonic diatoms: i. *cyclotella nana hustedt*, and *detonula confervacea* (cleve) gran. *Canadian Journal of Microbiology*, 8(2): 229–239.
- Hansen, P.J., Lundholm, N., and Rost, B., (2007). Growth limitation in marine red-tide dinoflagellates: effects of pH versus inorganic carbon availability. *Marine Ecology Progress Series*, 334: 63-71.
- Harwood, J.L. (2019). Algae: Critical Sources of Very Long-Chain Polyunsaturated Fatty Acids. *Biomolecules*, 9(11): 708.
- Heisler, J., Glibert, P.M., Burkholder, J.M., Anderson, D.M., Cochlan, W., Dennison, W.C., Dorth, Q., Gobler, C.J., Heil, C.A., Humphries, E., Lewitus, A.J., Magnien, R., Marshall, H.G., Sellner, K.G., Stockwell, D.A., Stoecker, D.K., and Suddleson, M. (2008). Eutrophication and harmful algal blooms: A scientific consensus. *Harmful Algae*, 8(1): 3–13.
- Henderson, L.J. (1908). Concerning the relationship between the strength of acids and their capacity to preserve neutrality. *American Journal of Physiology-Legacy Content*, 21(2), 173–179.
- Heredia-Arroyo, T., Wei, W., and Hu, B. (2010). Oil Accumulation via Heterotrophic/Mixotrophic *Chlorella protothecoides*. *Applied Biochemistry and Biotechnology*, 162(7): 1978–1995.
- Hodge, J.E., (1953). Chemistry of browning reactions in model systems. *Agriculture and food chemistry*, 1(15): 928-943.
- Hunziker, O.F and Nissen, B.H. (1926). Lactose solubility and lactose crystal formation: I. Lactose solubility. *Journal of dairy science*, 9(6): 517-537.
- Huot, Y. and Babin, M. (2011). Overview of Fluorescence Protocols: Theory, Basic Concepts, and Practice. In: Suggett DJ, Prasil O, Borowitzka MA (eds) Chlorophyll a Fluorescence Measurements in Aquatic Sciences: Methods and Applications. Springer, Berlin, pp 129-169.
- Jiang, Z.-P., Li, Y.-R., Wei, G.-P., Liao, Q., Su, T.-M., Meng, Y.-C., Zhang, H.-Y., and Lu, C.-Y. (2012). Effect of long-term vinasse application on physico-chemical properties of sugarcane field soils. *Sugar Technologies*, 14: 412– 417.
- Jónasdóttir, S. (2019). Fatty Acid Profiles and Production in Marine Phytoplankton. *Marine Drugs*, 17(3): 151.
- Jones, C.T., Craig, S.E., Barnett, A.B., MacIntyre, H.L., and Cullen, J.J. (2014). Curvature in models of the photosynthesis-irradiance response. *Journal of Phycology*, 50(2): 341–355.
- Kassim, M.A. and Meng, T.K. (2017). Carbon dioxide (CO2) biofixation by microalgae and its potential for biorefinery and biofuel production. *Science of The Total Environment*, 584-585: 1121–1129.
- Khethiwe, E., Clever, K., and Jerekias, G. (2020). Effects of Fatty Acids Composition on Fuel Properties of Jatropha Curcas Biodiesel. *Smart Grid and Renewable Energy*, 11:10.
- Kothari, R., Prasad, R., Kumar, V., and Singh, D.P. (2013). Production of biodiesel from microalgae *Chlamydomonas polypyrenoideum* grown on dairy industry wastewater. *Bioresource Technology*, 144: 499–503.
- Laney, S.R., Letelier, R., Abbott, M.R. (2009). Using a nonanalytical approach to model nonlinear dynamics in photosynthesis at the photosystem level. *Journal of Phycology*, 45:298–310.
- Langley, N.M., Harrison, S.T.L., and Van Hille, R.P. (2012). A critical evaluation of CO2 supplementation to algal systems by direct injection. *Biochemical Engineering Journal*, 68: 70–75.

- Leonardos, N., and Geider, R.J. (2004). Responses of elemental and biochemical composition of *Chaetoceros muelleri* to growth under varying light and nitrate: phosphate supply ratios and their influence on critical N:P. *Limnology and Oceanography*, 49: 2105-2114.
- Lewitus, A.J. and Kana, T.M. (1994). Responses of estuarine phytoplankton to exogenous glucose: Stimulation versus inhibition of photosynthesis and respiration. *Limnology and Oceanography*, 39(1): 182–189.
- Li, A., Liu, R., Liu, X., Xu, N, Zhang, C., and Duan, S. (2009). Effects of carbon sources on growth and fatty acid composition of *pinguiococcus pyrenoidosus* ccmp 2078[j]. *Acta hydrobiologica sinica*, 33(3): 461-467.
- Liefer, J.D., Garg, A., Fyfe, M.H., Irwin, A.J., Benner, I., Brown, C.M., Follows, M.J., Omta, A.W., and Finkel, Z.V. (2019). The Macromolecular Basis of Phytoplankton C:N:P Under Nitrogen Starvation. *Frontiers in Microbiology*, 10: 763.
- Liu, B., Eltanahy, E.E., Liu, H., Chua, E.T., Thomas-Hall, S.R., Wass, T J., Pan, K., and Schenk, P.M. (2020). Growth-promoting bacteria double eicosapentanoic acid yield in microalgae. *Bioresource Technology*, 123916.
- Lorenzen, C.J. (1966). A method for the continuous measurement of in vivo chlorophyll concentration. *Deep Sea Res*, 13:223–227.
- Lund, M.N., and Ray, C.A. (2017). Control of Maillard Reactions in Foods: Strategies and Chemical Mechanisms. *Journal of Agricultural and Food Chemistry*, 65(23): 4537–4552.
- Lundholm, N., Hansen, P.J., and Kotaki, Y., (2004). Effect of pH on growth and domoic acid production by potentially toxic diatoms of the genera *Pseudo-nitzschia* and *Nitzschia*. *Marine Ecology Progress Series*, 273: 1-15.
- MacIntyre, H.L. and Cullen, J.J. (2005). Using cultures to investigate the physiological ecology of microalgae. In: Andersen RA (ed) Algal Culture Techniques. *Academic Press*, New York, pp 287-326.
- MacIntyre, H.L. and Cullen, J.J. (2016). Classification of phytoplankton cells as live or dead using the vital stains fluorescein diacetate and 5-chloromethylfluorescein diacetate. *Journal of Phycology*, 52 (4):572-589.
- MacIntyre, H.L., Cullen, J.J., Whitsitt, T.J., and Petri, B. (2018). Enumerating viable phytoplankton using culture-based Most Probable Number assay following ultraviolet-C treatment. *Journal of Applied Phycology*, 30: 1073-1094.
- Marie, D., Simon, N., and Vaulot, D. (2005). Phytoplankton cell counting by flow cytometry. In: Andersen RA (ed) Algal Culture Techniques. *Academic Press*, New York, pp 253-267.
- Marwaha, S.S., and Kennedy, J.F. (1988). Whey-pollution problem and potential utilization. *International Journal of Food Science & Technology*, 23(4): 323–336.
- McGinnis, K. M., Dempster, T. A., and Sommerfeld, M. R. (1997). Characterization of the growth and lipid content of the diatom Chaetoceros muelleri. *Journal of Applied Phycology*, 9(1): 19–24.
- McManus, G., Mitra, A., Reguera, B., and Santoferrara, L. (2023). The Mixoplankton Paradigm in Plankton Ecology. In: Reguera, B. Harmful Algae News. The Association for the Sciences of Limnology and Oceanography (ASLO); 2023 June 4-9; Palma de Mallorca, Spain. Vigo, Spain: Intergovernmental Oceanographic Commission, UNESCO. P 15-18.
- Miller, J.N. and Miller, J.C. (2005). Statistics and Chemometrics for analytical chemistry. Edinburg Gate, England: *Pearson Education Limited*.
- Moheimani, N.R., and Borowitzka, M.A. (2011). Increased CO2 and the effect of pH on growth and calcification of *Pleurochrysis carterae* and *Emiliania huxleyi* (Haptophyta) in semicontinuous cultures. *Applied Microbiology and Biotechnology*, 90(4): 1399–1407.

- Mondal, M., Ghosh, A., Sharma, A.S., Tiwari, O.N., Gayen, K., Mandal, M.K., and Halder, G.N. (2016). Mixotrophic cultivation of Chlorella sp. BTA 9031 and *Chlamydomonas* sp. BTA 9032 isolated from coal field using various carbon sources for biodiesel production. *Energy Conversion and Management*, 124: 297–304.
- Nham, Q., Mattsson, L., Legrand, C., and Lindehoff, E. (2023) Whey permeate as a phosphorus source for algal cultivation. *Water Environment Research*, 95 (4).
- Nunez, M., and Quigg, A. (2015). Changes in growth and composition of the marine microalgae *Phaeodactylum tricornutum* and *Nannochloropsis salina* in response to changing sodium bicarbonate concentrations. *Journal of Applied Phycology*, 28(4), 2123–2138.
- Oberlander, J. (2023). Assessing the Impacts of Simulated Ocean Alkalinity Enhancement on Viability and Growth of Near-Shore Species of Phytoplankton [master's thesis]. Halifax (NS): Dalhousie University. 79 p. http://hdl.handle.net/10222/82384
- Ogbonna, J.C., Masui, H., Tanaka, H. (1997). Sequential heterotrophic/autotrophic cultivation – An efficient method of producing Chlorella biomass for health food and animal feed. *Journal of Applied Phycology*, 9: 359–366.
- Olguín, E. (2003). Phycoremediation: key issues for cost-effective nutrient removal processes. *Biotechnology Advances*, 22(1-2): 81–91.
- Oxborough, K., Hanlon, A.R.M., Underwood, A.J., and Baker, N.R. (2000). In vivo estimation of the photosystem II photochemical efficiency of individual microphytobenthic cells using high-resolution imaging of chlorophyll a fluorescence. *Limnology and Oceanography*, 45:1420-1425.
- Parrish, C.C. (1999). Determination of Total Lipid, Lipid Classes, and Fatty Acids in Aquatic Samples. *Lipids in Freshwater Ecosystems*, 4–20.
- Peltomaa, E., Johnson, M., and Taipale, S. (2017). Marine Cryptophytes Are Great Sources of EPA and DHA. *Marine Drugs*, 16(1): 3.
- Pulz, O., and Gross, W. (2004). Valuable products from biotechnology of microalgae. *Applied Microbiology and Biotechnology*, 65(6): 635–648.
- Quigg, A., Finkel, Z.V., Irwin, A.J., Rosenthal, Y., Ho, T.Y., Reinfelder, J.R., Schofield, O., Morel, F.M.M., and Falkowski, P.G. (2003). The evolutionary inheritance of elemental stoichiometry in marine phytoplankton. *Nature*, 425(6955): 291-294.
- Rabalais, N.N., Turner, R.E., Diaz, R.J., and Justic, D. (2009). Global change and eutrophication of coastal waters. *ICES Journal of Marine Sciences*, 66 (7):1528-1537.
- Rajakala, P. and Selvi, P.K., (2006). The effect of pH, Temperature and Alkali Metal Ions on the hydrolysis of Whey Lactose Catalysed by B-Galactosidase from *Kluyveromyces marxianus*. *International Journal of Dairy Science*, 1(2): 167-172.
- Ratomski, P., Hawrot-Paw, M., and Koniuszy, A. (2021). Utilisation of CO_2 from Sodium Bicarbonate to Produce Chlorella vulgaris Biomass in Tubular Photobioreactors for Biofuel Purposes. Sustainability, 13: 9118.
- Raven, J. (1997). Putting the C in phycology. *European Journal of Phycology*, 32(4): 319–333.
- Raven, J.A., Giordano, M., and Beardall, J. (2008). Insights into the evolution of CCMs from comparisons with other resource acquisition and assimilation processes. *Physiologia Plantarum*, 4-14.
- Rhee, G.-Y. (1978). Effects of N: P atomic ratios and nitrate limitation on algal growth, cell composition, and nitrate uptake. *Limnology and Oceanography*, 23: 10–25.

- Rigobello-Masini, M., Aidar, E., and Masini, J.C. (2003). Extra and intracelular activities of carbonic anhydrase of the marine microalga *Tetraselmis gracilis* (Chlorophyta). *Brazilian Journal of Microbiology*, 34(3).
- Roth, M.S., Westcott, D.J., Iwai, M., and Niyogi, K.K. (2019). Hexokinase is necessary for glucose-mediated photosynthesis repression and lipid accumulation in a green alga. *Communications Biology*, 2:347.
- Roy, S.S. and Pal, R. (2015). Microalgae in Aquaculture: A review with special references to nutritional value and fish dietetics. *Proceedings of the Zoological Society*, 68(1): 1-8.
- Salati, S., D'Imporzano, G., Menin, B., Veronesi, D., Scaglia, B., Abbruscato, P., Mariani, P., and Adani, F. (2017). Mixotrophic cultivation of Chlorella for local protein production using agro-food by-products. *Bioresource Technology*, 230: 82–89.
- Salbitani, G., Bolinesi, F., Affuso, M., Carraturo, F., Mangoni, O., and Carfagna, S. (2020). Rapid and Positive Effect of Bicarbonate Addition on Growth and Photosynthetic Efficiency of the Green Microalgae *Chlorella Sorokiniana* (Chlorophyta, Trebouxiophyceae). *Applied Sciences*, 10(13): 4515.
- Sang, M., Wang, M., Liu, J., Zhang, C., and Li, A. (2012). Effects of temperature, salinity, light intensity, and pH on the eicosapentaenoic acid production of *Pinguiococcus pyrenoidosus*. *Journal of Ocean University of China*, 11(2): 181–186.
- Shoaf, W.T. and Lium B.W. (1976). Improved extraction of chlorophyll a and b from algae using dimethyl sulfoxide. *Limnology and Oceanography*, 21(6), 926–928.
- Solórzano, L. and Sharp, J.H. (1980). Determination of total dissolved phosphorus and particulate phosphorus in natural waters. *Limnology and Oceanography*, 25(4): 754–758.
- Stancheva, M., Yemendzhiev, H., and Nenov, V. (2021). Phosphorus recovery from dairy processing waste streams. *Journal of Chemical Technology and Metallurgy*, 57(1): 119-125.
- Statista. (2023, January 12). Cheese market in Canada- statistics & facts. https://www.statista.com/topics/4202/cheese-market-in-canada/
- Taipale, S., Peltomaa, E., and Salmi, P. (2020). Variation in ω-3 and ω-6 Polyunsaturated Fatty Acids Produced by Different Phytoplankton Taxa at Early and Late Growth Phase. *Biomolecules*, 10(4): 559.
- Taraldsvik, M. and Myklestad, S.M., (2000). The effect of pH on growth rate, biochemical composition and extracellular carbohydrate production of the marine diatom *Skeletonema costatum*. *European Journal of Phycology*, 35(2): 189-194.
- The Global Goals (2023). Target 12: Responsible consumption and production. New York: The United Nations General Assembly; [accessed 2023 April 27]. https://www.globalgoals.org/goals/12-responsible-consumption-and-production/#things-to-do
- Tredici, M.R. (2010). Photobiology of microalgae mass cultures: understanding the tools for the next green revolution. *Biofuels*, 1(1): 143–162.
- Trivino, A., Godbout, S., Pelletier, F., and Heitz, M. (2016). Environmental study of valorization of cheese dairy residues. Written for presentation at the CSBE/SCGAB 2016 Annual Conference Halifax World Trade and Convention Centre 3-6 July 2016. *The Canadian Society for Bioengineering*. Paper No. CSBE16-066.
- Tsakali, E, Petrotos, K., Allessandro, A.D., and Goulas, P. (2010). A review on whey composition and the methods used for its utilization for food and pharmaceutical products. *Simulation and Modelling in Food and Bio Industries* FOODSIM'2010.
- Turner, L.G., Swaisgood, H.E., and Hansen, A.P. (1978). Interaction of Lactose and Proteins of Skim Milk during Ultra-High-Temperature Processing. *Journal of Dairy Science*, 61(4): 384–392.

- Ulrich, P. and Cerami, A. (2001). Protein glycation, diabetes, and aging; recent progress in hormone research. *The endocrine Society*.
- Ummalyma, S.B., and Sukumaran, R.K. (2014). Cultivation of microalgae in dairy effluent for oil production and removal of organic pollution load. *Bioresource Technology*, 165: 295–301.
- Vieira Salla, A.C., Margarites, A.C., Seibel, F.I., Holz, L.C., Brião, V.B., Bertolin, T.E., Colla, L.M., and Vieira, J.A. (2016). Increase in the carbohydrate content of the microalgae *Spirulina* in culture by nutrient starvation and the addition of residues of whey protein concentrate. *Bioresource Technology*, 209: 133-141.
- Wang, X.-W., Liang, J.-R., Luo, C.-S., Chen, C.-P., and Gao, Y.-H. (2014). Biomass, total lipid production, and fatty acid composition of the marine diatom Chaetoceros muelleri in response to different CO2 levels. *Bioresource Technology*, 161: 124–130.
- Welshmeyer, N.A. (1994). Fluorometric analysis of chlorophyll a in the presence of chlorophyll b and pheopigments. *Limnology and Oceanography*, 39(8): 1985-1992.
- Whitledge, T.E., Malloy, S.C., Patton, C.J., and Wirick, C.O. (1981). Automated nutrient analysis in seawater. *Brookhaven National Lab Report 51398, Brookhaven, NY.*
- Wiliams, A.G. and Withers, S.E. (1981). Hemicellulose-degrading Enzymes Synthesized by Rumen Bacteria. *Journal of applied Bacteriology*, 51(2), 375–385.
- Wood, A.M., Everroad, R.C., and Wingard, L.M. (2005). Measuring growth rates in microalgal cultures. In: Andersen RA (ed) Algal Culture Techniques. *Academic Press, New York*, pp 269-285.
- Wurts, W.A. (2000). Sustainable Aquaculture in the Twenty-First Century. *Reviews in Fisheries Science*, 8(2): 141–150.
- Yamamoto, C. (2023). Evaluating the potential of using food-grade wastes to enhance productivity of mixotrophic species of algae [master's thesis]. Halifax (NS): Dalhousie University. 125 p. http://hdl.handle.net/10222/82401
- Zall, R.R. (1992). Sources and Composition of Whey and Permeate. *Whey and Lactose Processing*, 1–72.
- Zwietering, M.H., Jongenburger, I., Rombouts, F.M., and Van't Riet, K. (1990). Modeling of the bacterial growth curve. *Applied and Environmental Microbiology*, 56(6):1875-1881.

Appendices

5.1. Photosynthesis ANOSIM, Cluster, and SIMPER analyses

Table 5.1. Results from one-way ANOSIM, CLUSTER, and SIMPER analyses comparing EXP cultures in CTRL, CTRL+DIC, and WP media. Analyses based on following variables: F_v/F_m, F_v/Chla, Chla/cell, and σ. Table shows ANOSIM global test R-statistic significance level from ANOSIM (only 10 permutations possible). Pairwise test results from ANOSIM shown when the CLUSTER analysis was significant, as well as variables contributing to the difference from SIMPER.

	R statistic (ANOSIM)	Significance level (ANOSIM)	Cluster analysis	Variable driving the difference (SIMPER) and % contribution
P. pyrenoidosus Global test	0.559	0.06	Non-significant	
C. mesostigmatica Global test	0.416	0.011	Non-significant	
C. muelleri Global test	0.588	0.021	Significant	
Pairwise tests				
CTRL and CTRL+DIC	-0.185	0.6		Fv/Chla (66.76%) and F_v/F_m (25.49%)
CTRL and WP	1	0.1		σ (59.26%) and F_v/Chla (31.23%)
CTRL+DIC and WP	1	0.1		σ (52.68%) and F_v/Chla (35.06%)
T. suecica Global test	0.835	0.007	Significant	
Pairwise tests				
CTRL and CTRL+DIC	0.259	0.2		Chla/cell (76.20%)
CTRL and WP	1	0.1		Chla/cell (95.76%)
CTRL+DIC and WP	1	0.1		Chla/cell (91.18%)

5.2. Fatty acids analyses

5.2.1. Fatty acid cumulative plots

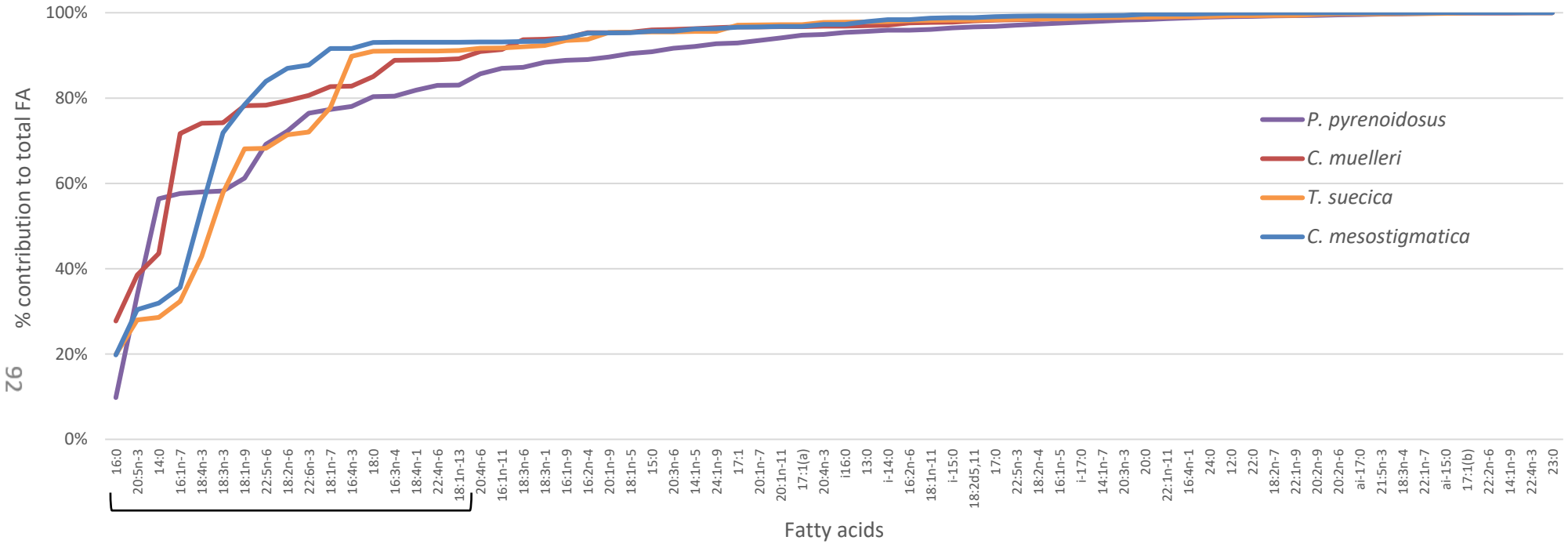

Figure 5.2. Cumulative contribution (%) of each all 68 fatty acids to the total for *P. pyrenoidosus*, *C. muelleri*, *T. suecica*, and *C. mesostigmatica*. Most abundant (17 first) were used for the analyses in this study.

5.2.2. Fatty acid profiles

Table 5.3. Fatty acid (µg/mL) profiles (average ± SD) of the 17 most abundant FA in cultures of *P. pyrenoidosus* grown in CTRL, CTRL+DIC, WP (0.05 g L^{-1}), and WP+DIC and harvested in EXP and STA phases. Data untransformed and unnormalized.

	CTRL		CTRL+DIC		WP		WP+DIC	
	EXP	STA	EXP	STA	EXP	STA	EXP	STA
Total 17 most abundant FA	1.47 ± 0.91	6.88 ± 3.98	3.68 ± 2.38	8.00 ± 2.57	3.05 ± 0.86	7.28 ± 0.68	2.65 ± 0.40	10.15 ± 1.43
Total all FA	1.87 ± 1.42	8.13 ± 4.89	5.73 ± 5.49	8.71 ± 2.64	3.29 ± 0.87	7.95 ± 0.69	2.90 ± 0.44	10.99 ± 1.54
14:0	0.35 ± 0.17	1.06 ± 0.57	1.07 ± 0.10	2.39 ± 1.02	0.99 ± 0.23	2.38 ± 0.07	0.91 ± 0.11	3.29 ± 0.79
16:0	0.10 ± 0.05	0.63 ± 0.22	0.42 ± 0.45	1.37 ± 0.40	0.18 ± 0.06	1.21 ± 0.29	0.18 ± 0.06	2.08 ± 0.31
16:1n-7	-	0.48 ± 0.50	0.02 ± 0.03	0.08 ± 0.02	-	0.05 ± 0.01	-	0.07 ± 0.01
16:3n-4	0.00 ± 0.00	0.02 ± 0.03	0.02 ± 0.04	-	-	-	-	0.00 ± 0.00
16:4n-3	0.06 ± 0.11	0.01 ± 0.01	-	0.01 ± 0.01	-	0.01 ± 0.00	-	0.00 ± 0.00
18:0	0.07 ± 0.02	0.07 ± 0.03	0.21 ± 0.32	0.11 ± 0.02	0.02 ± 0.03	0.32 ± 0.10	0.04 ± 0.02	0.19 ± 0.03
18:1n-9	-	0.87 ± 0.92	0.22 ± 0.38	0.17 ± 0.07	-	0.14 ± 0.01	-	0.15 ± 0.03
18:1n-13	-	-	0.00 ± 0.00	-	0.01 ± 0.00	0.01 ± 0.00	0.01 ± 0.00	0.01 ± 0.00
18:1n-7	-	0.14 ± 0.15	0.03 ± 0.06	0.01 ± 0.02	0.08 ± 0.01	0.05 ± 0.01	0.09 ± 0.02	0.04 ± 0.02
18:2n-6	0.03 ± 0.01	0.20 ± 0.06	0.15 ± 0.09	0.42 ± 0.13	0.09 ± 0.01	0.36 ± 0.03	0.11 ± 0.02	0.41 ± 0.01
18:3n-3	0.00 ± 0.01	0.04 ± 0.05	0.04 ± 0.07	0.00 ± 0.00	-	0.01 ± 0.00	-	-
18:4n-3	-	0.09 ± 0.12	0.05 ± 0.09	0.00 ± 0.01	-	-	-	-
18:4n-1	0.00 ± 0.00	0.02 ± 0.02	0.42 ± 0.73	0.00 ± 0.00	-	-	-	-
20:5n-3	0.57 ± 0.71	2.22 ± 1.77	0.70 ± 0.17	2.15 ± 0.71	0.76 ± 0.12	1.84 ± 0.11	0.91 ± 0.18	2.39 ± 0.19
22:4n-6	-	0.02 ± 0.00	-	0.19 ± 0.26	0.28 ± 0.48	0.03 ± 0.01	-	0.16 ± 0.06
22:5n-6	0.10 ± 0.03	0.31 ± 0.20	0.32 ± 0.04	0.98 ± 0.37	0.37 ± 0.04	0.80 ± 0.07	0.41 ± 0.04	1.24 ± 0.12
22:6n-3	0.17 ± 0.30	0.72 ± 0.88	-	0.10 ± 0.02	0.27 ± 0.47	0.08 ± 0.01	-	0.12 ± 0.01

Table 5.4. Fatty acid (µg/mL) profiles (average ± SD) of the 17 most abundant FA in cultures of *C. muelleri* grown in CTRL, CTRL+DIC, and WP (0.5 g L^{-1}) and harvested in EXP and STA phases. Data untransformed and unnormalized.

	CTRL		CTRL+DIC		WP	
	EXP	STA	EXP	STA	EXP	STA
Total 17 most abundant FA	1.43 ± 0.35	7.45 ± 3.94	1.41 ± 0.12	15.63 ± 1.36	2.49 ± 0.19	3.05 ± 0.86
Total all FA	1.51 ± 0.39	8.58 ± 4.29	1.50 ± 0.12	17.71 ± 1.16	2.79 ± 0.21	3.29 ± 0.87
14:0	0.12 ± 0.05	0.46 ± 0.26	0.13 ± 0.03	0.83 ± 0.09	0.04 ± 0.00	0.99 ± 0.23
16:0	0.02 ± 0.04	2.67 ± 1.64	0.01 ± 0.02	6.64 ± 0.75	0.59 ± 0.05	0.18 ± 0.06
16:1n-7	0.54 ± 0.10	2.26 ± 1.45	0.57 ± 0.04	4.32 ± 0.48	0.60 ± 0.04	-
16:3n-4	0.18 ± 0.04	0.29 ± 0.19	0.18 ± 0.02	0.47 ± 0.04	0.01 ± 0.00	-
16:4n-3	-	0.01 ± 0.00	-	0.03 ± 0.03	0.00 ± 0.00	-
18:0	-	0.14 ± 0.12	-	0.62 ± 0.05	0.09 ± 0.03	0.02 ± 0.03
18:1n-9	-	0.32 ± 0.27	-	0.38 ± 0.01	0.58 ± 0.03	-
18:1n-13	-	0.06 ± 0.10	-	0.03 ± 0.05	0.03 ± 0.00	0.01 ± 0.00
18:1n-7	-	0.07 ± 0.02	-	0.13 ± 0.01	0.41 ± 0.03	0.08 ± 0.01
18:2n-6	-	0.09 ± 0.02	-	0.25 ± 0.03	0.02 ± 0.00	0.09 ± 0.01
18:3n-3	-	0.01 ± 0.00	-	0.02 ± 0.02	0.00 ± 0.00	-
18:4n-3	0.08 ± 0.02	0.18 ± 0.11	0.08 ± 0.01	0.31 ± 0.01	0.03 ± 0.00	-
18:4n-1	-	0.00 ± 0.00	-	0.01 ± 0.01	-	-
20:5n-3	0.39 ± 0.11	0.78 ± 0.51	0.44 ± 0.02	1.44 ± 0.14	0.08 ± 0.00	0.76 ± 0.12
22:4n-6	0.00 ± 0.01	0.00 ± 0.00	-	0.00 ± 0.00	-	0.28 ± 0.48
22:5n-6	-	0.00 ± 0.00	-	0.01 ± 0.01	-	0.37 ± 0.04
22:6n-3	0.09 ± 0.15	0.09 ± 0.04	-	0.15 ± 0.03	0.01 ± 0.00	0.27 ± 0.47

Table 5.5. Fatty acid (µg/mL) profiles (average ± SD) of the 17 most abundant FA in cultures of *T. suecica* grown in CTRL, CTRL+DIC, and WP (0.5 g L^{-1}) and harvested in EXP and STA phases. Data untransformed and unnormalized.

	CTRL		CTRL+DIC		WP	
	EXP	STA	EXP	STA	EXP	STA
Total 17 most abundant FA	1.99 ± 0.52	4.49 ± 0.28	2.14 ± 0.21	8.57 ± 0.94	1.22 ± 0.15	1.74 ± 0.12
Total all FA	2.15 ± 0.62	4.93 ± 0.29	2.28 ± 0.22	9.54 ± 1.03	1.39 ± 0.18	1.98 ± 0.13
14:0	0.01 ± 0.01	0.01 ± 0.01	0.00 ± 0.00	0.03 ± 0.01	0.03 ± 0.01	0.04 ± 0.01
16:0	0.42 ± 0.10	1.11 ± 0.08	0.42 ± 0.04	2.11 ± 0.22	0.17 ± 0.03	0.30 ± 0.04
16:1n-7	0.06 ± 0.03	0.16 ± 0.02	0.06 ± 0.01	0.15 ± 0.00	0.13 ± 0.03	0.22 ± 0.03
16:3n-4	0.00 ± 0.00	0.00 ± 0.00	0.00 ± 0.00	0.00 ± 0.00	0.00 ± 0.00	-
16:4n-3	0.31 ± 0.02	0.64 ± 0.05	0.42 ± 0.04	1.18 ± 0.11	0.00 ± 0.00	0.00 ± 0.00
18:0	0.04 ± 0.04	0.02 ± 0.03	-	0.04 ± 0.02	0.06 ± 0.00	0.08 ± 0.02
18:1n-9	0.20 ± 0.15	0.36 ± 0.04	0.13 ± 0.01	1.52 ± 0.19	0.11 ± 0.01	0.30 ± 0.02
18:1n-13	0.00 ± 0.00	0.00 ± 0.00	0.00 ± 0.00	0.01 ± 0.00	-	-
18:1n-7	0.03 ± 0.01	0.06 ± 0.02	0.02 ± 0.00	0.12 ± 0.00	0.44 ± 0.04	0.60 ± 0.03
18:2n-6	0.07 ± 0.07	0.20 ± 0.04	0.05 ± 0.00	0.38 ± 0.03	0.00 ± 0.00	0.05 ± 0.00
18:3n-3	0.37 ± 0.02	0.80 ± 0.02	0.44 ± 0.04	1.56 ± 0.19	0.08 ± 0.00	0.00 ± 0.00
18:4n-3	0.31 ± 0.02	0.58 ± 0.07	0.44 ± 0.04	0.58 ± 0.07	0.04 ± 0.01	0.01 ± 0.00
18:4n-1	-	0.00 ± 0.00	-	0.00 ± 0.00	-	-
20:5n-3	0.14 ± 0.02	0.55 ± 0.06	0.16 ± 0.02	0.89 ± 0.17	0.10 ± 0.01	0.07 ± 0.01
22:4n-6	0.00 ± 0.00	-	0.00 ± 0.00	-	-	0.00 ± 0.00
22:5n-6	0.00 ± 0.01	0.00 ± 0.00	-	-	0.01 ± 0.00	0.01 ± 0.00
22:6n-3	0.02 ± 0.03	0.01 ± 0.01	-	-	0.05 ± 0.01	0.04 ± 0.01

Table 5.6. Fatty acid (µg/mL) profiles (average ± SD) of the 17 most abundant FA in cultures of *C. mesostigmatica* grown in CTRL, CTRL+DIC, and WP (0.15 g L^{-1}) and harvested in EXP and STA phases. Data untransformed and unnormalized.

	CTRL		CTRL+DIC		WP	
	EXP	STA	EXP	STA	EXP	STA
Total 17 most abundant FA	2.55 ± 0.22	3.09 ± 0.69	3.30 ± 0.79	9.84 ± 1.26	1.97 ± 0.29	8.44 ± 0.71
Total all FA	2.73 ± 0.23	3.38 ± 0.77	3.60 ± 0.91	10.60 ± 1.32	2.16 ± 0.35	8.88 ± 0.75
14:0	0.02 ± 0.00	0.02 ± 0.01	0.03 ± 0.02	0.15 ± 0.04	0.02 ± 0.01	0.28 ± 0.02
16:0	0.45 ± 0.05	0.55 ± 0.19	0.61 ± 0.25	2.06 ± 0.27	0.31 ± 0.06	2.33 ± 0.16
16:1n-7	0.08 ± 0.01	0.07 ± 0.03	0.11 ± 0.05	0.20 ± 0.02	0.21 ± 0.10	0.28 ± 0.03
16:3n-4	-	-	-	-	0.00 ± 0.00	-
16:4n-3	0.00 ± 0.00	0.00 ± 0.00	0.00 ± 0.00	0.00 ± 0.00	0.00 ± 0.00	0.00 ± 0.00
18:0	0.03 ± 0.01	0.03 ± 0.01	0.05 ± 0.00	0.12 ± 0.01	0.04 ± 0.01	0.16 ± 0.02
18:1n-9	0.09 ± 0.01	0.02 ± 0.00	0.09 ± 0.03	0.58 ± 0.15	0.14 ± 0.07	1.13 ± 0.09
18:1n-13	0.00 ± 0.00	-	-	-	-	-
18:1n-7	0.08 ± 0.01	0.03 ± 0.01	0.08 ± 0.01	0.16 ± 0.04	0.28 ± 0.07	0.34 ± 0.03
18:2n-6	0.07 ± 0.01	0.05 ± 0.01	0.08 ± 0.02	0.25 ± 0.05	0.05 ± 0.00	0.45 ± 0.04
18:3n-3	0.54 ± 0.05	0.45 ± 0.08	0.61 ± 0.13	1.75 ± 0.39	0.30 ± 0.01	1.89 ± 0.16
18:4n-3	0.69 ± 0.07	0.94 ± 0.22	0.88 ± 0.21	2.30 ± 0.24	0.32 ± 0.01	0.82 ± 0.09
18:4n-1	-	-	-	-	0.00 ± 0.00	-
20:5n-3	0.31 ± 0.02	0.57 ± 0.09	0.48 ± 0.07	1.48 ± 0.05	0.17 ± 0.00	0.51 ± 0.05
22:4n-6	-	-	-	0.00 ± 0.00	0.00 ± 0.00	0.00 ± 0.00
22:5n-6	0.17 ± 0.01	0.33 ± 0.05	0.26 ± 0.03	0.73 ± 0.03	0.09 ± 0.00	0.20 ± 0.03
22:6n-3	0.02 ± 0.00	0.03 ± 0.01	0.03 ± 0.00	0.07 ± 0.00	0.03 ± 0.01	0.04 ± 0.01

5.2.3. Fatty acid ANOSIM and SIMPER analyses

Table 5.7. Results from two-way crossed ANOSIM comparing growth phases (EXP and STA) and treatments (CTRL, CTRL+DIC, WP, and WP+DIC) based on data of the 17 most abundant fatty acids normalized to C biomass: 14:0, 16:0, 16:1n-7, 16:3n-4, 16:4n-3, 18:0, 18:1n-7, 18:1n-9, 18:1n-13, 18:2n-6, 18:3n-3, 18:4n-1, 18:4n-3, 20:5n-3, 22:4n-6, 22:5n-6, 22:6n-3. Global tests on growth phases and treatments display ANOSIM R-statistic and p-value for each species. Pairwise tests between treatments show R-statistic and significance level in codes: ^{o} for not significant, $^{\bullet}$ for $p < 0.05$, $^{\bullet\bullet}$ for $p = 0.01$.

P. pyrenoidosus Growth phases: R stats = 0.6, p = 0.005 Treatments: R stats = 0.24, p = 0.041			
	CTRL	CTRL+DIC	WP
CTRL+DIC	-0.038 ^{o}		
WP	0.403 ^{o}	0.086 ^{o}	
WP+DIC	0.667 $^{\bullet\bullet}$	0.298 $^{\bullet}$	-0.122 ^{o}

C. muelleri Growth phases: R stats = 0.83, p = 0.003 Treatments: R stats = 0.618, p = 0.004		
	CTRL	CTRL+DIC
CTRL+DIC	0.367 ^{o}	
WP	0.542 ^{o}	0.768 $^{\bullet}$

T. suecica Growth phases: R stats = 1, p = 0.003 Treatments: R stats = 0.988, p = 0.001		
	CTRL	CTRL+DIC
CTRL+DIC	0.934 $^{\bullet\bullet}$	
WP	1 $^{\bullet\bullet}$	1 $^{\bullet\bullet}$

C. mesostigmatica Growth phases: R stats =0.765, p = 0.002 Treatments: R stats = 0.761, p = 0.001		
	CTRL	CTRL+DIC
CTRL+DIC	0.463 ^{o}	
WP	1 $^{\bullet\bullet}$	0.87 $^{\bullet\bullet}$

Table 5.8. Results from SIMPER analyses showing the variables that contributes (%) the most to the significant differences in both EXP and STA cultures in CTRL, CTRL+DIC, WP, and WP+DIC. Analysis based on following fatty acids normalized to C biomass: 14:0, 16:0, 16:1n-7, 16:3n-4, 16:4n-3, 18:0, 18:1n-7, 18:1n-9, 18:1n-13, 18:2n-6, 18:3n-3, 18:4n-1, 18:4n-3, 20:5n-3, 22:4n-6, 22:5n-6, 22:6n-3.

Groups compared	***P. pyrenoidosus***	***C. muelleri***	***T. suecica***	***C. mesostigmatica***
STA and EXP	14:0 (44.1) 16:0 (30.4)	16:0 (71.4)	18:1n-9 (33.3) 16:0 (32.6) 18:4n-3 (13.4)	16:0 (49.5) 18:3n-3 (29.9)
CTRL and CTRL+DIC	Not significant	Not significant	18:1n-9 (51.6) 18:4n-3 (28.2)	Not significant
CTRL and WP	Not significant	Not significant	16 :0 (25.3) 18 :3n-3 (25.2) 16 :4n-3 (17.8) 18 :4h-3 (14.1)	16:0 (43.5) 18:3n-3 (28.68)
CTRL+DIC and WP	Not significant	16:0 (68.5) 16:1n-7 (16.2)	18:3n-3 (24.8) 16:0 (22.7) 16:4n-3 (19.5) 18:4n-3 (12.4)	16:0 (38.6) 18:3n-3 (23.3) 18:1n-9 (16.8)
CTRL+DIC and WP+DIC	14:0 (68.2) 20:5n-3 (20.3)			
WP and WP+DIC	Not significant			
CTRL and WP+DIC	14:0 (39.8) 16:0 (26.2) 20:5n-3 (18.2)			

5.2.4. FA coherence plots

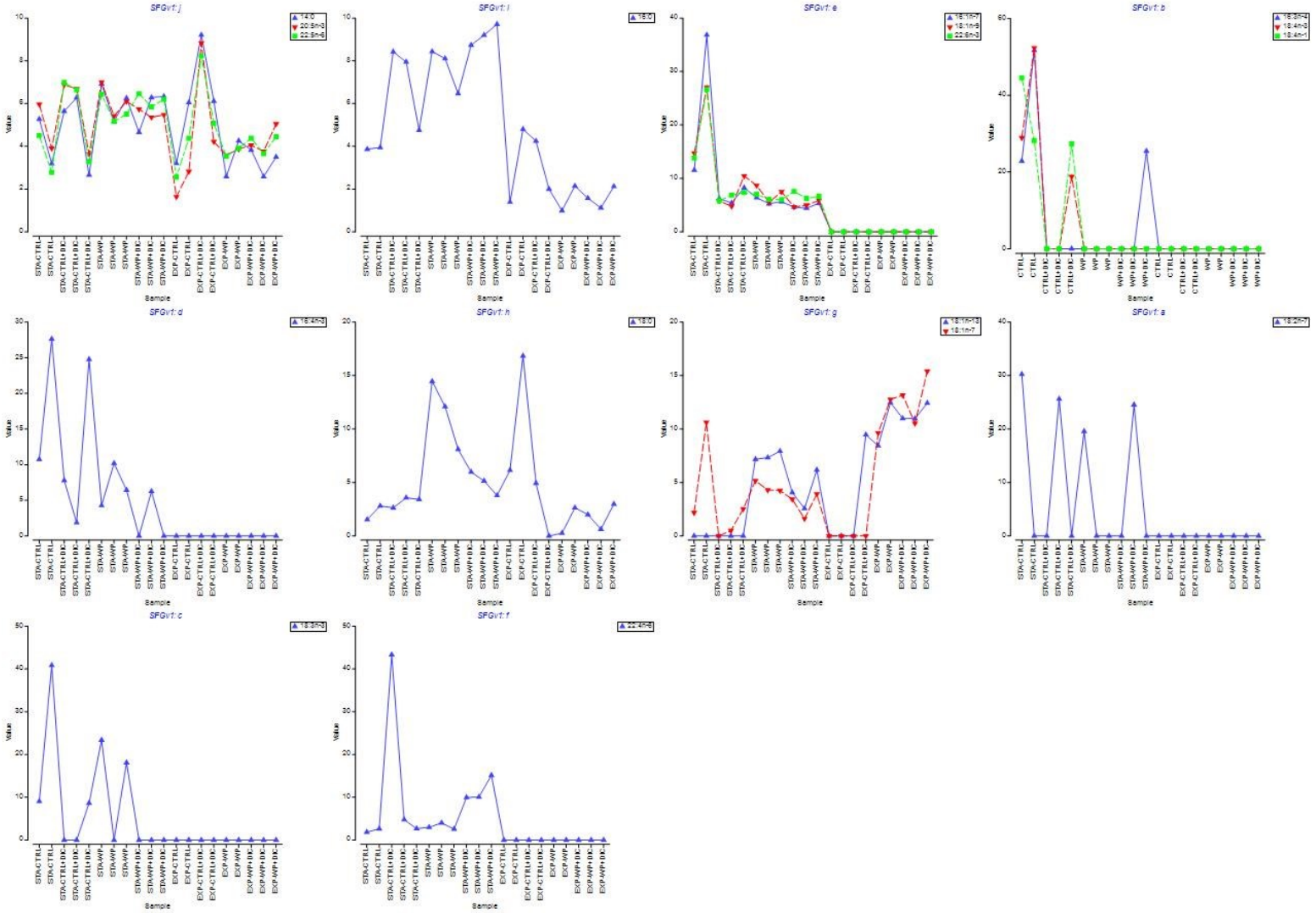

Figure 5.9. Coherence plots of fatty acid clusters from the 17 most abundant FA of *P. pyrenoidosus* showing clusters of FA composition observed across different growth phases and treatments (x axis order from left to right: STA-CTRL, -CTRL+DIC, -WP, -WP+DIC, EXP-CTRL, -CTRL+DIC, -WP, -WP+DIC). Data normalized to C biomass.

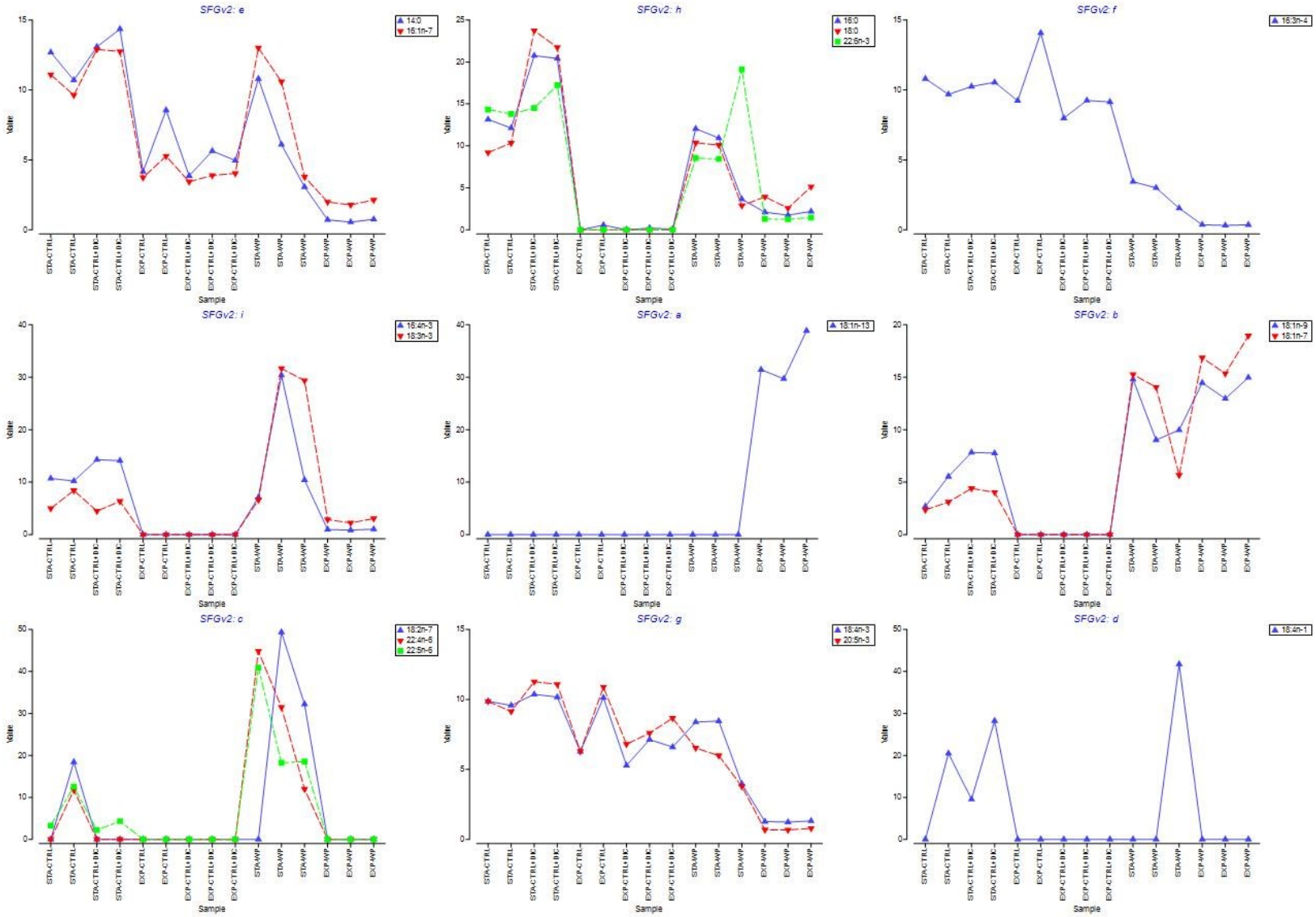

Figure 5.10. Coherence plots of fatty acid clusters from the 17 most abundant FA of *C. muelleri* showing clusters of FA composition observed across different growth phases and treatments (x axis order from left to right: STA-CTRL, -CTRL+DIC, EXP-CTRL, -CTRL+DIC, STA-WP, EXP-WP). Data normalized to C biomass.

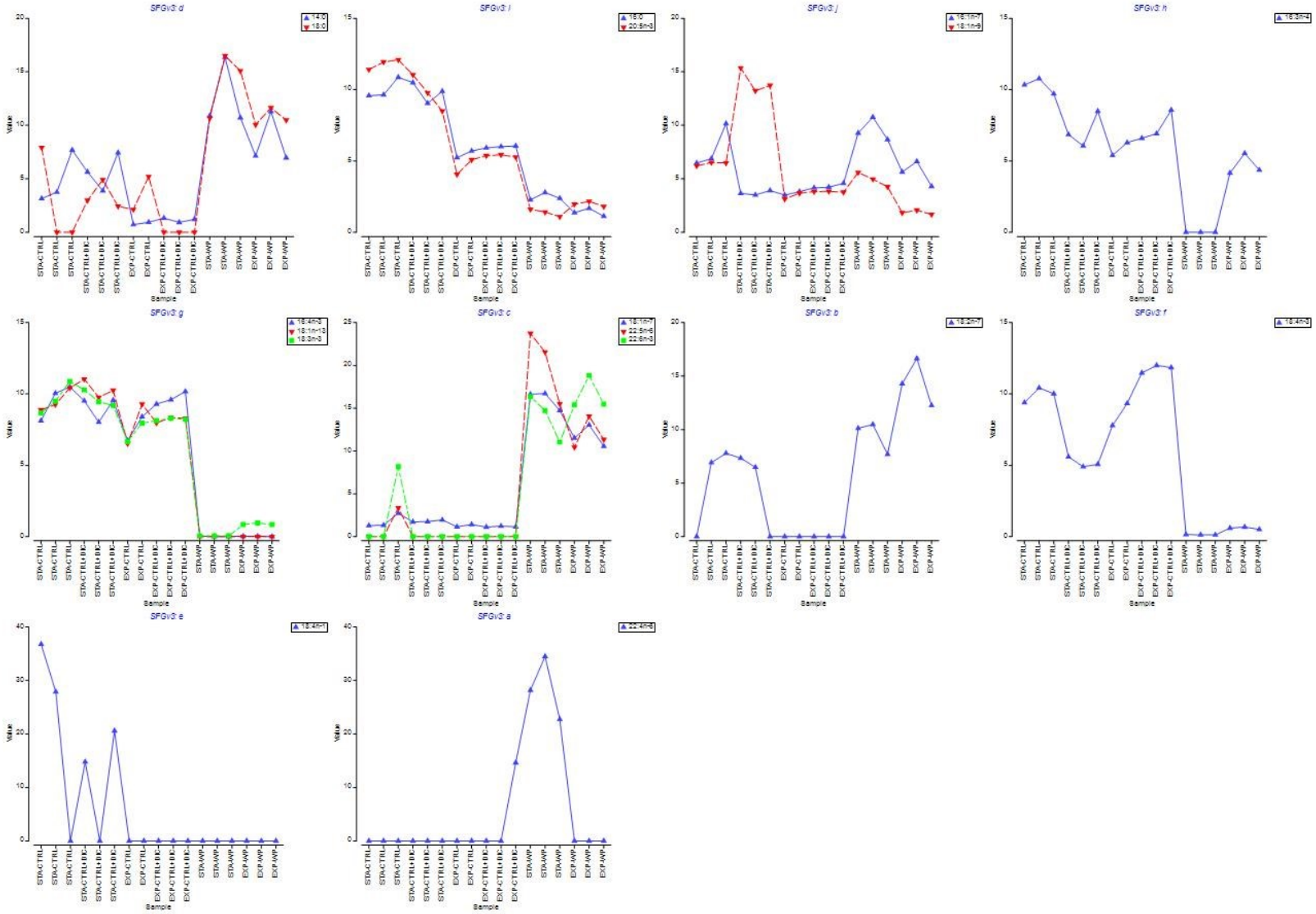

Figure 5.11. Coherence plots of fatty acid clusters from the 17 most abundant FA of *T. suecica* showing clusters of FA composition observed across different growth phases and treatments (x axis order from left to right: STA-CTRL, -CTRL+DIC, EXP-CTRL, -CTRL+DIC, STA-WP, EXP-WP). Data normalized to C biomass.

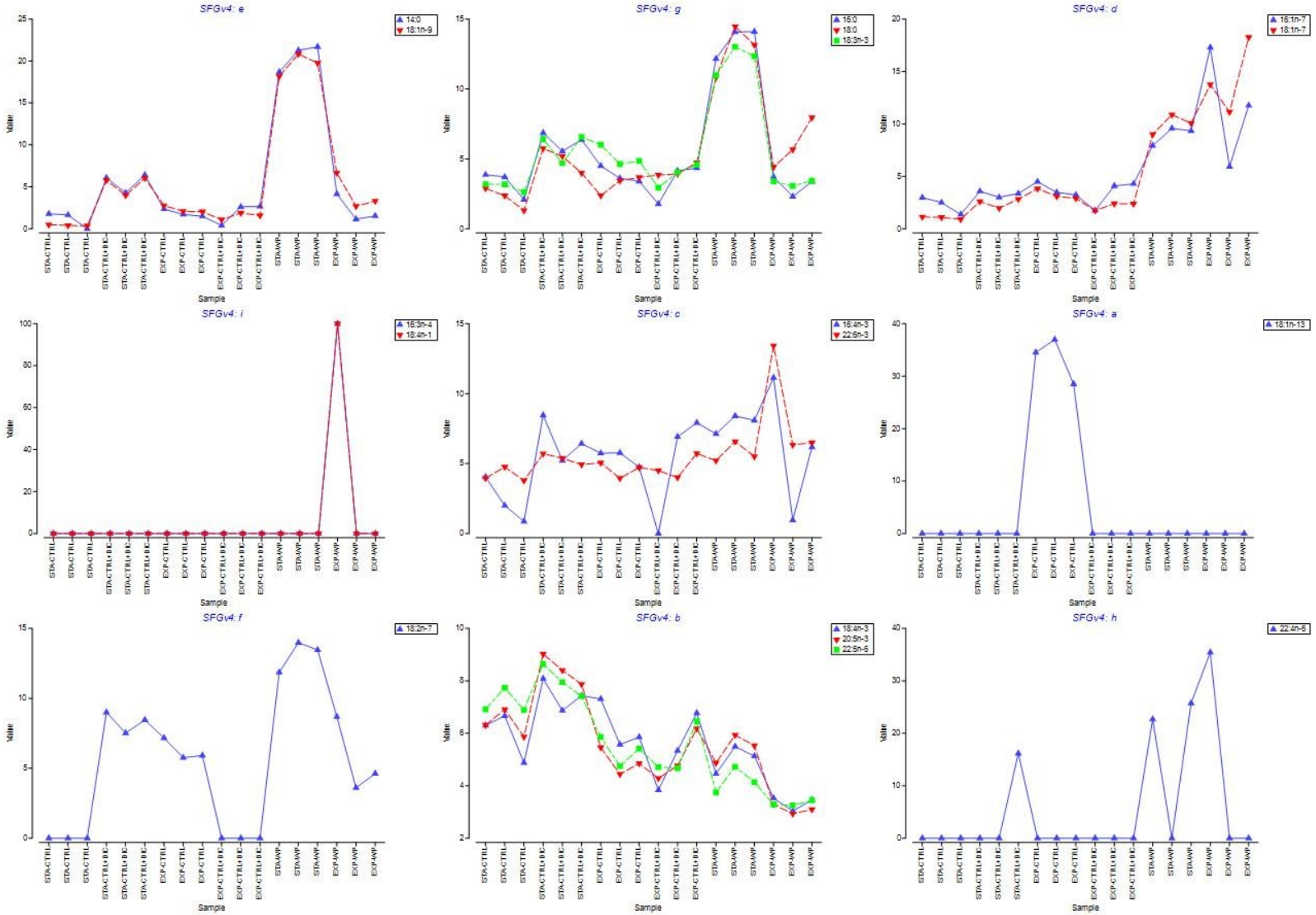

Figure 5.12. Coherence plots of fatty acid clusters from the 17 most abundant FA of *C. mesostigmatica* showing clusters of FA composition observed across different growth phases and treatments (x axis order from left to right: STA-CTRL, -CTRL+DIC, EXP-CTRL, -CTRL+DIC, STA-WP, EXP-WP). Data normalized to C biomass.

5.3. Biomass data

Table 5.13. Fluorescence and biomass data (average ± SD) of cultures of *P. pyrenoidosus*, *C. muelleri*, *T. suecica*, and *C. mesostigmatica* grown in CTRL, CTRL+DIC, WP, and WP+DIC media. Data untransformed and unnormalized.

		F **(Turner)**	F_0	F_m	**σ**	F_v	F_v/F_m	**Chla (µg/mL)**	**Cells/mL**	**C (µg/mL)**	**N (µg/mL)**	**P (µg/mL)**	**Total FA (µg/mL)**
P. pyrenoidosus													
CTRL	STA	111.70 ± 32.61	12199 ± 1787	17133 ± 2210	271 ± 62	4934 ± 540	0.29 ± 0.02	0.42 ± 0.03	930370 ± 127823	12.78 ± 1.07	2.11 ± 0.19	0.16 ± 0.12	8.13 ± 4.89
	EXP	52.10 ± 2.35	3601 ± 187	6321 ± 485	205 ± 11	2721 ± 562	0.43 ± 0.06	0.13 ± 0.01	536815 ± 27556	3.56 ± 1.35	0.78 ± 0.19	0.10 ± 0.05	1.87 ± 1.42
CTRL +DIC	STA	130.00 ± 13.00	11714 ± 1651	14751 ± 1891	297 ± 19	3037 ± 271	0.21 ± 0.01	0.46 ± 0.00	877185 ± 84717	19.89 ± 1.35	2.45 ± 0.19	0.13 ± 0.04	8.71 ± 2.64
	EXP	98.87 ± 2.72	6687 ± 732	12356 ± 811	214 ± 17	5669 ± 546	0.46 ± 0.04	0.29 ± 0.01	915926 ± 69941	6.22 ± 1.17	1.33 ± 0.33	0.16 ± 0.01	5.73 ± 5.49
WP	STA	193.67 ± 41.30	16206 ± 2202	22673 ± 3337	289 ± 21	6467 ± 1264	0.28 ± 0.02	0.43 ± 0.01	1409259 ± 333145	16.11 ± 2.91	2.22 ± 0.19	0.09 ± 0.02	7.95 ± 0.69
	EXP	108.67 ± 4.16	5485 ± 238	9373 ± 364	214 ± 15	3888 ± 126	0.41 ± 0.00	0.27 ± 0.00	1099259 ± 87998	11.33 ± 0.88	1.89 ± 0.19	0.25 ± 0.13	3.29 ± 0.87
WP +DIC	STA	127.67 ± 6.81	11588 ± 1722	15959 ± 3078	355 ± 49	4372 ± 1357	0.27 ± 0.03	0.34 ± 0.01	1354630 ± 188262	23.00 ± 2.19	2.22 ± 0.19	0.10 ± 0.03	10.99 ± 1.54
	EXP	99.73 ± 5.30	5060 ± 303	8714 ± 452	192 ± 10	3655 ± 277	0.42 ± 0.02	0.24 ± 0.01	1201481 ± 73806	11.33 ± 1.20	2.22 ± 0.19	0.15 ± 0.05	2.90 ± 0.44
C. muelleri													
CTRL	STA	153.71 ± 5.57	16269 ± 310	21015 ± 967	146 ± 6	4746 ± 677	0.23 ± 0.02	0.40 ± 0.01	1275556 ± 147802	17.78 ± 0.19	1.33 ± 0.33	0.11 ± 0.05	8.58 ± 4.29
	EXP	61.26 ± 0.50	5463 ± 564	13515 ± 198	106 ± 8	8051 ± 501	0.60 ± 0.04	0.25 ± 0.01	728333 ± 101749	7.53 ± 0.23	1.13 ± 0.12	0.07 ± 0.05	1.51 ± 0.39
CTRL +DIC	STA	143.04 ± 12.90	15727 ± 1672	22246 ± 2041	134 ± 2	6520 ± 388	0.29 ± 0.01	0.38 ± 0.01	887778 ± 157165	20.89 ± 0.96	1.44 ± 0.19	0.07 ± 0.00	17.71 ± 1.16
	EXP	61.60 ± 0.35	5013 ± 489	13199 ± 485	112 ± 1	8186 ± 973	0.62 ± 0.05	0.25 ± 0.01	651667 ± 41633	9.00 ± 0.87	1.13 ± 0.12	0.09 ± 0.03	1.50 ± 0.12
WP	STA	140.99 ± 48.79	9910 ± 3527	11706 ± 3234	328 ± 69	1797 ± 379	0.16 ± 0.07	0.19 ± 0.01	1152778 ± 226203	21.44 ± 2.36	2.67 ± 0.33	0.30 ± 0.14	10.66 ± 4.96
	EXP	16.26 ± 0.32	1165 ± 61	2071 ± 69	267 ± 32	906 ± 39	0.44 ± 0.02	0.04 ± 0.00	176333 ± 23629	18.00 ± 0.53	3.07 ± 0.12	0.44 ± 0.34	2.79 ± 0.21

		F (Turner)	F_0	F_m	σ	F_v	F_v/F_m	Chla (µg/mL)	Cells/mL	C (µg/mL)	N (µg/mL)	P (µg/mL)	Total FA (µg/mL)
T. suecica													
CTRL	STA	180.52 ± 18.33	17807 ± 1950	29108 ± 2254	292 ± 22	11301 ± 589	0.39 ± 0.02	0.91 ± 0.02	439333 ± 11930	16.33 ± 2.19	2.22 ± 0.19	0.16 ± 0.09	4.93 ± 0.29
	EXP	60.08 ± 2.07	4965 ± 33	12466 ± 269	226 ± 5	7501 ± 248	0.60 ± 0.01	0.51 ± 0.00	118333 ± 12702	9.49 ± 1.02	2.04 ± 0.27	1.67 ± 2.17	2.15 ± 0.62
CTRL +DIC	STA	216.85 ± 27.57	24062 ± 350	40582 ± 1554	361 ± 23	16520 ± 1239	0.41 ± 0.02	0.75 ± 0.04	490333 ± 96023	31.55 ± 2.22	2.22 ± 0.19	0.12 ± 0.05	9.54 ± 1.03
	EXP	67.86 ± 6.07	5138 ± 704	14237 ± 1493	206 ± 4	9099 ± 1373	0.64 ± 0.05	0.45 ± 0.03	119667 ± 16623	10.40 ± 1.11	2.13 ± 0.31	2.19 ± 1.37	2.28 ± 0.22
WP	STA	16.72 ± 0.82	937 ± 126	1063 ± 160	1076 ± 1759	125 ± 230	0.10 ± 0.19	0.08 ± 0.00	182667 ± 30436	18.00 ± 1.33	2.56 ± 0.19	0.03 ± 0.03	1.98 ± 0.13
	EXP	27.20 ± 1.23	1928 ± 58	3066 ± 110	343 ± 10	1138 ± 61	0.37 ± 0.01	0.08 ± 0.01	426333 ± 76840	17.93 ± 0.76	3.73 ± 0.12	0.04 ± 0.01	1.39 ± 0.18
C. mesostigmatica													
CTRL	STA	102.60 ± 2.65	7375 ± 266	11476 ± 713	118 ± 13	4101 ± 447	0.36 ± 0.02	0.64 ± 0.01	1089000 ± 132752	18.44 ± 1.50	3.78 ± 0.38	0.33 ± 0.34	3.38 ± 0.77
	EXP	46.19 ± 0.70	3572 ± 122	7100 ± 861	143 ± 8	3528 ± 740	0.49 ± 0.04	0.43 ± 0.00	345667 ± 7767	13.07 ± 0.70	2.33 ± 0.12	0.07 ± 0.02	2.73 ± 0.23
CTRL +DIC	STA	151.60 ± 4.36	12344 ± 1138	18842 ± 885	145 ± 6	6498 ± 253	0.35 ± 0.03	0.87 ± 0.04	1446667 ± 132035	36.33 ± 2.91	6.33 ± 0.33	0.11 ± 0.04	10.60 ± 1.32
	EXP	69.59 ± 1.44	4972 ± 54	9291 ± 228	145 ± 7	4319 ± 279	0.46 ± 0.02	0.61 ± 0.02	458333 ± 163531	19.60 ± 1.40	3.53 ± 0.23	0.07 ± 0.03	3.60 ± 0.91
WP	STA	53.28 ± 1.90	3835 ± 338	5973 ± 665	162 ± 6	2138 ± 342	0.36 ± 0.02	0.19 ± 0.01	416667 ± 4933	19.22 ± 1.07	1.78 ± 0.19	0.20 ± 0.05	8.88 ± 0.75
	EXP	28.52 ± 0.60	2038 ± 34	4232 ± 566	151 ± 6	2194 ± 559	0.51 ± 0.06	0.19 ± 0.00	195667 ± 4509	11.13 ± 0.42	2.27 ± 0.12	0.03 ± 0.01	2.16 ± 0.35

5.4. Model fit parameters

Table 5.14. Gompertz and Blackman fit parameters (average ± SD) according to Equations 3.2 and 3.3 of cultures of *P. pyrenoidosus*, *C. muelleri*, *T. suecica*, and *C. mesostigmatica* grown in CTRL, CTRL+DIC, WP, and WP+DIC media.

		Modified Gompertz model (Equation 3.2)			
Species	**Treatment**	F_{max}	μ_{max}	λ	F_{init}
P. pyrenoidosus	CTRL	5.31 ± 0.34	1.24 ± 0.09	1.69 ± 0.24	-0.38 ± 0.11
	CTRL+DIC	5.60 ± 0.10	1.13 ± 0.04	1.35 ± 0.10	-0.45 ± 0.02
	WP	5.54 ± 0.18	1.20 ± 0.11	1.16 ± 0.53	-0.07 ± 0.12
	WP+DIC	5.14 ± 0.08	1.00 ± 0.06	1.12 ± 0.18	-0.06 ± 0.05
C. muelleri	CTRL	8.65 ± 1.20	3.58 ± 2.13	-0.70 ± 0.84	-3.48 ± 1.30
	CTRL+DIC	5.30 ± 0.13	2.49 ± 0.04	-0.07 ± 0.06	-0.33 ± 0.07
	WP	2.45 ± 0.51	0.39 ± 0.06	0.00 ± 0.00	2.42 ± 0.10
T. suecica	CTRL	5.33 ± 0.14	1.70 ± 0.02	0.17 ± 0.16	0.00 ± 0.00
	CTRL+DIC	5.42 ± 0.15	1.59 ± 0.02	0.04 ± 0.07	0.00 ± 0.00
	WP	1.15 ± 0.09	5.12 ± 0.08	0.85 ± 0.02	2.28 ± 0.02
C. mesostigmatica	CTRL	3.81 ± 0.06	1.37 ± 0.01	0.00 ± 0.00	0.83 ± 0.04
	CTRL+DIC	4.12 ± 0.05	1.41 ± 0.07	0.00 ± 0.00	0.89 ± 0.05
	WP	2.69 ± 0.04	1.18 ± 0.03	0.53 ± 0.01	1.39 ± 0.01
			Modified Blackman model (Equation 3.3)		
Species	**Treatment**	F_{init}	F_{max}	t_{sat}	λ
P. pyrenoidosus	CTRL	-0.36 ± 0.06	4.67 ± 0.14	4.96 ± 0.31	1.39 ± 0.16
	CTRL+DIC	-0.36 ± 0.02	4.76 ± 0.11	5.22 ± 0.16	1.18 ± 0.13
	WP	0.05 ± 0.07	5.17 ± 0.09	5.14 ± 0.26	0.99 ± 0.46
	WP+DIC	-0.03 ± 0.02	4.76 ± 0.02	5.90 ± 0.30	0.72 ± 0.13
C. muelleri	CTRL	-1.48 ± 2.90	4.76 ± 0.15	2.25 ± 0.62	0.10 ± 0.18
	CTRL+DIC	0.20 ± 0.04	4.85 ± 0.07	2.38 ± 0.03	0.00 ± 0.00
	WP	2.63 ± 0.09	4.77 ± 0.35	7.39 ± 0.09	-0.03 ± 0.00
T. suecica	CTRL	0.09 ± 0.06	5.17 ± 0.12	3.89 ± 0.21	-0.09 ± 0.07
	CTRL+DIC	0.11 ± 0.03	5.15 ± 0.14	3.78 ± 0.02	-0.11 ± 0.04
	WP	2.28 ± 0.02	3.43 ± 0.10	1.03 ± 0.10	0.36 ± 0.04
C. mesostigmatica	CTRL	1.12 ± 0.05	4.56 ± 0.01	3.37 ± 0.04	-0.04 ± 0.00
	CTRL+DIC	1.18 ± 0.04	4.88 ± 0.03	3.43 ± 0.11	-0.04 ± 0.00
	WP	1.39 ± 0.01	3.97 ± 0.02	2.79 ± 0.02	0.32± 0.03